國立成功大學

化學研究所

碩士論文

建立細胞或酵素之試驗方法以分析人類疾病相關之聚醣代謝

Establishment of the cell- or enzyme-based approaches to analyze disease-associated human glycan metabolism

陳昱心

Yu-Hsin Chen

指導教授：鄭偉杰 博士

共同指導教授：周鶴軒 博士

Advisor: Wei-Chieh Cheng, Ph.D.

Co-Advisor: Ho-Hsuan Chou, Ph.D.

中華民國 108 年 7 月

doi:10.6844/NCKU201900656

國立成功大學

碩士論文

建立細胞或酵素之試驗方法以分析人類疾病相關之聚醣代謝

Establishment of the cell- or enzyme-based approaches to analyze disease-associated human glycan metabolism

研究生：陳昱心

本論文業經審查及口試合格特此證明

論文考試委員：

周鶴軒

徐翠珍

指導教授：[illegible]

系(所)主管：許輝煌（代主任）

中　華　民　國　108　年　7　月　26　日

doi:10.6844/NCKU201900656

本研究榮獲財團法人罕見疾病基金會

「第十九屆罕見疾病碩博士論文獎助學金」獎助

謹於此特別感謝

doi:10.6844/NCKU201900656

中文摘要

聚醣是一種在人體中必需的生物材料，其功能為調節人體中細胞或是訊息傳遞等生理功能，像是細胞與細胞之連結與傳遞訊息之橋樑以及細胞與周邊胞內間質的交互作用。聚醣包括了寡醣或是多醣存在於人體中，而這些醣類的生合成以及代謝在特定疾病中扮演了可能誘發致病的重要角色。本篇論文主要分為兩個部分，第一部分講述了罕見疾病-溶小體儲積症，其致病機制為遺傳基因的缺陷造成特定的溶小體酵素失去正常功能，導致其受質大量堆積於溶小體中，使得細胞功能異常並更進一步造成組織以及器官無法正常運作。現行的溶小體儲積症的治療方法包括了酵素取代療法、藥理小分子伴護療法以及小分子穩定劑共同治療等。然而在溶小體儲積症中，其中又以黏多醣症的小分子藥物開發最為艱困，原因為現行平台不夠完備以致無法有效率地進行分子庫的篩選。本篇論文將以第二型黏多醣症為主要的研究方向，第二型黏多醣症又稱作韓特氏症，其致病機制為病患體中缺乏了己醛糖酸鹽硫酸酶，導致其受質皮膚素硫酸鹽及肝黏醣硫酸鹽兩種多醣類的代謝異常並堆積。為了要建立小分子檢測平台作為治療第二型黏多醣症的藥物開發，我們嘗試開發酵素以及細胞之檢測平台並且針對酵素標靶或是受質致病表徵的改變來檢測小分子的潛在應用。另外，瞭解黏多醣症病人與正常人之間的差異也是一個重要的指標來判斷小分子的效果，因此我們建立了黏多醣症病人或正常人的酵素平台對於酵素的熱穩定性與細胞內的酵素活性實驗來針對小分子酵素穩定劑作評估。另一方面，觀察其受質致病表徵也是一種評判小分子效果的方法，主要目的為判斷其大量累積的受質在小分子參與下是否能夠減少以達到治療效果，但其受質為大分子多醣在藥物研究中其難以檢測，因此我們嘗試了化學標誌方法以及酸水解甲基化法。然而在開發化學標誌方法中，我們尚須在製備艾杜醣醛酸的標準品以及樣品的前處理中進行可行性的評估。同時，我們成功利用酸水解甲基化法藉由液相串聯式質譜儀評估肝黏醣硫酸鹽在正常人與黏多醣症病人細胞中的差異。在此初步成果中，希望此酵素與細胞試驗在未來能夠運用在分子庫檢測以利開發治療

doi:10.6844/NCKU201900656

黏多醣症的小分子藥物。

在第二部分中，高程度甘露醣聚醣在癌症細胞或是正常細胞中扮演著細胞增生的重要角色。人類高基氏體甘露醣酶是一種水解酵素並且是一個藥物開發中已知的癌症標靶，而目前已知具有抗癌活性的天然物苦馬豆素是一種強力的高基氏體甘露醣酶抑制劑，但同時也會抑制溶小體甘露醣酶而造成了高程度甘露醣聚醣無法正常代謝並累積在溶小體中並在藥物臨床開發中造成負面影響。為了克服苦馬豆素對於高基氏體甘露醣酶與溶小體甘露醣酶的不良選擇性，其具有潛力的選擇性抑制劑會透過人工螢光受質試驗篩選出來。然而在簡易版的人工螢光受質試驗無法精確的探討抑制劑在酵素與真實受質的結合情況。因此我們嘗試建立以寡醣作為真實受質的檢測平台，來更進一步確認具有潛力之選擇性抑制劑的抑制效果。最後我們成功利用酵素化學合成法製備螢光標定的寡醣作為高基氏體甘露醣酶與溶小體甘露醣酶的受質。與此同時，我們也建立寡醣受質檢測方法來評估了具有潛力的高基氏體甘露醣酶抑制劑的選擇性抑制能力，並且更進一步利用此平台來探討酵素動力學之抑制模式。最後我們發現利用了不同受質的檢測平台來評估具有潛力之抑制劑確實會觀察到不同的抑制效果，並且也會在酵素動力學研究中造成不同抑制模式。針對此結果，我們提供了真實的寡糖受質檢測平台來幫助未來在高基氏體甘露醣酶選擇性抑制劑的開發。

關鍵字 ： 溶小體儲積症; 第二型黏多醣症; 己醛糖酸鹽硫酸酶; 肝黏醣硫酸鹽; 酸水解甲基化法; 小分子酵素穩定劑; 高程度甘露醣聚醣; 高基氏體甘露醣酶; 寡醣受質; 選擇性抑制劑

doi:10.6844/NCKU201900656

Abstract

Glycans are necessary bio-materials for physiological function regulating like cell-cell communication or cell-matrix interaction. Moreover, the balance of biosynthesis and metabolism toward the many oligo- or polysaccharides is very important and relates to diseases.

The first part described lysosomal storage diseases (LSDs), a kind of rare inherited diseases caused by genetic deficiency. The major pathogenic mechanism is the abnormal accumulation of the substrates in the lysosomes, resulting in progressive cellular and multi-organ dysfunction. Nowadays, the treatments of LSD include enzyme replacement therapy, pharmacological chaperone, and small molecule enzyme stabilizer. However, the small molecule drug discovery of mucopolysaccharidosis (MPS) is the most challenging among all the LSDs, because the assay platform for screening is incomplete to screening the library efficiently. In this work, we focus on the mucopolysaccharidosis type II (LSDs), is also called Hunter syndrome, which is caused by the deficiency of iduronate-2-sulfatase to lead the substrate accumulation of glycosaminoglycans (GAGs). To establish the assay platform for small molecule screening in the drug discovery, we attempt to develop the enzyme- and cell-based assays to observe the variation of specific target or phenotype. Besides, differentiation of the level of substrates toward the normal person and MPS patient is crucial information to judge the potency of the small molecule. Thus, we established the enzymatic bio-assays include the thermal stability and enzyme activity in the cell-based assay to evaluate the property of small molecules. Also, the observation of the pathological phenotype of the substrate accumulation is a direct approach to link with the potency of the small molecule. Because the substrate of polysaccharides is difficult to detect, so we attempt to use the methods of tag chemicals and methanolysis. Unexpectedly, in the development of tag chemical method, we still need to evaluate the feasibility of the

doi:10.6844/NCKU201900656

preparation of standard and sample pretreatments. At the same time, we successfully established the method of methanolysis in the cell-based assay to evaluate the differentiation of HS levels by LCMS/MS toward the normal person and MPS patient. In our efforts of this work, we hope these established assay platforms include the enzyme- and the cell-based assay can apply in the small molecules screening for the drug discovery of MPS.

The second part is the topic about the high mannose-type glycan, a key role in the cell-cell communication toward cell proliferation in normal cell and cancer cell. Human Golgi α-mannosidase II (hGMII) is a glycosyl hydrolase, and also is a pharmaceutical target for the anticancer therapies. A well-known potent inhibitor of hGMII called Swainsonine, a natural product which has the anti-tumor activity but co-inhibition of human lysosomal α-mannosidase (hLM) cause the accumulation of high-mannose oligosaccharides in lysosomes which limits the application in the clinical trials. To overcome the challenge arising from poor selective inhibition between hGMII and hLM, the potential small molecules have been analyzed the selective inhibition through the common used fluorometric assay by the artificial substrate. However, the artificial substrate is not the insight to express the binding situation of the inhibitor between the real substrate and enzyme. Thus, we attempt to establish the real oligosaccharide-based assay to characterize the potency of the selective inhibitors. On the other hand, we successfully prepared the labeled oligosaccharides and the real substrate of hGMII by chemoenzymatic synthesis. By using the oligosaccharide-based substrate, we establish the assay platform to evaluate the potential selective inhibitors and the binding mode in the enzyme kinetic studies.

Keywords: LSDs; MPS II; GAGs; Iduronate-2-sulfatase; heparan sulfate; methanolysis; High-mannose type glycan; hGMII; Oligosccharide-based substrate; Selective inhibitor

doi:10.6844/NCKU201900656

Acknowledgment

兩年的研究所生涯，途中的失敗與不如預期不勝枚舉，儘管路途顛簸，走來跌跌撞撞，但這趟旅程著實讓我成長許多，無論是待人處事、邏輯思維或是解決問題的能力。首先特別感謝指導教授鄭偉杰老師，用心且認真教導學術知識與實驗邏輯，鄭老師對於教學之熱忱以及研究的嚴謹與敬責態度是我在碩士生涯中最好的學習榜樣。在學期間，因為鄭老師的鼓勵以及無私的協助，讓我能夠申請到罕見疾病基金會之碩博士獎學金以及在台灣藥學會獲得口頭論文報告佳作，其中也得到了王光昭教授學術基金會以及科技部的出國會議經費補助，另外也讓我參與了許多學術研討會來增進學術領域的視野。在此特別感謝補助參與美國化學年會的台灣藥學會之王光昭教授學術基金會以及科技部。同時感謝共同指導教授周鶴軒老師在學期間的指導與關心，讓我在一年級奠定了書報討論以及簡報製作的正確觀念。由衷感謝口試委員徐翠玲老師在實驗上的建議以及認真的指導，讓後續實驗能夠順利進行，並使論文內容更加完善。

在實驗過程中，需要透過自我思考判斷並不停的自我修正才能使結果更加明確。但因自我能力有限，有時免不了的無所適從，都能從身邊的同儕以及實驗室同仁得到幫助、建議以及經驗的傳授。所以在此感謝實驗室的大家對我的關心以及幫忙，讓我在實驗過程中能夠圓滿順利。最後要感謝父母讓我就學期間食衣住行無後顧之憂，並給予關懷以及支持讓我能專心於研究與學習。

2019.8.20　陳昱心

doi:10.6844/NCKU201900656

Table of Contents

doi:10.6844/NCKU201900656

doi:10.6844/NCKU201900656

doi:10.6844/NCKU201900656

Index of Figures

Chapter 1 Part A

doi:10.6844/NCKU201900656

Chapter 1 Part B

doi:10.6844/NCKU201900656

Chapter 2

doi:10.6844/NCKU201900656

Index of Tables

Chapter 1 Part A

Chapter 1 Part B

Chapter 2

Index of Schemes

Chapter 1 Part B

Chapter 2

doi:10.6844/NCKU201900656

Chapter 1 Develop the analytical platform toward mucopolysaccharidosis type II

Part A. Establish enzyme-based assays for small molecules evaluation

1A.1 Introduction

1A.1.1 Lysosomal storage diseases

Lysosomal storage diseases (LSDs) are inherited lysosomal metabolic disorder because of the genetic defect caused by the deficient function of a specific enzyme[1]. There are currently more than 50 rare diseases caused by dysfunction of the lysosome, such as Fabry disease, Pompe disease, and Mucopolysaccharidoses. The mutant enzyme fails to pass through the quality control mechanism in the endoplasmic reticulum and result in degradation or loss-function. Due to insufficient enzyme activity, the substrate will accumulate in the patient's cell and further cause the organ dysfunction[2] (Figure 1A.1).

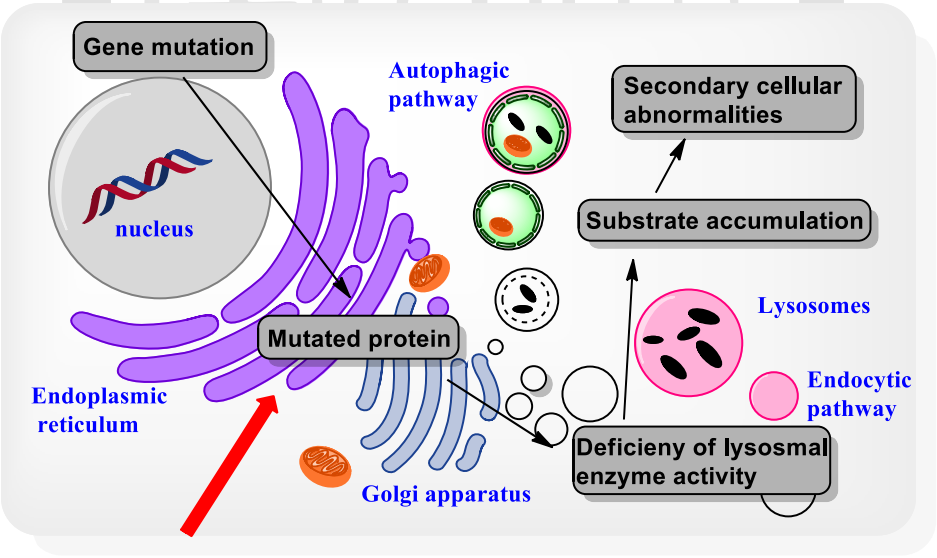

Figure 1A. 1 The pathogenic pathway of LSDs

doi:10.6844/NCKU201900656

1A.1.2 Mucopolysaccharidoses

Mucopolysaccharidoses (MPS) belongs to a group of LSDs caused by an inborn error of metabolism. The mutant enzyme fails to pass through the quality control mechanism in the endoplasmic reticulum and result in degrading or loss-function. Due to insufficient enzyme activity, the substrate will not be degraded and accumulate in the patient's cell further cause organ dysfunction[3]. The lack of essential enzyme activities will cause mucopolysaccharidosis. MPS are classified by the deficient enzymes and the clinical phenotypes. All of types MPS are autosomal recessive disorders except for MPS II is X-linked (Table 1A.1).

The incidence of MPS was reported to be 1 per 50,000 in Taiwan[4, 5]. Of these cases, MPS II had the highest birth incidence of 1 per 100,000 live births (2 per 100,000 male of live births). MPS II caused by a deficiency of iduronate-2-sulfatase (IDS, EC.3.1.6.13), an enzyme encoded by a gene located on Xq28[6]. *IDS* genes were classified into nonsense mutation, missense mutation, deletions mutation, and insertion nutation. At least 530 mutations will lead to mild or severe phenotypes in MPS II.

doi:10.6844/NCKU201900656

Table 1A. 1 The types of Mucopolysaccharidoses

Disease	**Deficient enzyme**	**Storage product**
MPS I (Hurler-Scheie)	α-L-Iduronidase (*IDUA*)	Dermatan sulfate Heparan sulfate
MPS II (Hunter)	Iduronate-2-sulfatase (*IDS*)	Dermatan sulfate Heparan sulfate
MPS III (Sanfilippo A)	N-sulfoglucosamine sulfohydrolase (Sulfamidase, *SGSH*)	Heparan sulfate
MPS III (Sanfilippo B)	N-acetyl-α-glucoaminidase (*NAGLU*)	
MPS III (Sanfilippo C)	Acetyl Co-A: α-glucosaminide N-acetyltransferase (*HGSNAT*)	
MPS III (Sanfilippo D)	Glucosamine (N-acetyl)-6-sulfatase (*GNS*)	
MPS III (Sanfilippo E)	N-sulfoglucosamine-3-sulfatase (*ARSG*)	
MPS IV (Morquio A)	Galactose/N-acetyl-6-sulfatase (*GALNS*)	Keratin sulfate Chondroitin-6-sulfate Dermatan sulfate
MPS IV (Morquio B)	β-galactosidase (*GLB1*)	Keratin sulfate
MPS VI (Maroteaux−Lamy)	N-acetylgalactosamine 4-sulfatase (*ARSB*)	Dermatan sulfate Chondroitin sulfate
MPS VII (Sly)	β-glucuronidase (*GUSB*)	Chondroitin sulfate Dermatan sulfate Heparan sulfate
MPS IX (Natowicz)	Hyaluronidase (*HYAL1*)	Hyaluronan

doi:10.6844/NCKU201900656

1A.1.3 Glycosaminoglycans

Glycosaminoglycans (GAGs) are long unbranched polysaccharides with repeating disaccharides. GAGs include heparan sulfate (HS), dermatan sulfate (DS), chondroitin sulfate (CS), keratan sulfate (KS), and hyaluronan, which are consisting of different amino sugar and uronic acid with variable sulfation levels. These negatively charged molecules distributed on outer of cell membranes and many tissues like skin, bone, and cartilage. Their functions are lubrication and providing physiological specificity functions such as angiogenesis and cell proliferation[7].

For example, the heparan sulfate constituted by the repeating subunit, glucuronic acid or iduronic acid plus glucosamine, derived in various sulfation (GlcA or IdoA + GlcN). The heparan sulfate chains are covalently O-linked with the core protein called heparan sulfate proteoglycans (HSPGs) which are widespread macromolecules associated with the cell surface and extracellular matrix of a wide range of cells[8]. In the degradation of heparan sulfate proteoglycans and the formation of short, functional heparan sulfate chains may need multiple heparanase enzymes. Heparanases are family of mammalian endoglycosidases which cleave HSPGs from proteoglycan core proteins and further degrade them into shorter chains. The latent heparanase is thought to act primarily outside the cell and bind the heparan sulfate to transfer into the cell by endocytosis[9, 10]. Next, the heparanase will active in the endosome to cleave the HS chains to 5~7 kDa pieces and then transfer to lysosomes. Finally, the short fragments of HS chain will be catalyzed by a series of hydrolyases to undergrade step-wise degradation, and the residues will return to the cycle of metabolism. Therefore, the heparan sulfate will accumulate because of the loss-function IDS in the MPS II patients (Figure 1A.2).

doi:10.6844/NCKU201900656

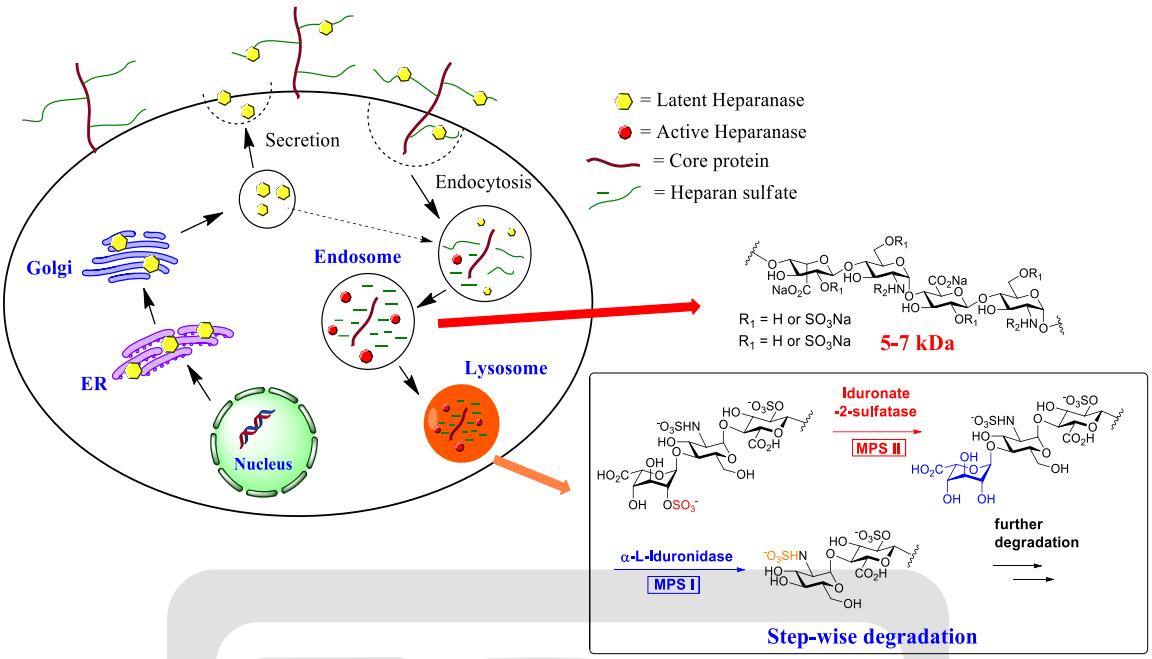

Figure 1A. 2 Degradation of heparan sulfate

1A.1.4. The characterization of iduronate-2-sulfatase

Recently, the X-ray crystal of human iduronate-2-sulfatase has been reported with a sulfate ion bond covalently in the active site[11]. According to those results, the residual amino acids nearby active site can be observed. There are some of the basic side chains which have positive charge can play important roles in catalysis, making direct contact with the hydroxyl group. And the divalent metal ion, Ca^{2+}, is essential for the stability of the active site and sulfate-ester (Figure 1A.3).

Additionally, the docking results between IDS and 2-O-sulfo-α-L-iduronic acid were investigated recently. The 2S-IdoA monosaccharide form additional hydrogen bonds to R273, N167, Y348, K479 and have low energy in $^4C_1$ conformation (Figure 1A.4), though the population of conformer at the polysaccharides is $^1C_4$ more than $^4C_1$[12]. The mechanism of IDS is transesterification-elimination (TE)[13]. Cα-formylglycine (FGly) is a crucial amino acid result from the cysteine residue oxidation. FGly aldehyde-hydrate (FGH) is an intermediate which can perform an SN_2 nucleophilic attack on the sulfur atom to get the FGS

doi:10.6844/NCKU201900656

adduct. And then FGS will eliminate the bound sulfate and return to the FGly aldehyde (Figure 1A.5).

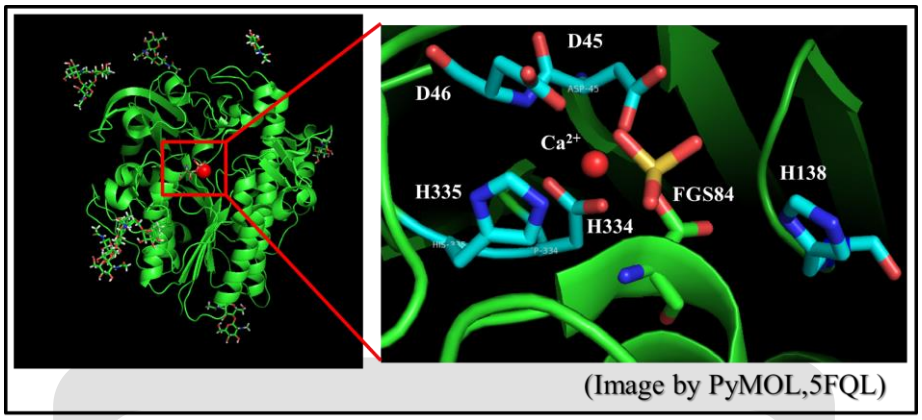

Figure 1A. 3 A simulated image of iduronate-2-sulfatase

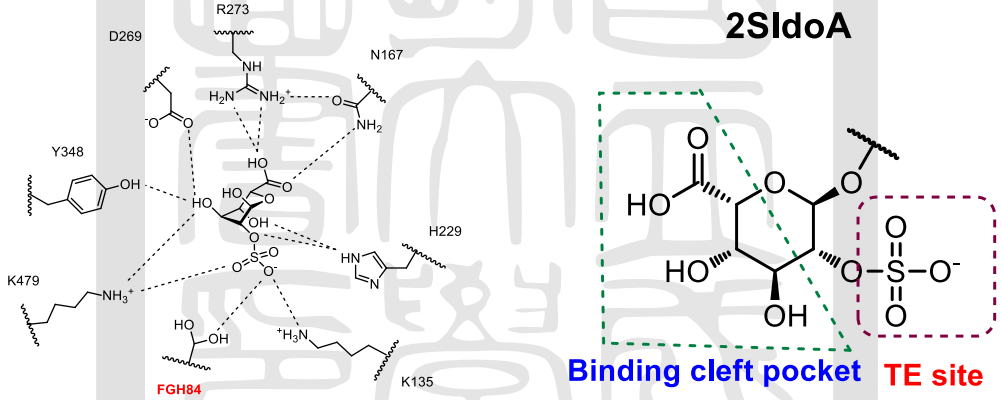

Figure 1A. 4 The active site interaction between IDS and 2-O-sulfo-α-L-iduronic acid

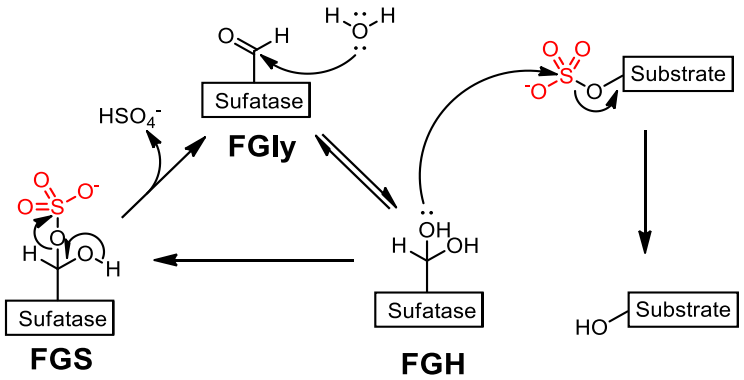

Figure 1A. 5 Mechanism of FGly-mediated sulfate ester hydrolysis

doi:10.6844/NCKU201900656

1A.1.5. Treatments of Mucopolysaccharidosis type II

Mucopolysaccharidosis type II (MPS II, OMIM # 309900), or Hunter syndrome, is an X-linked lysosomal storage disease caused by a genetic deficiency of the enzyme iduronate-2-sulfatase (IDS), required for the step-wise degradation and recycling of complex glycosaminoglycans (GAGs). Loss of IDS activity results in abnormal accumulation of GAGs (i.e., HS and DS) in multiple tissues and organs, following by progressive cellular and multi-organ dysfunction[14]. The enzyme replacement therapy (ERT) is one of the treatments for MPS II patients. Elaprase® (Idursulfase), a recombinant human IDS for ERT was approved in the United States in 2006 and Europe in 2007[15, 16]. This drug is the most expensive medical treatments at the present time, which cost ten million NTD per year for one patient out today. The delivery of the enzyme is through mannose-6-receptor pathways[17], and these receptors also expressed into the cell membrane (Figure 1A.6). Therefore, the enzyme follows the route of endocytosis to be carried to the lysosome and play a role. In contrast to the natural continuous enzyme production, the infusion of recombinant enzymes act as a bolus as it is distributed and eliminated immediately after the infusion stops. On the other hand, this implies the need for weekly (MPS) or biweekly (other LSDs) infusions[18]. Because of the limitation of ERT, different therapies are developing to overcome the negative effects of enzyme deficiency[19, 20]. In the clinical trial of MPS II, a gene therapy called SB-913 is a ZFN-mediated in *vivo* human genome editing to let the patient provide IDS from liver continuously to treat MPS II[21]. However, this ZFN-based genome editing therapy for MPS II shows the unfavorable result in a clinical trial of phase I/II.

doi:10.6844/NCKU201900656

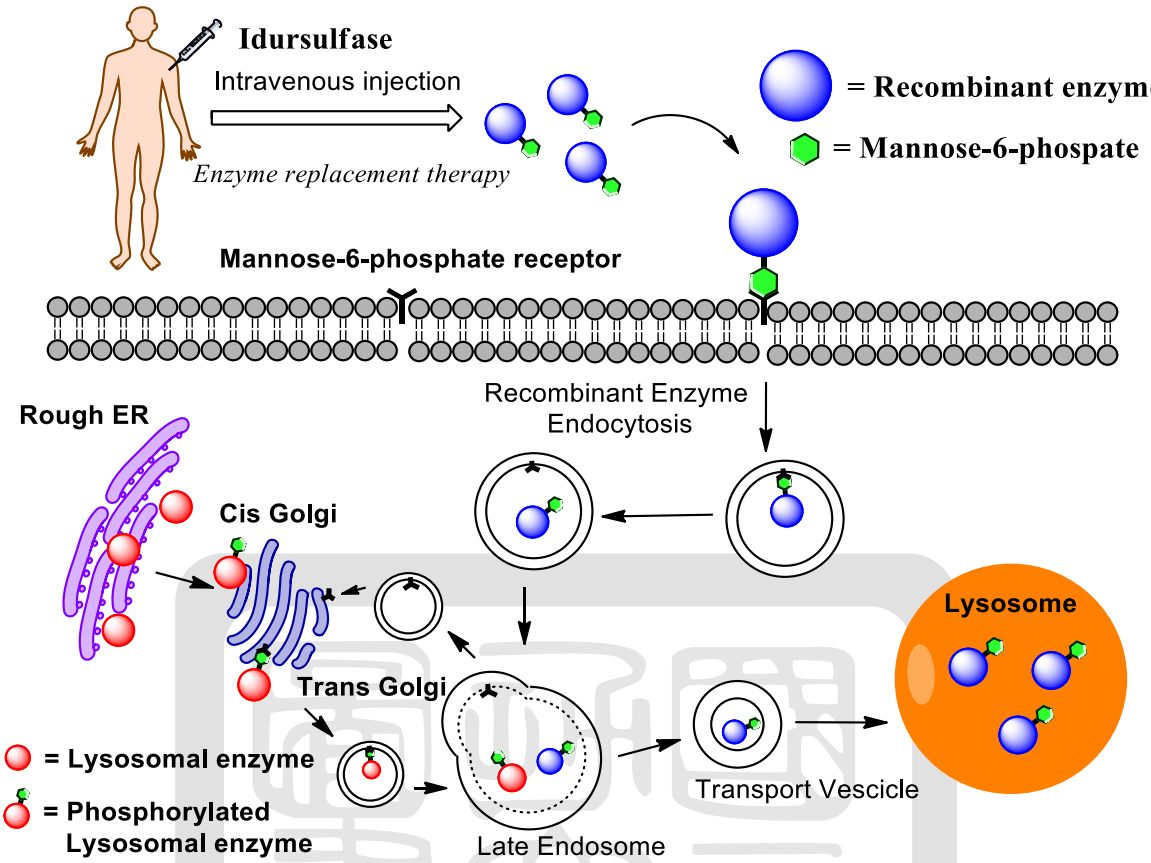

Figure 1A. 6 Lysosomal recombinant iduronate-2-sulfatase transport

1A.1.6 Chaperone and Stabilizer

LSDs, caused by the missense mutation of gene sequence, which leads to the expressed protein misfolding and loss-of-function. There is a novel approach to treat the misfolding protein diseases called small molecule pharmacological chaperones (PC) therapy[22]. Such small molecule as the PC can interact with the mutant protein to enhance the stability and recover the misfolding protein to the correct conformation[23, 24]. Therefore, the small molecule chaperone has the potency to rescue the mutant protein and prevent degradation in the human body (Figure 1A.7).

Pharmacological chaperone (PC) therapy has been investigated as a potential treatment for several LSDs, including Fabry[25-28], Gaucher[29], GM1-gangliosidosis[30], and Pompe diseases[31] caused by missense mutations. Currently, the therapy for Fabry disease was

doi:10.6844/NCKU201900656

approved by the European Medicines Agency in 2016[32].

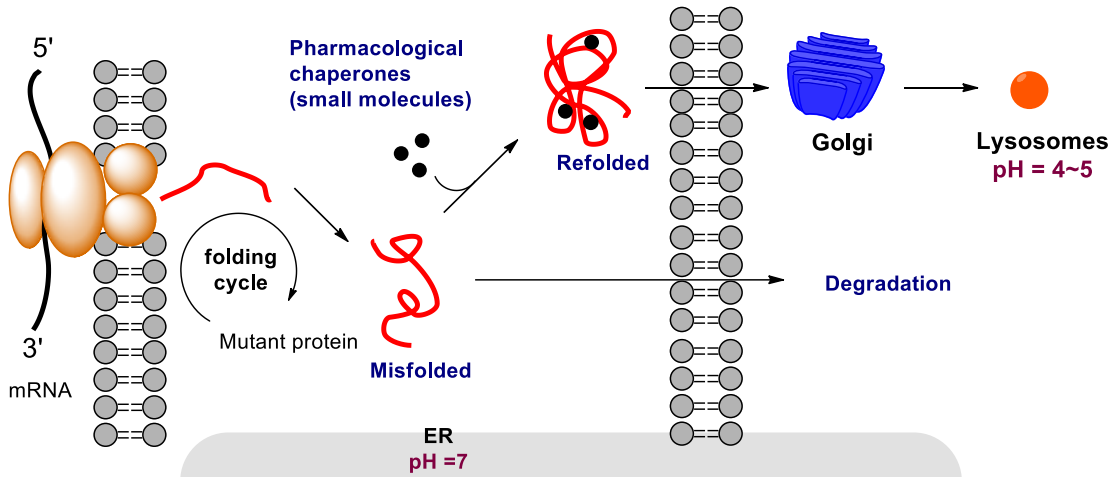

Figure 1A. 7 A proposed mechanism of pharmacological chaperones

Recently, the potential pharmacological chaperone for MPS II was reported by *Y.shimada et al*., that the **D2S0**, a sulfated disaccharide derived from heparin can attenuate the thermal degeneration of the recombinant human IDS (rhIDS) *in vitro*[33] . Also, **D2S0** improved the enzyme activity of IDS mutants derived from different mutations in the cell-based assay. D2S0 is produced by the bacterial heparinase from heparin. The structure of D2S0 is Δ-unsaturated 2-sulfouronic acid-N-sulfoglucosamine, which has a similar structure with the natural substrate of IDS[34](Figure 1A.8). The function of heparinase is cleaving the non-reducing end and generate a double bond between C4 and C5 in sugar acids such as IdoA and GlcA. It is known that the chaperone compounds for LSDs are substrate analogs and act as competitive inhibitors in a dose-dependent manner. In the inhibition study, the **D2S0** is competing with the artificial substrate and bind directly to IDS, which is similar to chaperone compounds for other LSDs.

doi:10.6844/NCKU201900656

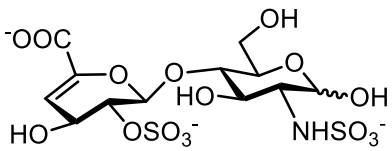

D2S0

Figure 1A. 8 The structure of D2S0 derived from heparin

Different from the PC, the strategy of the enzyme stabilizer is to enhance the stability of the enzyme. Because the recombinant enzyme in ERT is highly expensive and inherently unstable, it's an important issue to create enzyme stabilizer to prolong the half-time of enzyme drug in the patient's circulatory system[28] (Figure 1A.9).

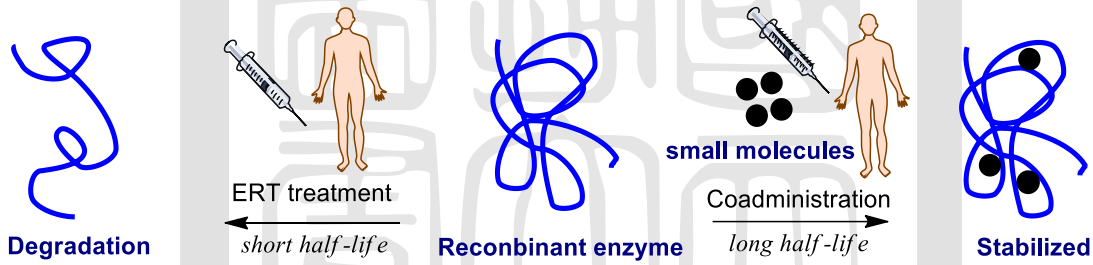

Figure 1A. 9 The strategy of enzyme drug stabilizers

MPS II can be treated by enzyme replacement therapy (ERT). Recombinant human Iduronate-2 sulfatase (rhIDS) is injected into the patient, after which it will be transported into cells through endocytosis, eventually reducing accumulated substrates, and alleviating clinical symptoms. But rhIDS is prodigiously expensive and inherently unstable, and its administration constitutes a significant hardship to the patient, involving intravenous infusions, usually once every two weeks, for life. One possible approach towards enzyme stabilization is through the use of reversible inhibitors, especially competitive inhibitors, because their binding affinity can maintain protein folding. Recently, the application of this concept to stabilize enzymes implicated in LSDs was explored. For example, 1-

doi:10.6844/NCKU201900656

deoxynojirimycin (DNJ), a naturally occurring inhibitor of various α-glucosidases, was found to improve the enzyme stability of Myozyme, a recombinant human α-glucosidase for the ERT treatment of Pompe disease[35, 36], and another well-known piperidine, 1-deoxygalactonojirimycin (DGJ), was found to increase the physical stability of recombinant human α-galactosidase in *vitro*[37].

1A.1.7. The fluorimetric enzyme assay for IDS

The artificial substrate, 4-Methylumbelliferyl-α-iduronate-2-sulfate (4MU-2SIdoA), is a specific substrate for IDS to characterize the enzyme activity or the study of inhibitor. This fluorimetric enzyme assay is also a common method for the diagnosis of MPS II by using dried blood spots and patient cell[38-40]. In the principle of the fluorimetric enzyme assay, the 4-Methylumbelliferone needed to be cleaved the glycosidic linkages from the sugar and read out the fluorescence in the basic solution. Two enzymes are required to liberate the 4MU from 4MU-2SIdoA sequentially. In the first, the action of desulfation by IDS to form the 4-Methylumbelliferyl-α-iduronide (4MU-IdoA), which is the artificial substrate for α-iduronidase. The hydrolysis of 4MU-IdoA by IDUA is the second step in the reaction of IDS treated 4MU-2SIdoA, so the excess of IDUA is needed to liberate the 4MU from the 4MU-IdoA completely (Figure 1A.10). Though the fluorimetric enzyme assay is a regular approach in the evaluation of the enzyme activity of IDS, there are some factors needed to be concerned, such as couple enzyme involved and time consuming.

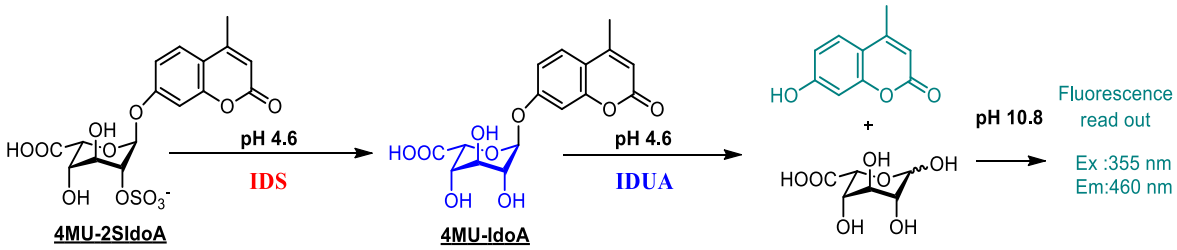

Figure 1A. 10 The principle of fluorometric enzyme assay by artificial substrate

doi:10.6844/NCKU201900656

1A.1.8 Motivation

In our previous work, some enzyme-based assay platforms toward glycolipids-related disorders, such as Fabry disease[26, 28] and Gaucher disease[27], have been developed. With the assistance of these assays, the new small molecule-based chemical chaperones or enzyme stabilizers have been successfully discovered. In our recent study, we also successfully developed the non-cleavable substrate-based small molecule in our enzyme activity study toward the potential treatment of MPS I as the first example in this research field[41].

Herein, we would like to establish various key analytical platforms toward MPS II to evaluate the characteristic of IDS in the enzyme-based and cell-based assays for small molecule screening (Figure1A.11).

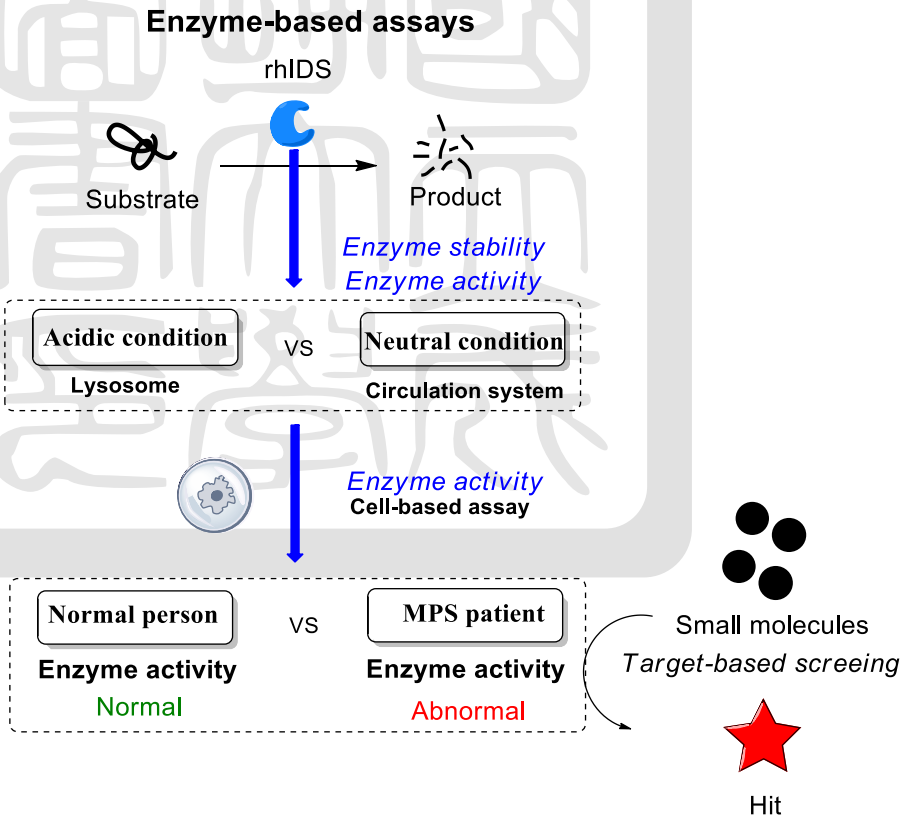

Figure 1A. 11 The aims of enzyme-based assay

doi:10.6844/NCKU201900656

1A.2. Results and discussions

1A.2.1 The initial enzyme-based assay

Generally, the enzyme-based assay for IDS activity is common to use in the various studies and experiments such as the enzyme kinetic assay, enzyme stability, and enzyme inhibition. In recent studies, the potential chaperone for IDS was sieved out by the enzyme thermal stability assay and enzyme inhibition assay. The enzyme activity of IDS was depicted by 4MU substrate assay include 4MU-2SIdoA. At first, the enzyme kinetic of IDS was tested to understanding the information of the K_m of rhIDS was 0.406 ± 0.193 mM, and the followed reference[40] shows that the K_m from leukocytes and fibroblasts was 0.6 mM (Figure 1A.12).

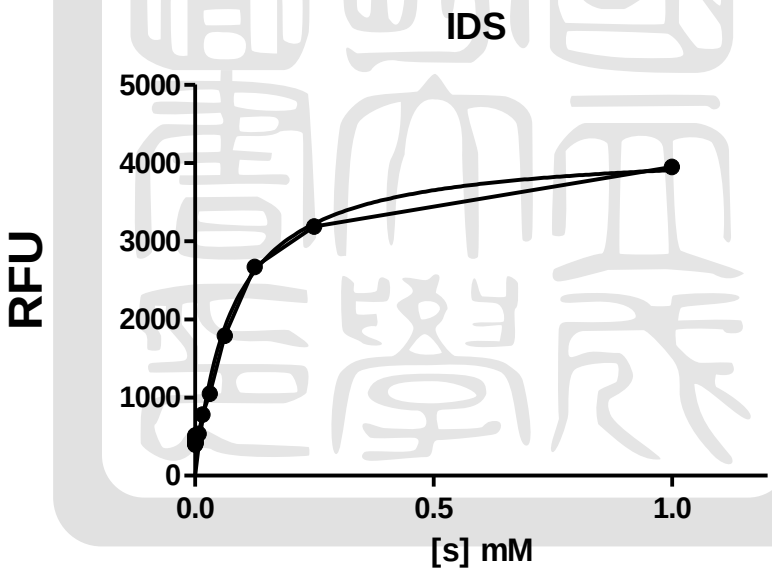

Figure 1A. 12 The enzyme kinetic of IDS by Michaelis-Menten equation

doi:10.6844/NCKU201900656

A thermal shift assay is a common approach to evaluate the protein conformational and colloidal stability in biopharmaceutical development. The conformational stability is determined by the protein melting temperature (T_m), which defined as the temperature at the half of protein is in the unfolded state. This method is available to be a useful tool for high-throughput screening to serve out the potential candidates in the first step, because of (1) low sample volume requirement (2) high sample throughput, (3) ease of preparation (4) rapid analysis[42]. Therefore, the suitable fluorescent dye is an important role to measure the change in fluorescence intensity as a function of temperature. 4-(4-(dimethylamino)styryl)-Nmethylpyridinium iodide (DASPMI)[43] is a fluorescent molecular rotor dye for use with differential scanning fluorimetry (DSF), which is reported to decrease the background interference from surfactants to modify the determination of T_m and other characterization. The most commonly used fluorescent dye, SYPRO orange is a polarity-sensitive dye for DSF measurements, but the extensive background interference from surfactants will obscure the determination of a T_m and other characterization (Figure 1A.13).

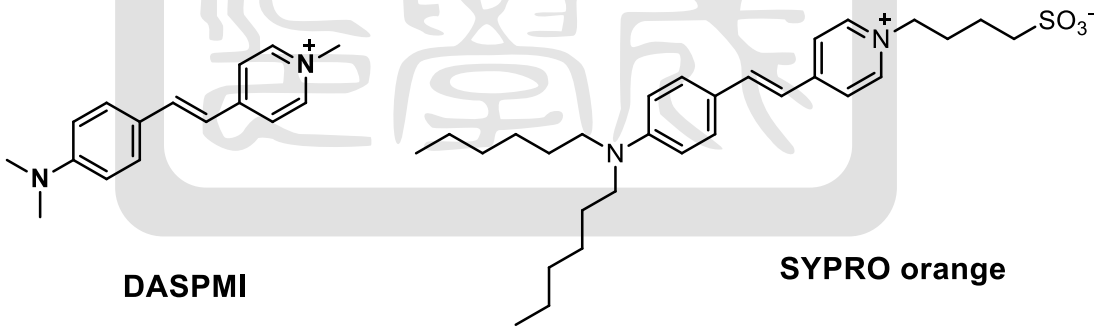

Figure 1A. 13 The fluorescent molecular rotor dyes used in the thermal shift assay

doi:10.6844/NCKU201900656

The concept of thermal shift assay is that the enzyme will denature by heating, and *Tm* presents the stability of the enzyme in such conditions. If the small molecule binds to the enzyme, the enzyme melting temperature will shift to higher or lower. The small molecules with increasing *Tm* are considered to be a candidate of enzyme stabilizers which stabilize the enzyme in unfavorable condition (Figure 1A.14).

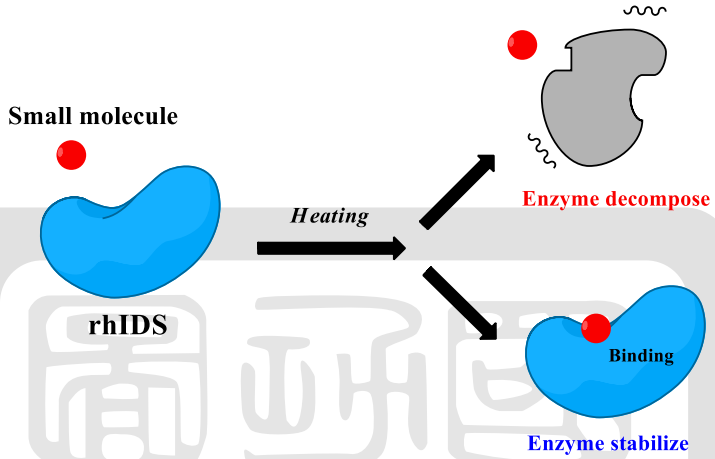

Figure 1A. 14 The concept of thermal shift assay

The endogenous IDS is work at the lysosome in the pH 4.6, but the exogenous rhIDS, the commercial protein drug, exposed in the neutral pH condition and transported through the circulation system by intravenous injection. To calculate *Tm* in the thermal shift assay, rhIDS was incubated in the pH 4.6, pH 7.4, pH 8.5 buffer and heated to the 90°C to calculate the *Tm* by the thermal shift assay. The different fluorescent dyes would be tested to qualify the condition for thermal shift assay. In our results, DASPMI was not suitable for rhIDS to measurement (See the Appendix), but the *Tm* of rhIDS could be calculated by SYPRO orange in the different pH values. The results showed the rhIDS had lower Tm in the neutral condition, which presented this enzyme was unstable in the human circulation system.

Conversely, rhIDS was more stable in the acidic condition, which determined the function was maintained in the lysosome. Besides, the IDS was quite unstable in the basic condition. In our results, we successfully found the qualified fluorescent dye to characterize

doi:10.6844/NCKU201900656

the stability of rhIDS in the different pH values, and further determined the protein drug would expose to the unfavorable environment during the transportation

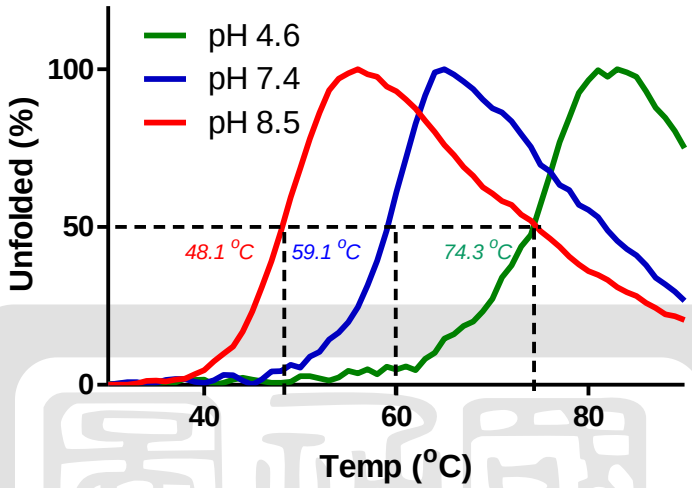

Figure 1A. 15 The Tm of IDS in the various pH conditions in thermal shift assay by SYPRO orange

For the high-throughput screening, thermal shift assay was an initial assay to the recognition of the enzyme stability treated the small molecules before and after. Also, the enzyme activity is crucial information for the characterization of the small molecule treatments. Furthermore, the heat-induced denaturation assay was designed for understanding the residual enzyme activity incubated in high temperatures by the fluorimetric enzyme assay[40, 44]. A heat-induced denaturation assay was performed by treatment of pH 4.6 or 7.0 buffer with rhIDS at various temperature for the time-dependent to evaluate the enzyme activity (Figure 1A.16). Due to the neutral buffer is an unfavorable condition for the hydrolysis of the substrate, 4-Methylumbelliferyl-α-iduronate-2-sulfate (4MU-2SIdoA), the higher concentration of rhIDS was needed for incubation. At the end of the experiment, the high concentration of rhIDS would dilute by the appropriate buffer for the hydrolysis of 4MU-2SIdoA into the highly fluorescent product 4MU. From our results,

doi:10.6844/NCKU201900656

the enzyme activity of rhIDS incubated in the natural condition was loss quickly at a short time, and the enzyme activity was almost disappeared in the 60 min incubation. By contrast, the rhIDS incubated in the acidic condition was maintained in half of the enzyme activity. In the heat-induced denaturation assay, we chose the modified parameter of temperature was 60°C, which was the appropriate window to observe the changing after the small molecules treatments. Thus, the condition was determined in our enzyme-based assay, and the results indicated rhIDS was unstable at the neutral condition, whatever the conformation and activity of the enzyme.

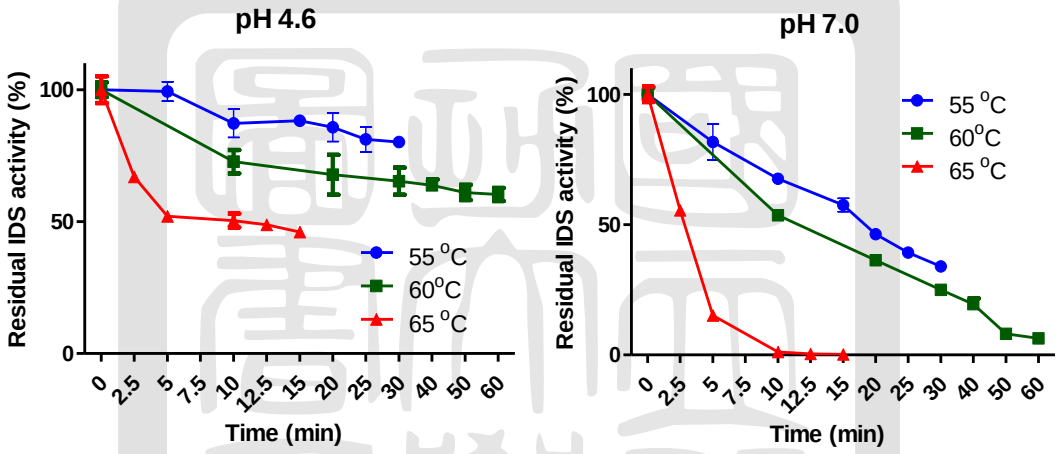

Figure 1A. 16 The residual enzyme activity of rhIDS by heat-induced denaturation in time-dependent and different pH values

Not only the thermal shift assay shows the rhIDS was unstable at neutral condition but also the heat-induced denaturation assay indicates that the enzyme activity of IDS decreases quickly at a short time in the nutrual buffer. However, the rhIDS had a lower elimination half-life compared with other enzyme drugs approved in ERT in clinical pharmacokinetic studies (See the Table in Appendix). Thus, we established the enzyme-based assay platform include the thermal shift assay for a small molecule as the enzyme binder to stabilize the conformation and the heat-induced denaturation assay which can

doi:10.6844/NCKU201900656

correspond to the result of thermal shift assay to understand the residual enzyme activity treated by small molecule in the unsuitable condition. We hope these assay platforms can be used in the screening of small molecule libraries to find the potential hits to be the enzyme stabilizers of rhIDS and characterize the further property in the cell-based assay.

1A.2.2. Enzyme activity of cell-based assay

Followed the concept of the enzyme-based assay, we attempted to understand the enzyme activity of endogenous IDS in the normal fibroblast and the severe types of MPS II fibroblast. In the experimental design, the first step was to lyse the cells by the different lysis buffer to release the enzyme out and treat by the 4MU-substrate to readout the fluorescence. The lysis buffer in the neutral condition called RIPA buffer (50 mM Tris-HCl, 50 mM NaCl, pH 7.4, containing 0.1% Triton X-100) was commonly used for cell lysis. On the other hand, the sodium acetate buffer (0.1 M sodium acetate, pH 4.6, containing 0.1% Triton X-100) is used to be the appropriate condition of IDS for the cell lysis. The cell line of normal fibroblast was C-015, friendly assistance from Taipei Veterans General Hospital, and the cell line of severe types of MPS II patient fibroblast purchased from Coriell® (GM00615).

doi:10.6844/NCKU201900656

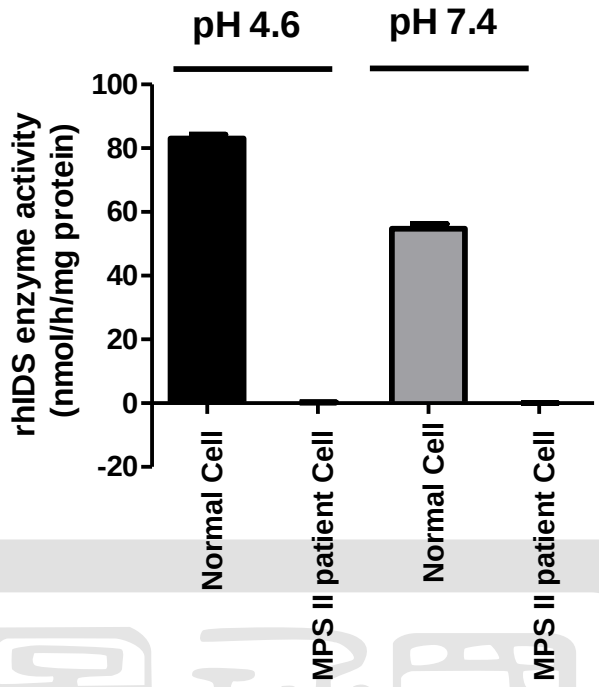

Figure 1A. 17 The enzyme activity of endogenous IDS of normal and patient fibroblast

The result shows the enzyme activity of endogenous IDS is almost none in the severe type of MPS II patient fibroblast whatever buffer was used. Furthermore, the enzyme activity of normal fibroblast in pH 4.6 buffer is 80%. When the endogenous IDS exposed in the neutral condition, the enzyme activity drops to 60%, prove that the IDS is unstable in the pH 7.0 condition of the cell-based assay (Figure 1A .17). Therefore, we choose the sodium acetate buffer in pH 4.6 as the lysis buffer to apply in the cell-based assay.

With the evaluation of enzyme activity in the cell-based assay, we attempted to design the assay platform for small molecule co-treatment with the rhIDS. Thus, the rhIDS was added in the medium to incubate with the MPS II patient fibroblast for 24 h at 37°C. At the end of the experiment, the medium washed by PBS twice to remove the extra residual rhIDS.

doi:10.6844/NCKU201900656

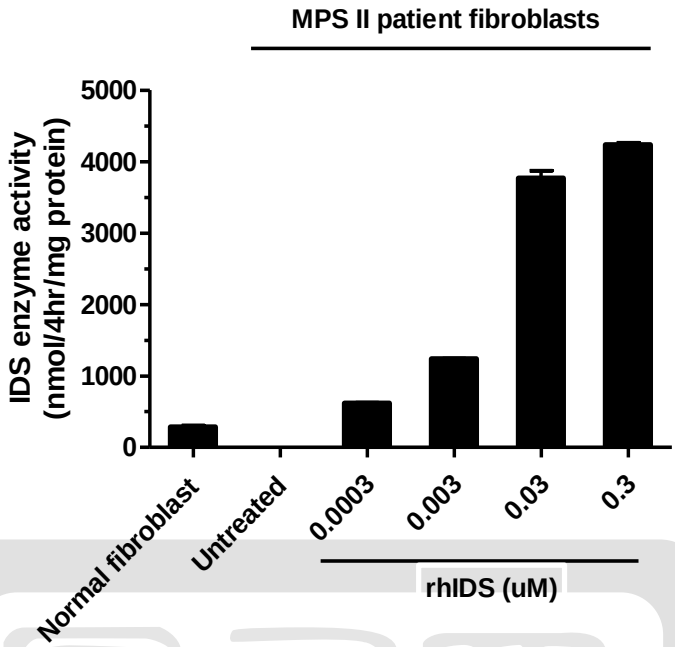

Figure 1A. 18 The enzyme activity of patient fibroblast treated by rhIDS

From the results, the enzyme activity of IDS in the MPS II patient fibroblast is enhanced by treated the rhIDS with dose-dependent (Figure 1A.18). Currently, the minimum concentration of rhIDS is 0.3 nM, which could improve the enzyme activity of MPS II patient fibroblast even higher than normal fibroblasts.

1A.2.3. Small molecule evaluation

With the enzyme-based and cell-based assay in hand, the interesting small molecule would be evaluated the property of potential hit. We tested the seven GAG-related compounds(Figure 1A. 19) as our preliminary small molecule pool in the inhibition studies against IDS. The data showed the **D2S6** and **D2S0** exhibit a high inhibition potency at 250 μM, and these two were chosen for further characterization. Next, the thermal shift assay was performed toward these two; unfortunately, no significant stability was observed (See the appendix). Although the results of the thermal shift assay did not show clearly beneficial, two further assays including cell-based chaperone assay and cell-based co-administration

doi:10.6844/NCKU201900656

assay were still carried out.

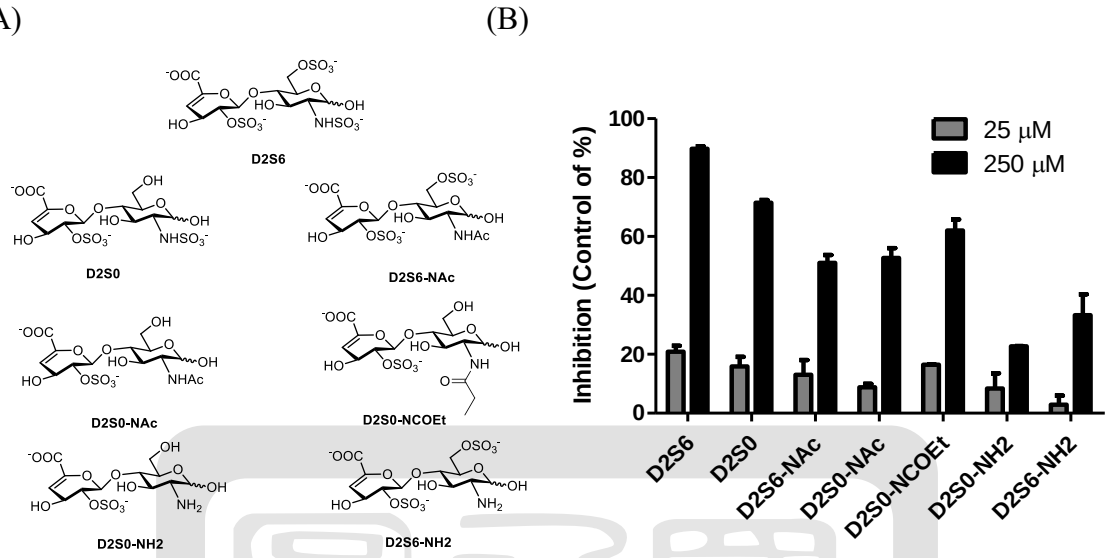

Figure 1A. 19 (A) The structure of seven disaccharides are purchased by Iduron® (B) The seven disaccharides and their inhibition activity at 25 or 250 μM against rhIDS

Notably, since **D2S0** has been reported as a chemical chaperone of the several mutants IDS in MPS II cells[33], we were interested to test its chaperoning activity toward our MPS II (a severe type, E521V) mutant cell line.

As shown in Figure 1A.20A, the results showed no chaperoning effect toward the MPS II E521V mutant fibroblast cell line. In our opinion, this severe mutant type can not be rescued by these two molecules, even other small molecules. On the other hand, the co-administration of the different concentrations of **D2S0** and **D2S6** disease to the medium and incubated with rhIDS in the MPS II patient fibroblast (E521V) for 24h at 37ºC (Figure 1A.20B). No promising co-administration result was obtained. The enzyme activity was inhibited by the treatment of **D2S6**, but the **D2S0** could slightly increase s the enzyme activity of rhIDS at the concentration of 0.03 μM.

doi:10.6844/NCKU201900656

(A) (B)

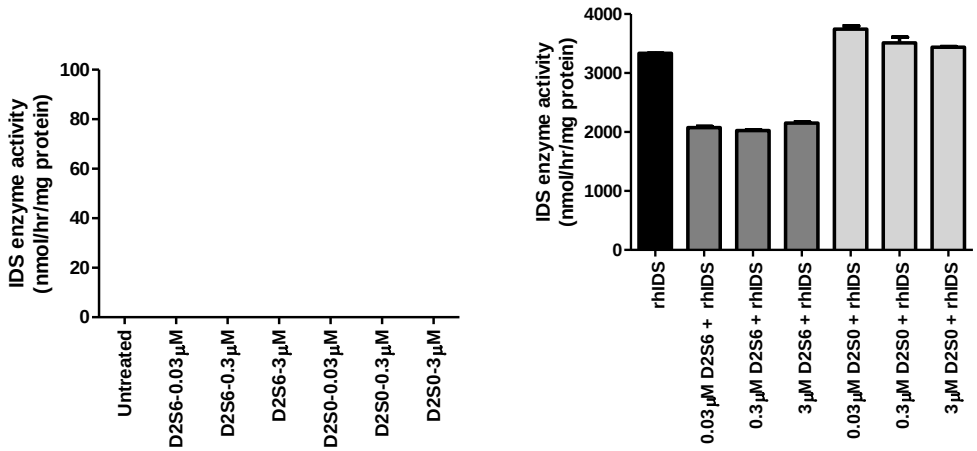

Figure 1A. 20 **C**haracterization of residual enzymatic activity of rhIDS in MPS II patient fibroblast. (A) The chaperoning effects were evaluated by single treatment of different concentrations of **D2S6** or **D2S0**, and the mutant type of severe patient fibroblast is E521V (B) The co-treated effects of 3 nM IDS and different concentrations o**f D2S6** or **D2S0** are treated in the patient fibroblast in 24 h

From our unexpected results of co-administration, we were curious whether they are the IDS substrates because structures of **D2S0** and **D2S6** are similar to the heparan sulfates and similar to the natural substrate. The results showed that the peak of **D0S6** (16.5 min) was observed when **D2S6** treated by IDS, and the ratio conversion was recognized obviously. On the other hand, the **D2S0** treated by IDS was also showed the peak of product, **D0S0** (13.9 min) corresponding to the standard, but the ratio of conversion was lower than **D2S6** treated by rhIDS (Figure 1A.21). Based on our HPLC results, the **D2S0** and **D2S6** could be the substrates of IDS, and the level of sulfation strongly affects the potency of IDS recognition. This finding inspires us for further small-molecule design in order to develop a non-cleavable scaffold bearing more negative charged moieties for developing new IDS enzyme stabilizers in the future.

doi:10.6844/NCKU201900656

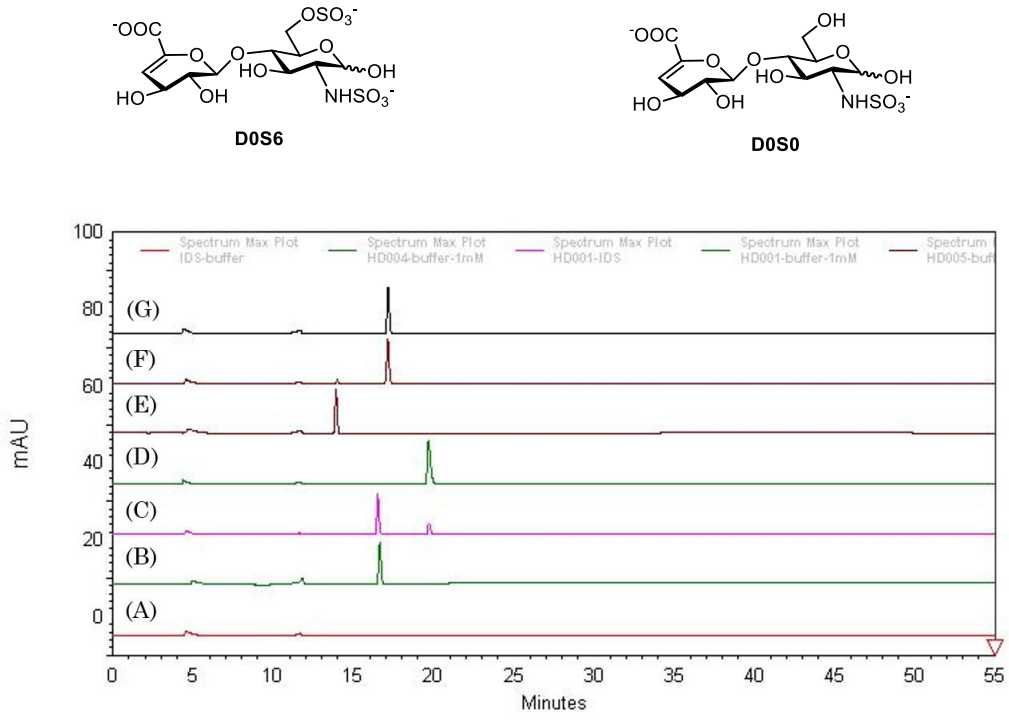

Figure 1A. 21 HPLC profile of four disaccharides in the reaction treated by rhIDS from the disaccharide standards. (A) Blank (B) **D0S6** standard (C) Mixture of **D2S6** treated by rhIDS (D) **D2S6** standard (E) **D0S0** standard (F) Mixture of **D2S0** treated by rhIDS (G) **D2S0** standard

1A.3 Sub-summary

In this work, we have established several key assay platforms including, (i) IDS enzyme inhibition assay, (ii) IDS thermal-shift assay, (iii) IDS heat-induced denaturation assay, (iv) cell-based chaperone assay, (v) cell-based co-administration assay. Among them, the assays (ii) and (v) are the first platforms applied in IDS According to the basic enzyme-based assay, we confirmed that rhIDS is unstable at the neutral condition by thermal shift assay and the enzyme activity of rhIDS dropped at the short term in the unsuitable condition by heat-induced denaturation assay. On the other hand, the enzyme activity of endogenous IDS from normal fibroblast decreased in the neutral condition, which simulated the human's circulation system. In the severe type of MPS II patient fibroblast, the enzyme activity of endogenous IDS almost disappeared, causing the large accumulation of substrate in the cell.

doi:10.6844/NCKU201900656

Moreover, the enzyme activity in the MPS II patient fibroblast enhanced by the rhIDS treatment. By characterization of enzyme activity in the cell-based assay, we attempted to evaluate the interesting molecule by the co-treatment with rhIDS in our assay platform for discovering the potential hits to be the enzyme stabilizer of rhIDS. The Δ-unsaturated disaccharide, **D2S0** derived from heparin reported to be a chaperone compound for mutant IDS in the cell-based assay. Therefore, we chose the **D2S6** and **D2S0** to evaluate the effect of stabilization by co-administration in the MPS II patient fibroblast. Unexpectedly, the results showed the enzyme activity is inhibited by **D2S6**, and the enzyme activity increased slightly by **D2S0** in the MPS II patient fibroblast by co-treatment with rhIDS. Thus, we curious about why the potential chaperone compound, **D2S0** showed the negative result of co-administration in the cell-based assay. Although the structures of **D2S0** and **D2S6** are similar to the natural substrate, there is no report to describe their possibility of acting as the substrate to affect the potency of enzyme stabilizer. Therefore, the **D2S0** and **D2S6** are treated by rhIDS, respectively, and the products of desulfation are observed by using HPLC-based assay. The results of co-administration with **D2S0** and **D2S6** were unfavorable, but the effort of assay establishment will provide the platform of evaluation for screening the potential enzyme stabilizers of rhIDS. Besides, through the evaluation of **D2S0** and **D2S6** by co-administration in the cell-based assay, the structures will be the reference for inspiration of the small-molecule design to develop the enzyme stabilizers of rhIDS in the future work.

doi:10.6844/NCKU201900656

Part B. Establish cell-based assays for metabolic processing toward the normal and MPS patient cell.

1B.1 Introduction

1B.1.1 GAGs as the biomarker of MPS

Mucopolysaccharidoses (MPS) is a subset of LSDs in which deficiencies occur in multiple enzymes involved in the degradation of glycosaminoglycans (GAGs)[45]. A family of at least 11 enzymes catalyzes the lysosomal degradation of GAGs, including several glycosidases and sulfatases, an acetyltransferase, and an enzyme required for generating the catalytically active form of all known sulfatases (Figure 1B.1). For example, the heparan sulfate is a glycan-based biomarker that has been used to characterize the animal models, tissue or urine of patients with MPS for diagnosis and monitoring therapy based on enzyme replacement therapy[46-48]. Actually, the heparan sulfate is a complex, linear polysaccharide composed of repeating disaccharide subunits of uronic acid, GlcA or IdoA, GlcN, and decorated by various patterns of sulfation. The largest challenges are analysis and quantification of the high molecular weight and a remarkable degree of structural heterogeneity. Therefore, the approaches of sample preparation of HS are enzymatic digestion[49, 50] and acid hydrolysis[51-53,] to release the specific repeating units, such as monosaccharide or disaccharide with low molecular weight to handle easier.

doi:10.6844/NCKU201900656

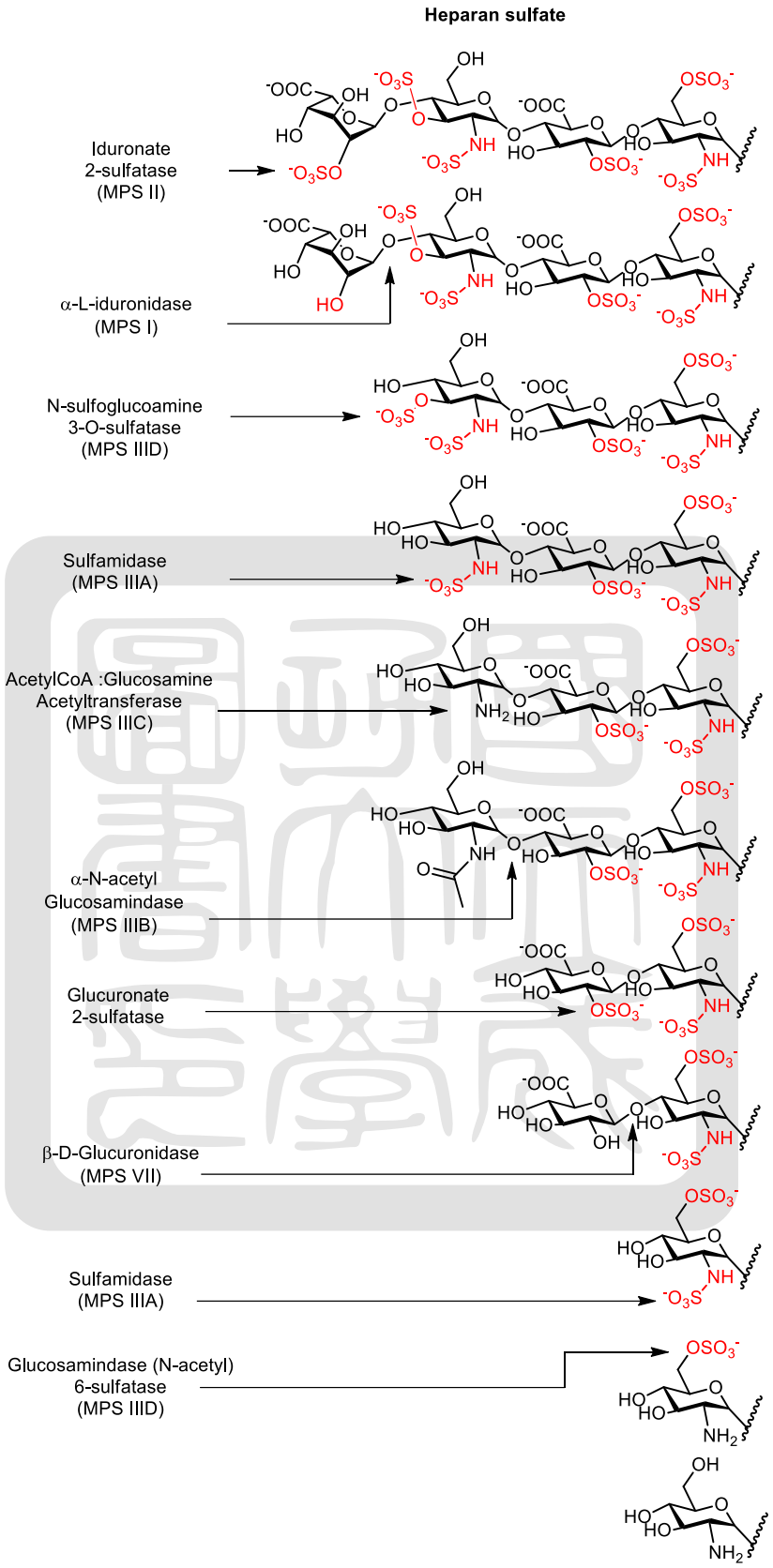

Figure 1B. 1 Glycosaminoglycan catabolism of heparan sulfate and the diseases correspond to the deficient lysosomal enzyme

doi:10.6844/NCKU201900656

1B.1.2 The assay platforms of GAGs detection by LC or LCMS/MS

Because of GAGs are long unbranched and negatively charged polysaccharides, the detention of GAGs is extremely challenging in the diagnosis of MPS. On the other hand, several assay platforms are developed to analyze the accumulated GAGs in the animal model, tissue or urine of MPS patients[51, 54-57]. In recent years, the LC or LCMS/MS technology was improved significantly to making it possible to measure different GAGs at the same time in smaller volumes of different biological matrices. The enzymatic digestion and chemical cleavage are the common methods to apply in the sample preparation of GAGs for LC or LCMS[58]. A simple method for methanolysis of GAGs is developed to analyze the urine and cerebrospinal fluid samples of MPS patients[54, 59, 60]. Thus, this method has been used in the initial screening test for MPS and also help the monitoring of the effectiveness of enzyme replacement therapy. Methanolysis can degrade the HS into simple desulfated and deacetylated repeating disaccharides (Figure 1B. 2), which is available to analyze by liquid chromatography/tandem mass spectrometry (LC-MS/MS).

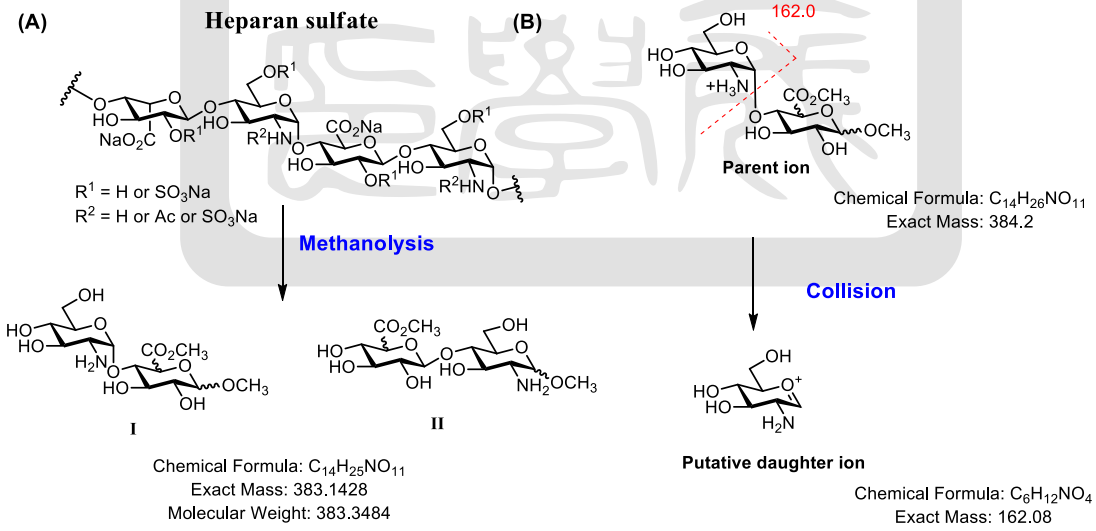

Figure 1B. 2 (A) Degradation by methanolysis of HS to get desulfated and methylated disaccharide (B) MS/MS of the major parent and putative daughter ion obtained from the methanolysis of HS

doi:10.6844/NCKU201900656

Through the methanolysis of HS, the complexity is greatly reduced to analyze the sample by MS/MS. However, the process of methanolysis will yield several isobaric and isomeric disaccharide products. The fragment of type I that the GlcN-(1,4)- uronic acid disaccharides are indicated to the major reaction products of HS methanolysis[61]. On the other hand, the fragment of type II as the minor disaccharides products are unknown in the identity of HS methanolysis.

Moreover, the novel assay platform used the liquid chromatography-tandem mass spectrometry to apply in the diagnosis of MPSs called Sensi-Pro assay[62, 63]. The HS is treated by bacterial heparin lyase to generate the disaccharides containing Δ4,5-unsaturated uronic and hexosamine containing a variable number of sulfate group. The method involves depolymerization of GAG chains to liberate the non-reducing end (NRE) carbohydrates and tag the aniline by reductive amination. For example, the specific biomarker of MPS II by lyase-generated is the NRE consisting of 2-sulfo-iduronic linked to N-sulfoglucosamine-6-sulfate (I2S6, m/z = 671) (Figure 1B.3). The concept is the MPS disorders resulting from a deficiency of sulfatase or glycosidase that act strictly at the NRE of the glycan; each LSDs should, in theory, give rise to a unique set of NRE structures, which define candidate biomarkers for each subclass of MPS.

doi:10.6844/NCKU201900656

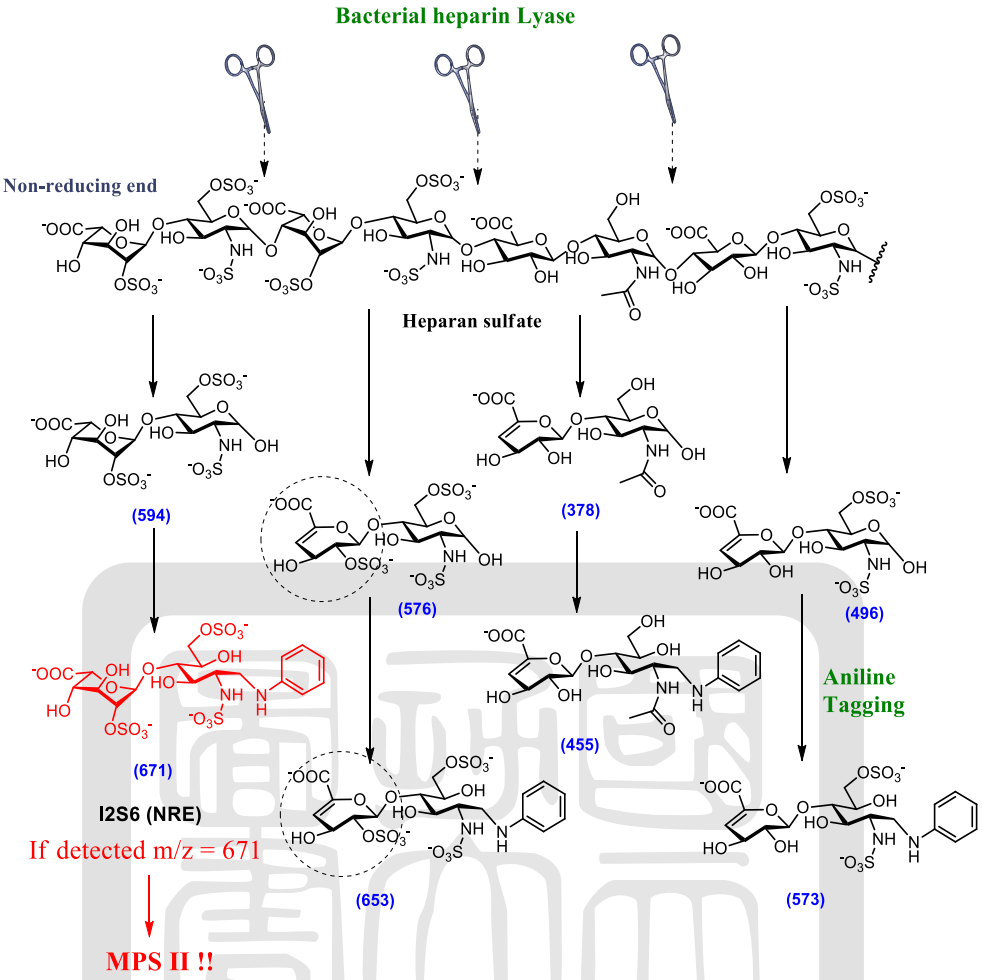

Figure 1B. 3 The concept of Sensi-Pro assay

Recently, a novel approach has been reported is called pathological iduronic acid assay[64] (PIA assay). This method is used in the study of the potential chaperone compound, **D2S0** to evaluate the improvement of accumulated GAGs in the patient fibroblasts by LCMS/MS[33]. The principle of PIA assay used iduronic acid to serve as the specific biomarker, which is liberated by the IDS and IDUA catalyze the accumulated GAGs. The chemical tag, *p*-aminobenzoic ethyl ester (ABEE) is used to enhance the sensitivity by reductive amination to detect the ABEE-labeled IdoA by the LC system (Figure 1B. 4). This method can quantify and monitor the metabolic processing of substrate accumulated in the bio-matrices of MPS II to develop the assay platform of the drug discovery toward chaperone therapy.

doi:10.6844/NCKU201900656

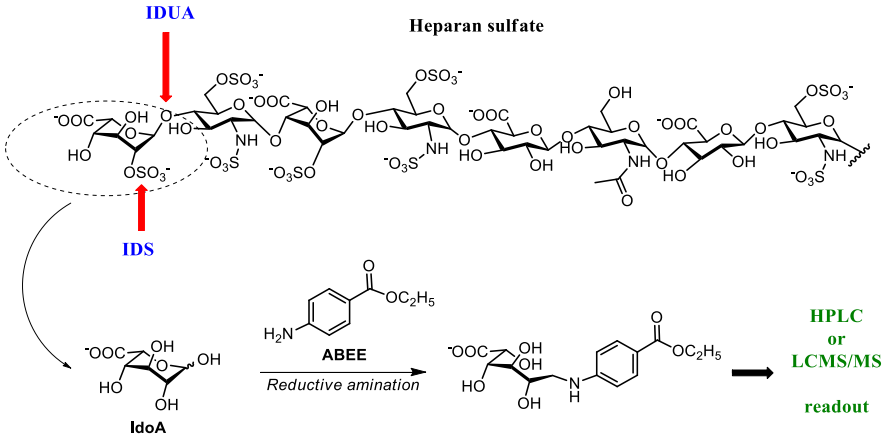

Figure 1B. 4 Development of the pathological iduronic acid assay for MPS II

1B.1.3 Derivatization of carbohydrates for analysis

Carbohydrates are the largest group of compounds found in nature, and the size diversity is the width of the monosaccharides to the large molecular polysaccharides. The analysis of carbohydrates is a large challenge for several reasons: the complexity of the isomeric structure about the monosaccharides (ring-opened or closed, different ring size and conformations), and the variation of the branch about the oligosaccharides, unlike the other common biopolymers[65, 66]. In the lack of chromophores or fluorophores to recognition, the detection of carbohydrates becomes difficult. Hence, many analytical approaches depend on the application of chemical modifications such as hydrolysis or derivative formation are investigated(Figure 1B. 5)[67].

doi:10.6844/NCKU201900656

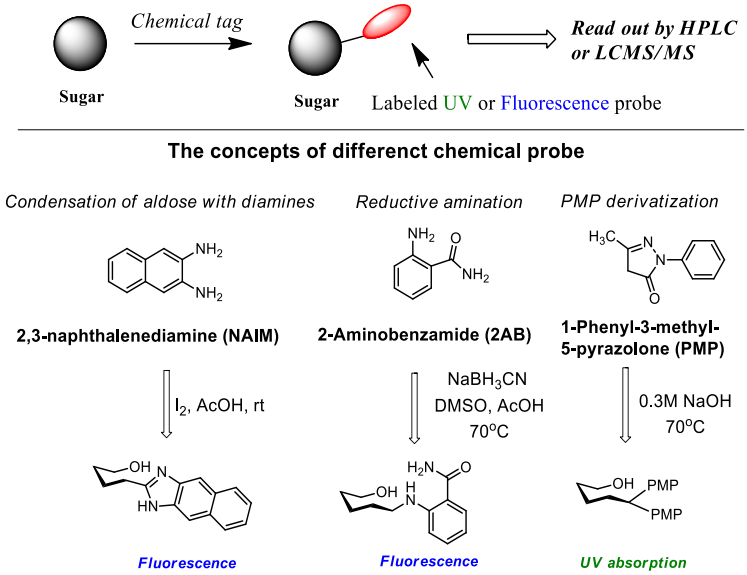

Figure 1B. 5 The derivatization of carbohydrates of different chemical tags

1B.1.4 Motivation

Up to date, most studies are applied for newborn screening, not for small molecule drug discovery. Besides, the current cell-based assay toward the GAG metabolic readout is still limited and not reliable. For example, dye-spectrometric methods are commonly used in the direct analysis of GAGs; dimethylmethylene blue (DMMB), which are the cationic dyes can interact with sulfated GAGs and result in an absorbance shift. However, the disadvantage of this assay is the certain false-negative results occur because of salt, protein concentration, or the buffer issue. Thus, more reliable metabolic approach toward MPS II for small molecule screening platform remains to be explored. Therefore, we attempt to find a suitable method, including the chemical tag and acid hydrolysis to develop the platform of the cell-based assay. Because of the important biomarker of GAGs, iduronic acid (IdoA) of the commercial product is too expensive to obtain in a large scale; the efficient synthesis route is used to the preparation of IdoA for derivatization by chemical tag. On the other hand, we were curious about the differentiation of levels of the accumulated GAGs in the MPS patient between the normal person in the cell-based assay. Herein, the specific aim of this part is to establish a

doi:10.6844/NCKU201900656

suitable method which is easily handled to evaluate the accumulated GAGs to distinguish the normal person and MPS patient in the cell-based assay (Figure 1B. 6).

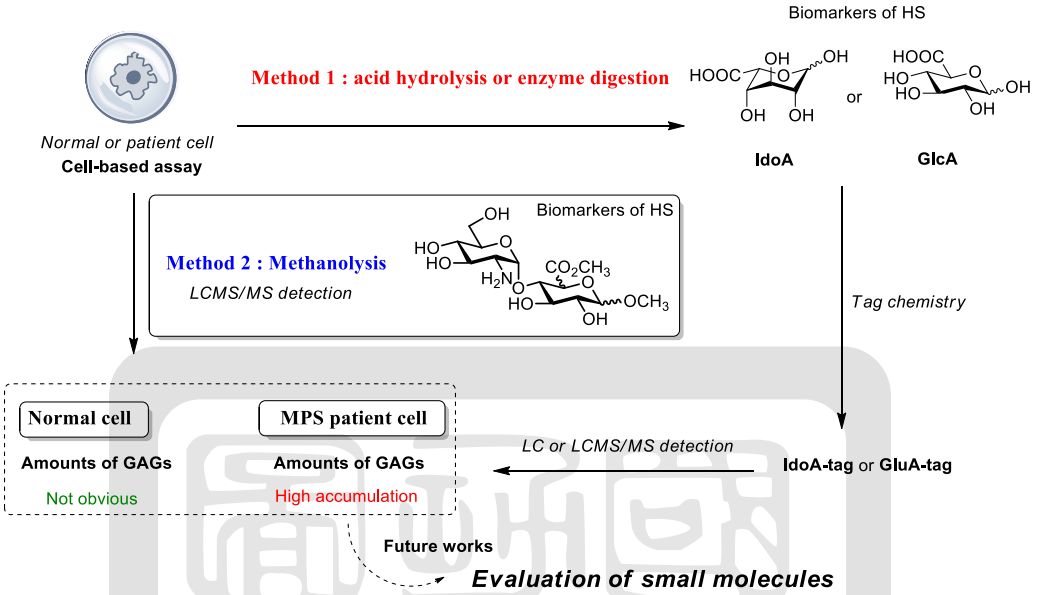

Figure 1B. 6 The concepts of differentiation in a cell-based assay

1B.2. Results and discussions

1B.2.1 Design

Our design was to develop a straightforward approach toward metabolic processing of accumulated GAGs to differentiate the cell lines of the patient and normal person. In the cell-based assay, the biggest challenge was the detective sensitivity of the biomarkers derived from GAGs corresponds to the amounts of cell numbers. Therefore, Method I utilized the acid hydrolysis or enzyme digestion to release the IdoA and GlcA as the key biomarkers of GAGs and the chemical tag is labeled to the monosaccharides to enhance the sensitivity to detect by LC or LCMS/MS (Scheme 1B.1). Due to the analysis of complexity in the cell-based assay, the standard compound is essential for the qualification and quantification of the labeled monosaccharides. Hence, the suitable chemical tag was selected by the model reaction and evaluated the convenience of operation to apply in the sample

doi:10.6844/NCKU201900656

preparation. Besides, the methods of cell sample pretreatment in Method I was also a factor to influence the efficiency of the sample preparation. Acid hydrolysis is a common approach to depolymerize the glycans to analyze the components of monosaccharides. However, the partial monosaccharides may be decomposed by the harsh condition to influence the accuracy of analysis, but the advantage is that it is much easier to operate for sample preparation (Scheme 1B.2). Another method of sample preparation is enzyme digestion, IDS, and IDUA can cleave the IdoA from the non-reducing end of GAGs. Although the enzyme digestion can release the specific biomarker of GAGs precisely, the extremely challenging is the sensitivity of the chemical tag. Besides, the more complicated protocol of sample preparation by enzyme digestion results in a decrease of operational convenience.

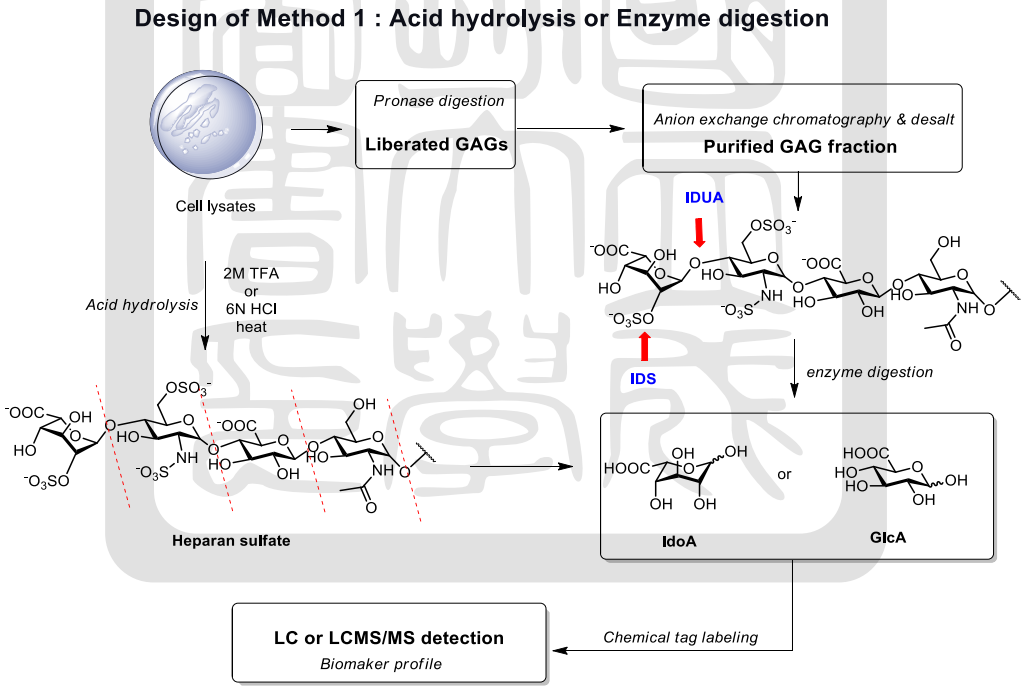

Scheme 1B. 1 The analytical approaches of Method I

At the same time, we also demonstrated the Method II of methanolysis in the analysis of GAGs in a cell-based assay. This approach is very convenient for the sample preparation, and the method of detection is highly sensitive by the LCMS/MS for the biomarker of GAGs. However, the disadvantage is lack of the authentic disaccharide standards to quantify the

doi:10.6844/NCKU201900656

GAGs at the MPS patient and normal person in a cell-based assay. Despite the well-known pros and cons of Method I and Method II, we decided to attempt both approaches to discuss the feasibility and efficiency of the assay platform establishment.

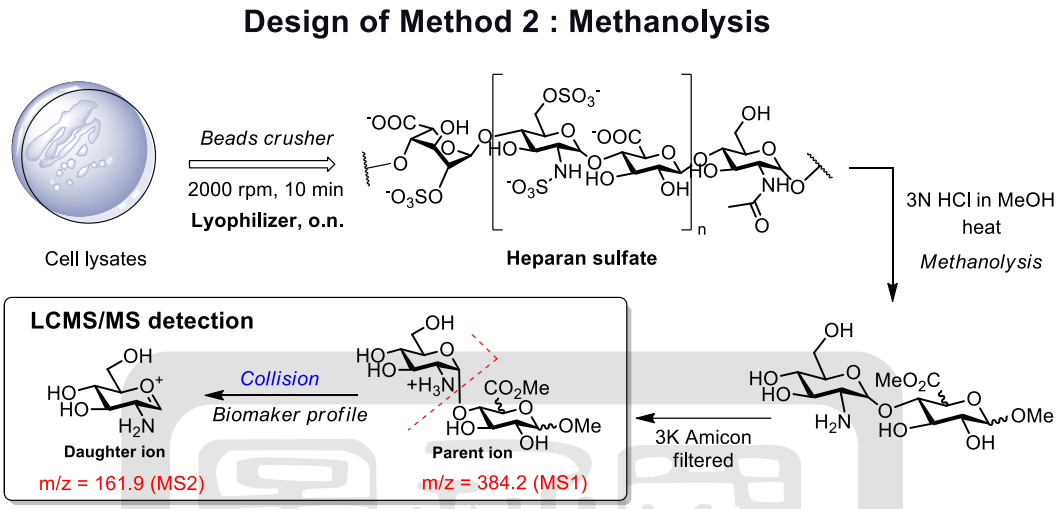

Scheme 1B. 2 The analytical approach of Method II

1B.2.2 Tag chemistry to enhancing the sensitivity

Followed the protocol of Method I, the essential labeled standards are needed at first to characterize the products in the cell sample. To understand the efficiency and the conversion of the tag chemistry, the GlcA was used in the model reaction to select the suitable chemical tag. At first, we used the 2,3-naphthalenediamine (NAIM) to test the model reaction (Scheme 1B.3), and the preparation of the condensation of aldoses with diamines followed the previous report[68].

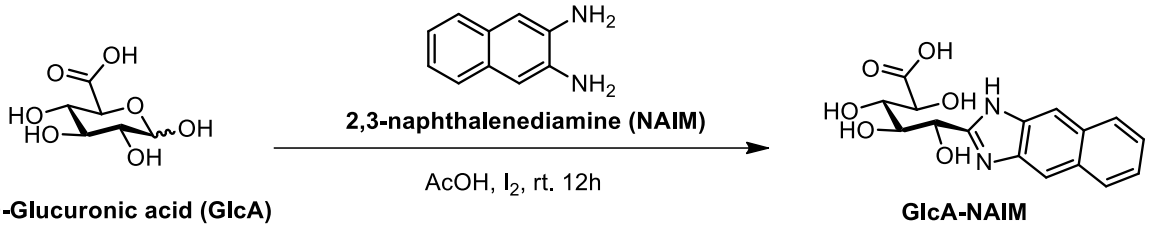

Scheme 1B. 3 The model reaction of NAIM by oxidative condensation

doi:10.6844/NCKU201900656

The speculated mechanism of the reaction initiated by the formation of a Schiff base (Intermediate **A** in Scheme 1B.4), followed by condensation of the aldose with one of the amino group in NAIM. The process of the formation of the Schiff base is reversible in the condensation of an aldehyde with the amine group. The acetic acid was chosen as a mild acidic solvent in this reaction for the Schiff base forming.

When the formation of aldo-imidazoles, the subsequent nucleophilic addition of the other amino group of NAIM undergo nucleophilic attack and produce the imidazoline intermediate **B**, which could be oxidized in the air or by iodine to obtain the product. Another pathway is the aldo-imidazole products would process the prior N-iodination of the imine moiety in Schiff base to form the intermediate **C**. The desired product would be produced by the subsequent elimination of HI molecule, which can be oxidized in air to regenerate iodine in the acetic acid media.

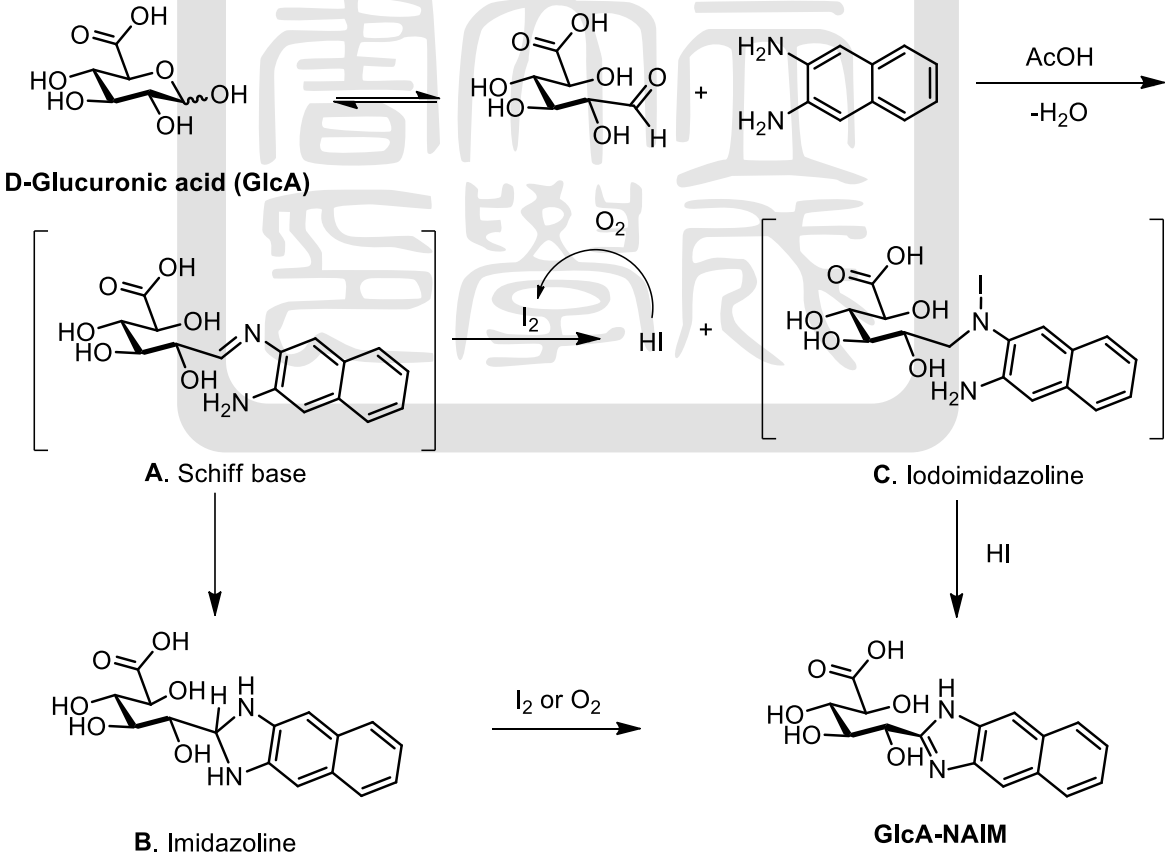

Scheme 1B. 4 Oxidative condensation of GlcA with NAIM by iodine mediated

doi:10.6844/NCKU201900656

We tested the oxidative condensation of GlcA with 2,3-naphthalenediamine using I_2 (0.1 equiv) as the promoter gave the negative results with difficult purification for the standard preparation. On the other hand, the acetic acid in the reaction was difficult to handle and remove in the sample for the subsequent analysis.

The other chemical tag called 2-Aminobenzamide (2AB) is used in the model reaction by reductive amination[69] (Scheme 1B.5**)**. The 2-Aminobenzamide (2AB) is a common fluorescence tag attached to reducing end of saccharides to apply in the analysis of glycan widely. Unfortunately, the product of GlcA-2AB was also difficult to purify because of the hydrophilic property. The results of the fluorescent tags, NAIM and 2AB were unfavorable chemical tag in the standards preparation, and the acetic acid is also involved in both reactions causing the processes of sample preparation would be inconvenient and complicated.

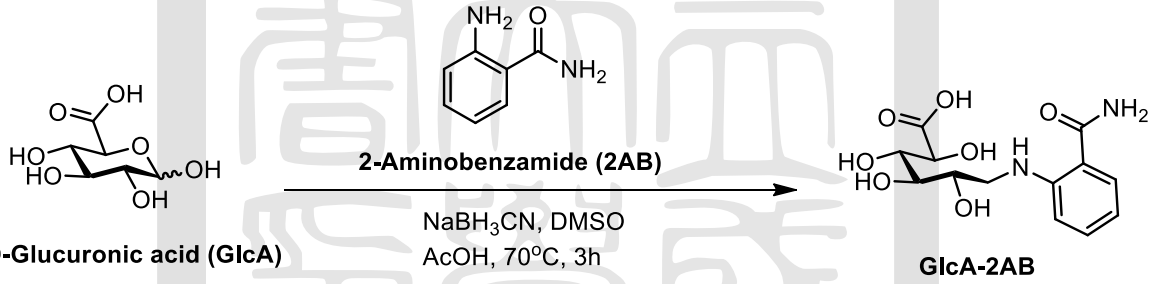

Scheme 1B. 5 The model reaction of 2AB by reductive amination

At this stage, we attempted to test the 1-phenyl-3-methyl-5-pyrazolone (PMP), which can yield the strongly UV-absorbing at 245 nm and available for extraction when the reaction completed. The procedure of PMP-derivatization followed the previously reported by *Honda et al.*[70], which is a simple method and results in few side products; no additional chromatographic step required. From the result of the model reaction, the PMP labeled glucuronic acid compound **1'** gave the yield 88% to be the reference for the other standard preparation (Scheme 1B.6).

doi:10.6844/NCKU201900656

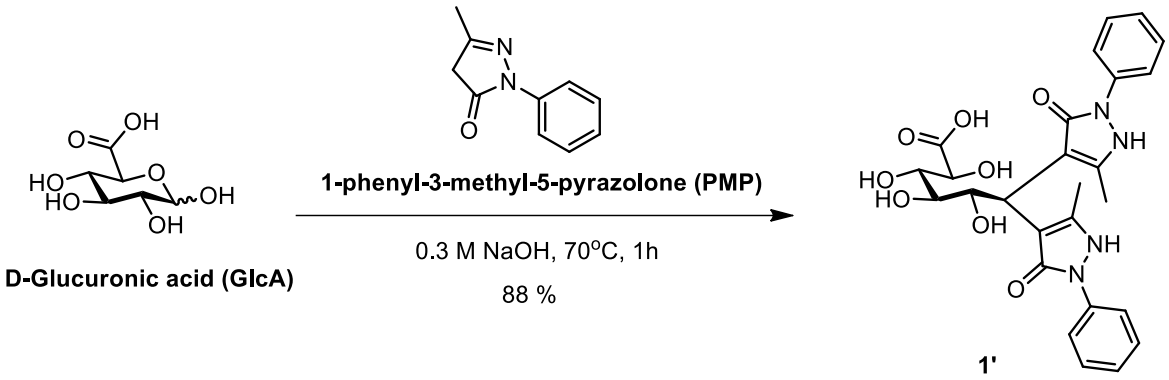

Mechanism

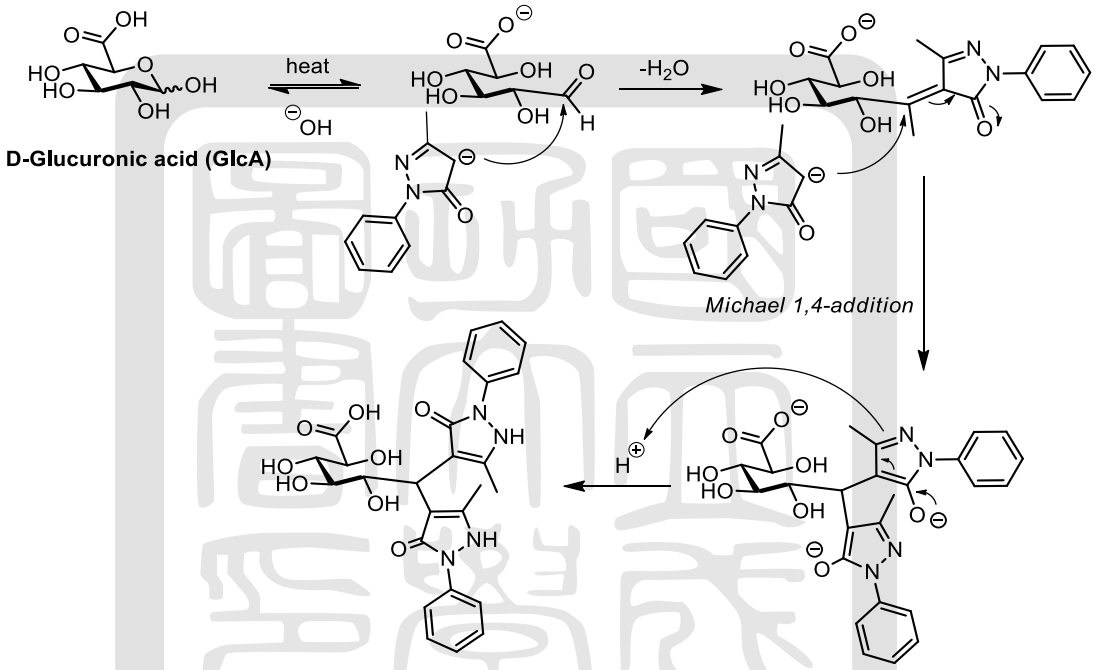

Scheme 1B. 6 The model reaction of PMP labeling

On the other hand, acid hydrolysis was one of the analytical approach in Method I; this approach would release the other monosaccharides include the glucosamine (GlcN) in the reaction. Besides, the xylose would be the internal standard to normalize the divergence of instrument responses and the operational error. To establish the assay platform and to profile the monosaccharides of GAGs by acid hydrolysis, the Xyl and GlcN are labeled by PMP to obtain the **2'**and **3'** for standard preparation (Figure 1B.7).

doi:10.6844/NCKU201900656

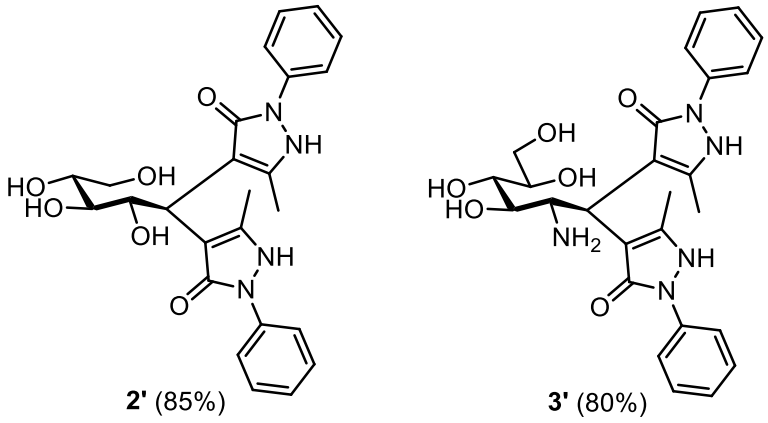

Figure 1B. 7 The yield of the several monosaccharides labeled by PMP

Next, the key biomarkers of GAGs, iduronic acid (IdoA) would be synthesized by the PMP labeling to act as the authentic standard for detecting in the cell-based assay. However, commercial IdoA is too expensive and to obtain on a large scale for standard preparation. Therefore, the IdoA was synthesized in-house via the efficiently synthetic route developed by the effort of the lab's members.

In previous work in our lab, the synthesis of the iduronic acid derivative was investigated when synthesizing the artificial substrate and the potential enzyme stabilizers of MPS I[41]. As shown in (Scheme 1B.7), L-idoA was prepared with D-glucuronolactone as a starting material, and the sodium hydroxide and methanol were used to induce ring-opened and form the structure of chair form. Next, the methanolysis mixtures followed by peracetylation gave a mixture of α- and β-anomers of **1**. Bromination of **1** at the C5 position under photo-induced radical conditions using N-bromosuccinimide gave **2** (70%). Next, **2** treated with tributyltin hydride and azobisisobutyronitrile (AIBN) under reflux THF, which gave a separable mixture of **3** and **1** (**3**/ **1** = 1/2) in 90% yield. Based on NMR analysis and literature reports, **3** was confirmed to be a $^{1}C_{4}$ conformer because of the smaller coupling constants of $J^{4,5}$, and $J^{4,3}$ (2.7 and 3.8 Hz, respectively) observed. The L-idoA obtained by the deprotection of **3** in the basic condition in 95 % yield.

doi:10.6844/NCKU201900656

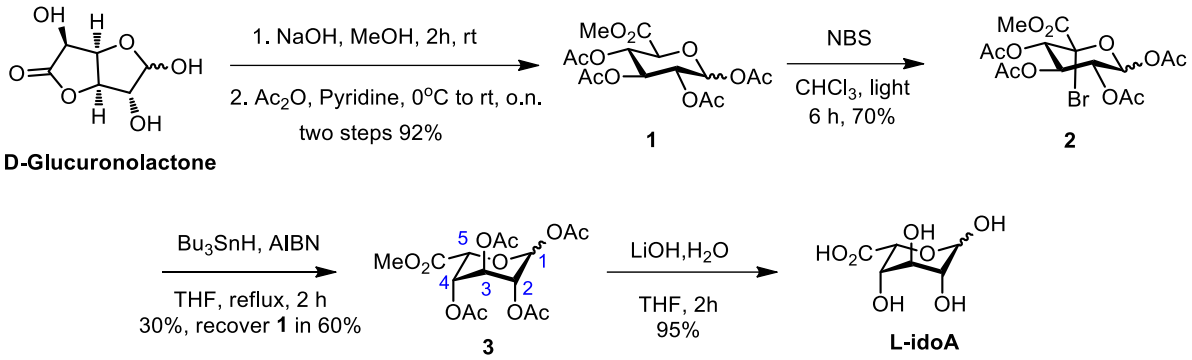

Scheme 1B. 7 The preparation of L-IdoA

With the synthetic L-idoA ready, the reaction of PMP labeling used for the sample preparation (Scheme 1B. 8). Unfortunately, the results of the labeling of L-idoA by PMP showed that reaction yield is low and difficult to characterization by the NMR spectrum. However, we could observe a reasonable spot in the monitoring of reaction by TLC, and the small amount of product checked by HRMS (Figure 1B. 8). Besides, the **5'** has not been reported and it difficult to demonstrated by the HRMS spectrum or NMR spectrum.

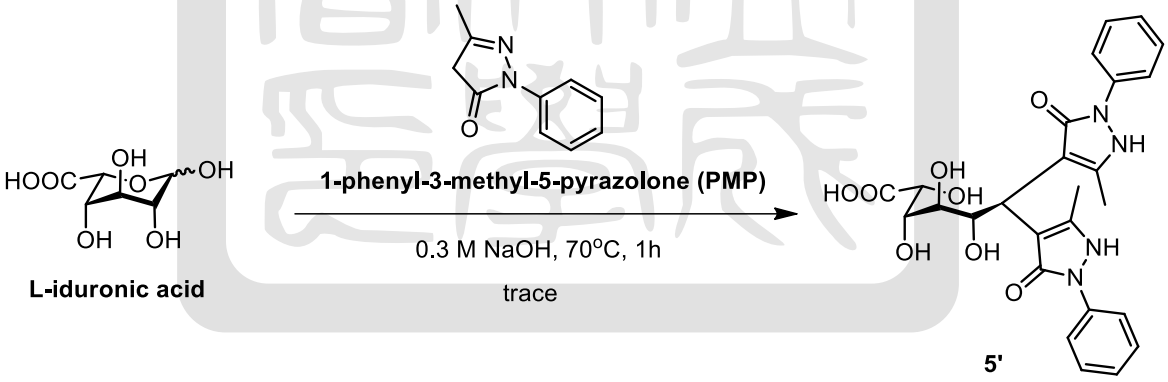

Scheme 1B. 8 The standard preparation of key biomarker, L-IdoA labeled by PMP

doi:10.6844/NCKU201900656

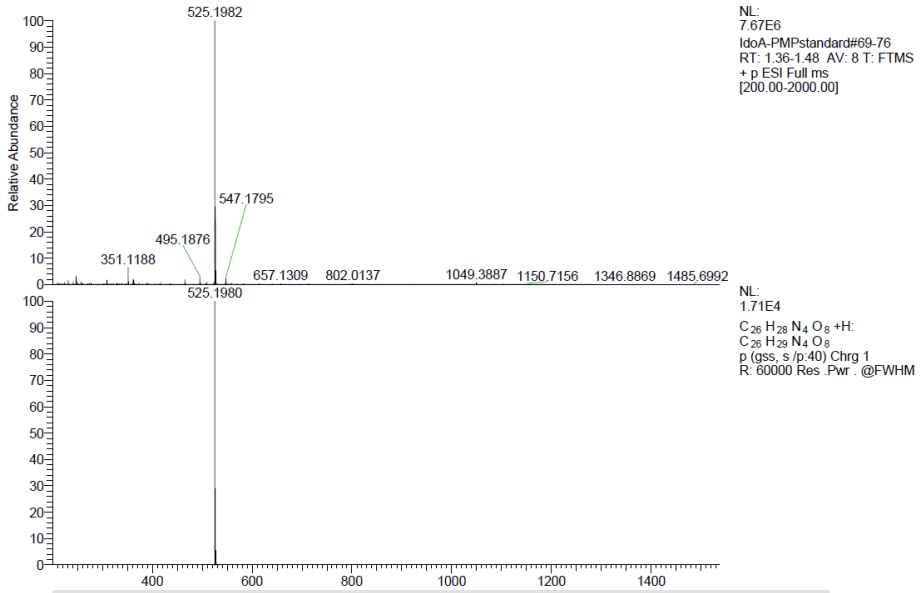

Figure 1B. 8 The HRMS spectrum of **5'**, calculated for $[C_{26}H_{28}N_4O_8+H]^+$ 525.1980, found 525.1982

The preparation of an authentic standard of the key biomarker **5'** was unexpected to obtain with the high yield, because of the low reactivity in the tag chemistry would cause the mistakes in the qualification and quantitation. The low yield of L-idoA labeling reaction may result from the unstable conformation of L-IdoA in the solution. The NMR spectrum indicates the mixture of L-IdoA compound exists as a mixture of conformations in water solution (Figure 1B. 9). As a result, the standard preparation of key biomarker is unavailable to use in the Method I, because of the low reactivity is a large risk of the tag chemistry in the complex bio-matrices.

doi:10.6844/NCKU201900656

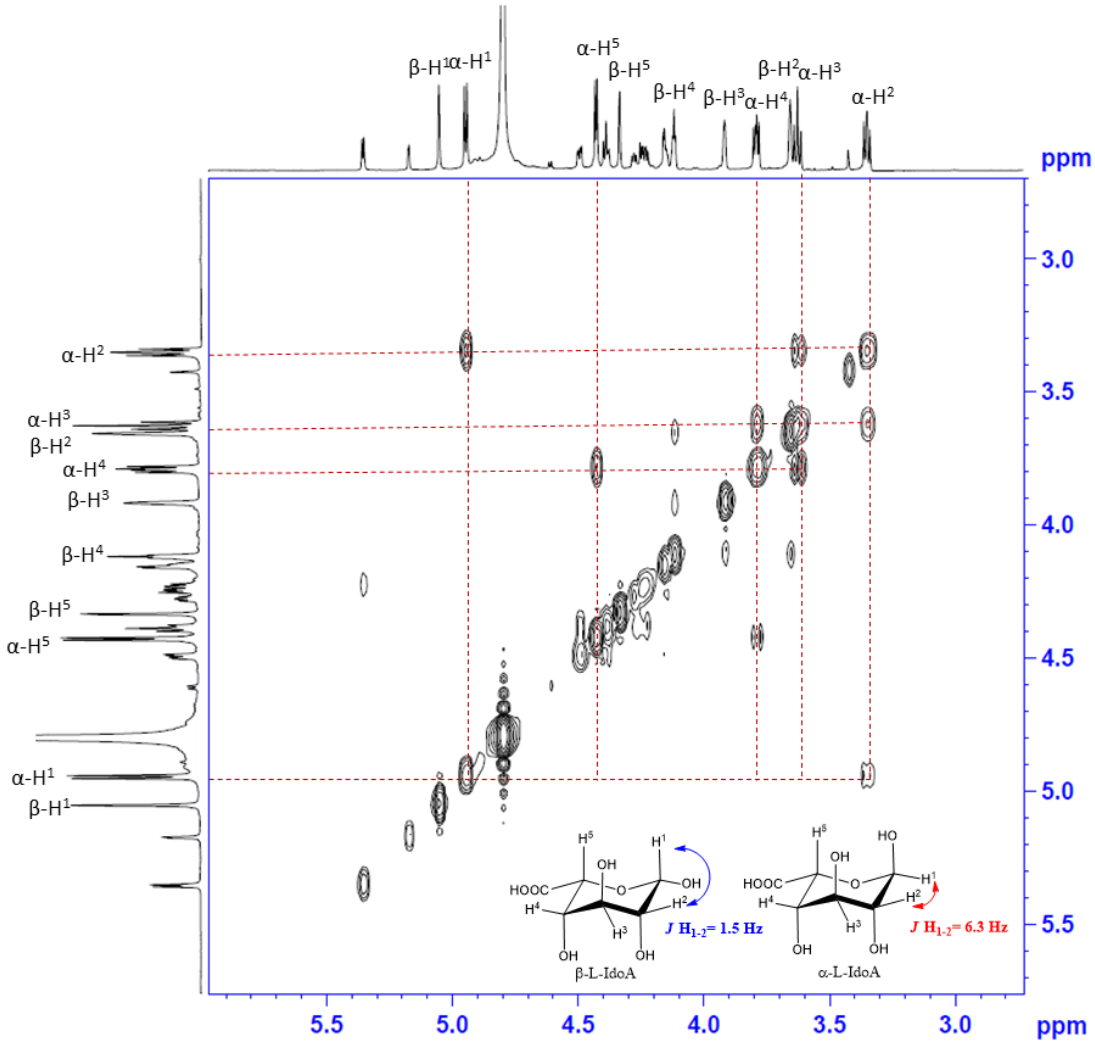

Figure 1B. 9 The COSY of synthetic L-IdoA

1B.2.3 Comparison of the normal and patient cell by methanolysis

In previous studies of MPS, the methanolysis is a simple method for the identification of the GAGs in the patient urine or tissues. The methanolysis of GAGs would generate the specific disaccharides (Scheme 1B. 9), and the major type products are detected by LCMS/MS. The heparan sulfate is one of the GAGs, which numerously accumulated in the MPS II patient. Therefore, the MPS II patient fibroblast was used to detect the HS for methanolysis digestion in the cell-based assay.

doi:10.6844/NCKU201900656

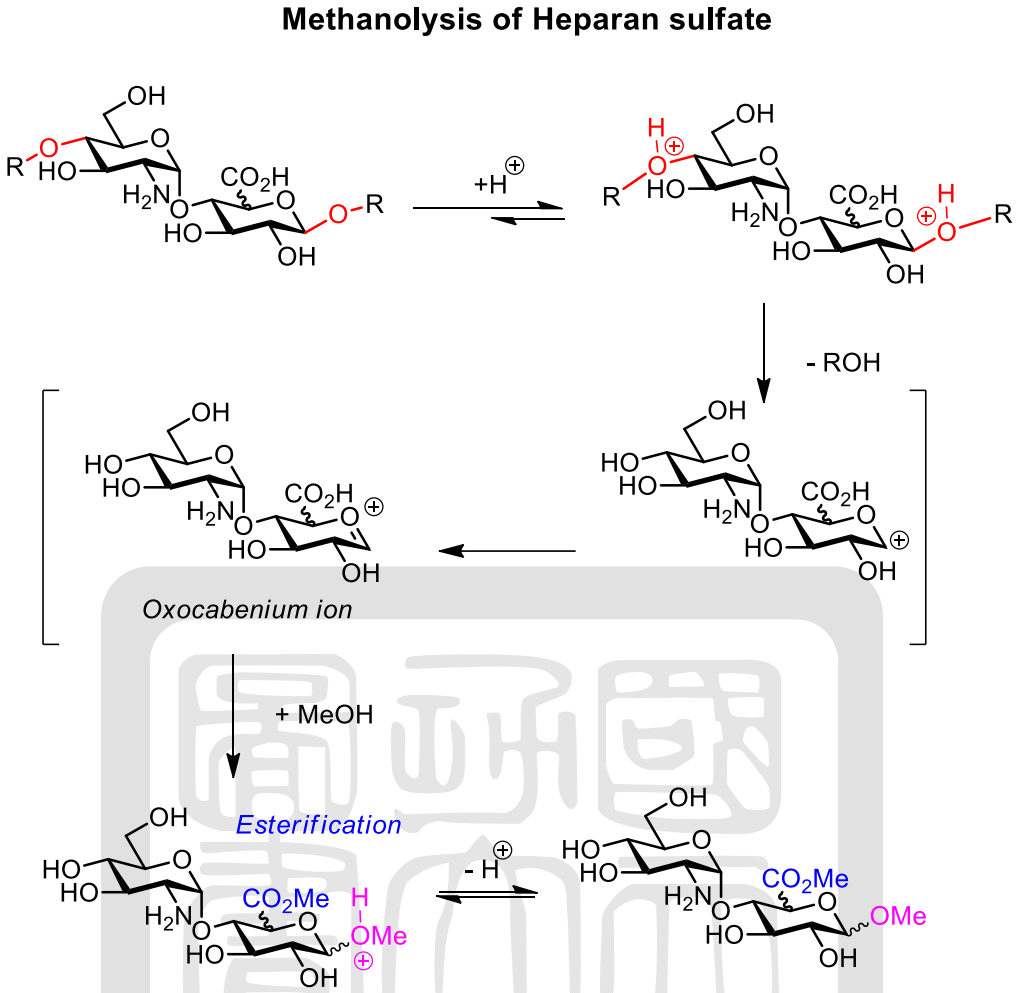

Scheme 1B. 9 The mechanism of HS methanolysis digestion

To obtain the model for the condition tuning in the HS methanolysis digestion detected by LCMS/MS, standard heparin sulfate was treated by 3N HCl in MeOD, then dropwise addition of acetyl chloride. The mixtures of the sample are filtered by 3K Amicon device to clean up the impurities, and reconstituted by 60 μL DMSO after the detection.

doi:10.6844/NCKU201900656

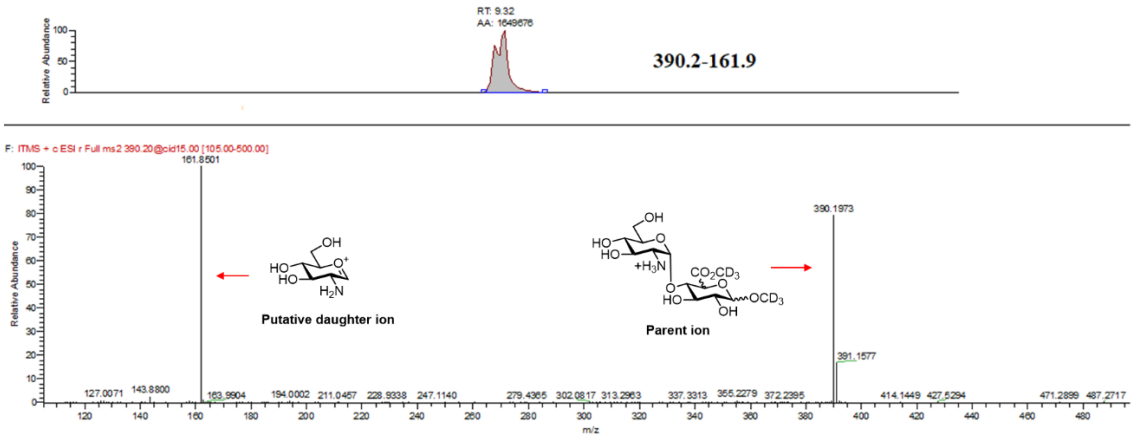

Figure 1B. 10 The model of deuteriomethanolysis of heparan sulfate standard

The mass spectrum of the deuteriomethanolysis product, [$^2H_6$] HS disaccharides showed the incorporation of +6 atoms of deuterium (Figure 1B. 10). The deuteriomethanolysis of HS standard produced a corresponding signal at m/z 390.2, was the parent ion, and the fragmented signal at m/z 161.9 was the putative daughter ion (retention time = 9.25 $\pm$ 0.12 min). Therefore, the peak areas are presented the rough amounts of HS involved in methanolysis digestion. On the other hand, the [$^2H_6$] HS disaccharides have a similar property with the HS disaccharides derived from methanolysis digestion by 3N HCl in methanol. Therefore, we presumed the methylated disaccharides is yielded a protonated molecular ion predominantly at m/z 384.2 as the parent ion and m/z 161.9 for HS after the collision.

doi:10.6844/NCKU201900656

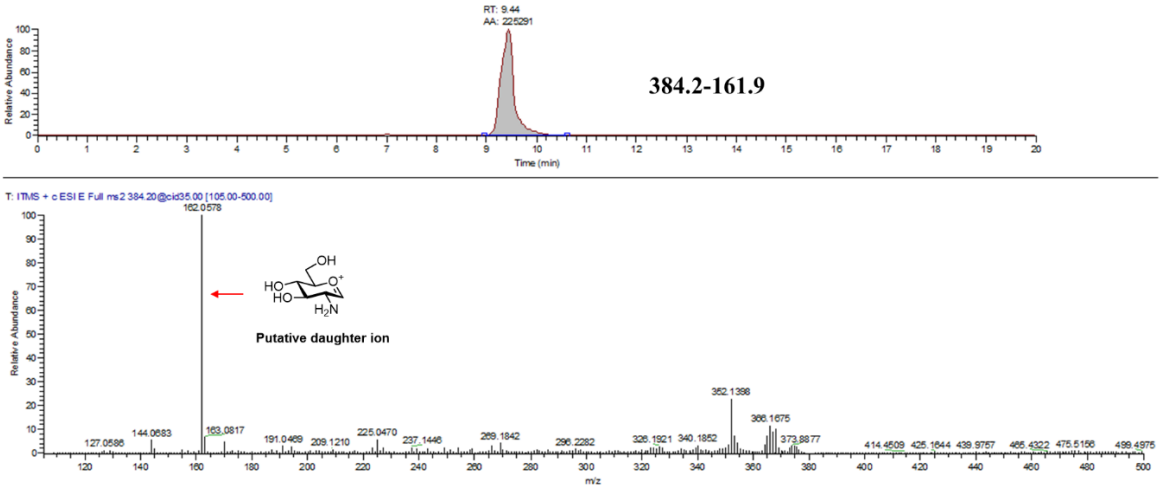

Figure 1B. 11 The model of methanolysis of heparan sulfate standard

Form the result of the methanolysis of HS standard by 3N HCl in methanol, and the condition-tuning let completely collision of parent ion to form the daughter ion. The peak area calculated from the signal of MS2 at m/z 161.9 (Figure 1B. 11), and the retention time (retention time = 9.36 ± 0.11 min) is similar to the [$^2H_6$] HS disaccharides.

Up to date, several newborn screening methods have been established and the patient samples can be obtained from patient plasma or urine. In contrast, no much study for cell-based metabolic analysis for small molecule screening toward MPSI or MPSII diseases. Presumably, the preparation of cell-based samples is not straightforward. In addition, the hydrolysis of GAGs is highly dependent on operating conditions such as time, temperature, operation procedures, and detection methods. In this work, we also would like to test the initial conditions for detection of the differences in the degree of GAG metabolite accumulation between the patient (E521V, a severe mutation) and normal cells. Initial attempts to hydrolyze GAG in the harsh condition (6N HCl, 100ºC, 1h) to become mono iduronic acid (IdoA) in the did not work promising in our hand, and the sample turned dark and black during heating; the certain decomposition was observed. Thus, we decided to choose a milder condition (3N HCl, 65ºC, 1.5 h) to find the disaccharide (GlcN-(1,4)- uronic

doi:10.6844/NCKU201900656

acid) amount. Based on our design, we would like to analyze the methylated disaccharide (m/z = 384.2) via acidic methylation conditions, followed by LCMS/MS analysis (MS2) to detect daughter ion (m/z = 161.9). After testing different cell numbers from $0.05x10^6$ to $1x10^6$ (Figure 1B.12), our results showed the intensity ratios (PC/NC) from 8.8 to 163. To be a delight, when the $0.05x10^6$ cell numbers were applied, the difference of metabolite accumulation intensity still be readout clearly and the ratio can be reached to 35, suggesting the cell numbers can reduce to fit into the microtiter plate format to let the operation become more practical for further small molecule screening (See the appendix)

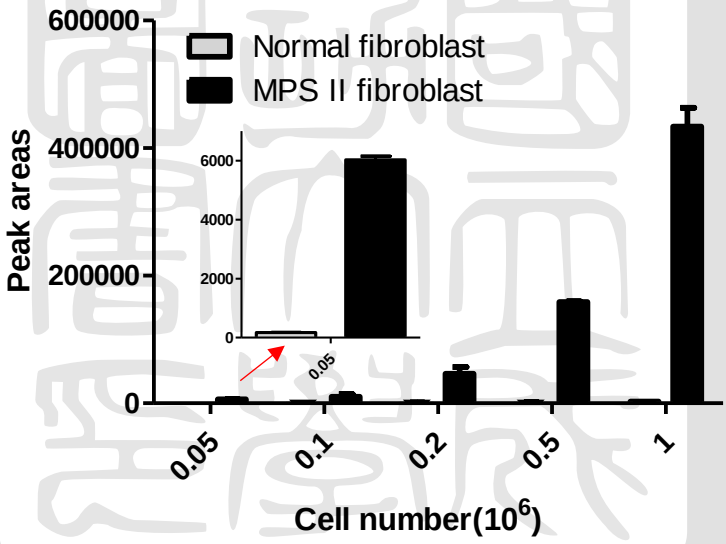

Figure 1B. 12 The peak areas of methylated HS disaccharide in the different cell numbers of MPS II patient between the normal person

By using the methanolysis of HS detected by LCMS/MS in the cell-based assay, we described the difference of patient cell and normal cell in various cell numbers. Besides, we determine the appropriate numbers of the cell to analyze the amounts of HS. On the other hand, the ratio of the patient cell and normal cell existed a gap to present the accumulated GAGs in the severe type MPS II patient. Therefore, Method II was an available assay

doi:10.6844/NCKU201900656

platform to evaluate the small molecules that affect the metabolic processing of accumulated GAGs in MPS disorders.

Next, we tried to modify the condition of time in the methanolysis reaction. The MPS II cell sample was treated the 3N HCl in MeOH in time-dependent (0.5 h to 6h). As the results showed in Figure 1B.13, the amount of methylated HS disaccharide was increased in time-dependent. Therefore, we decided to choose the more efficient condition, 1.5 h apply in the subsequent cell-based assay.

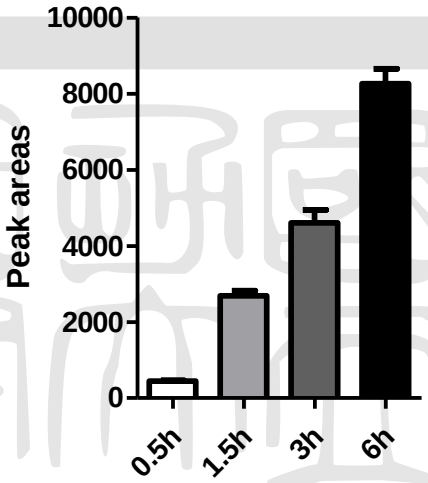

Figure 1B. 13 The amount of methylated HS disaccharide in the reaction of time-dependent

1B.2.4 Demonstration of the assay platform for small molecule evaluation

To prove the feasibility of this assay platform, some positive controls were needed to apply in the cell-based assay. Genistein is a kind of isoflavone, which has been proposed as a potential drug for substrate reduction therapy toward mucopolysaccharidoses[71]. Genistein is a tyrosine kinase inhibitor, which has been shown that the major mechanism of genistein-mediated inhibition of GAG synthesis involves epidermal growth factor (EGF), resulting in genistein affected EGF receptor-catalyzed phosphorylation efficiency[72]. On the other hand, genistein can inhibit mTORC1 of the transcription factor EB (TFEB) phosphorylation to cause the translocation of TFEB from cytoplasm to the nucleus[73]. Both EGF and TFEC were

doi:10.6844/NCKU201900656

the key roles to result in the stimulation of certain lysosome-related gene expression and enhancement of degradation of lysosomal aggregates by genistein-mediated (Figure 1B. 14). A decreased production of GAGs was observed in fibroblasts of MPS I, MPS II, MPS IIIA, and MPS III patients even though the animal models[74-76]. Therefore, genistein was a primary positive control to verify the feasibility of the established assay platform by us.

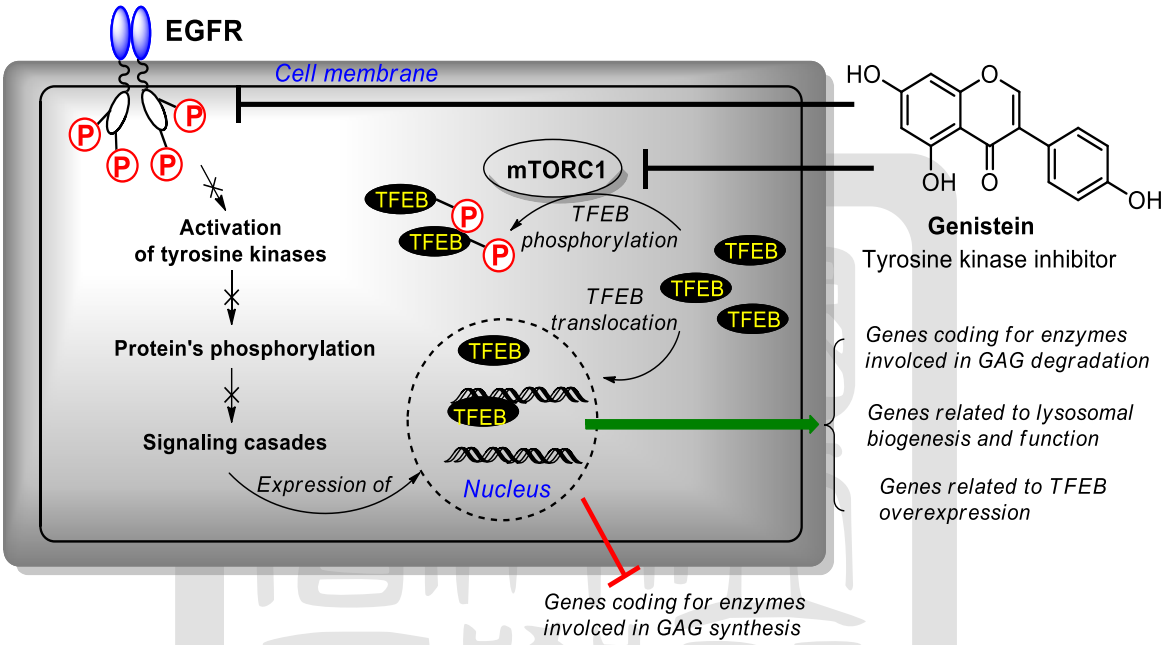

Figure 1B. 14 Schematic representation of the mechanism of genistein-mediated the lysosomal metabolism-related genes and TFEB

At first, we used $0.05x10^6$ seeding in the 24-well plate to treat the IDS and genistein in the dose- and time-dependent. From our results, the amounts of methylated HS disaccharide indeed reduce by treated the IDS and genistein (Figure 1B.15). However, the amounts of GAG would re-accumulation in the low concentration of IDS, due to the enzyme activity was unavailable in the long term of treatment (48 h). Based on this experience, we would use the fewer cell numbers to fit in the 96-well microplate to access the rapid analysis of small molecule.

doi:10.6844/NCKU201900656

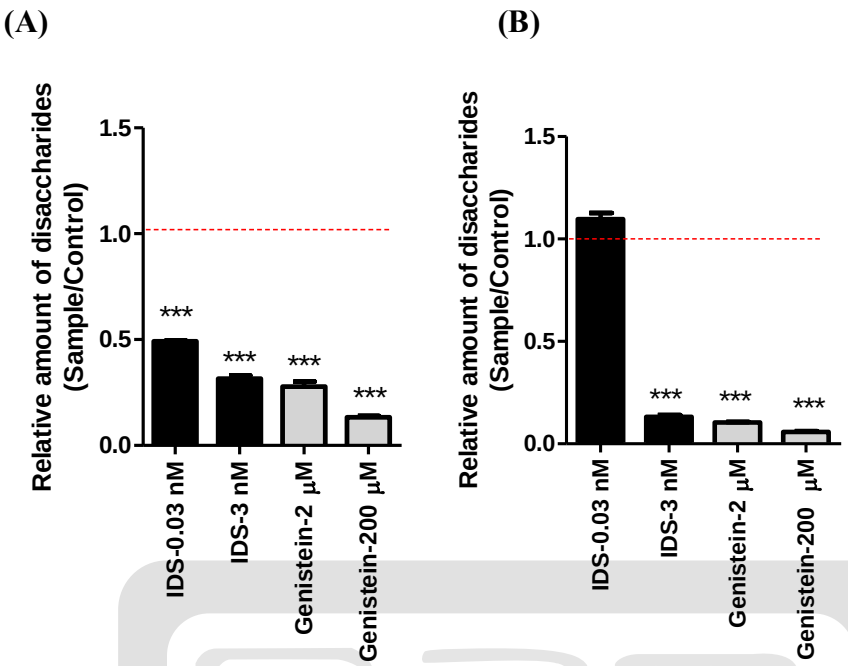

Figure 1B. 15 The relative amount of methylated HS disaccharide treated by IDS and genistein in MPS II cell in (A) 24 h (B) 48 h. Control is the untreated cell sample. The results were presented as mean ± S.D. ***P<0.001 vs. control group.

The purpose of the rapid analysis of small molecules evaluation in the cell-based assay is a helpful tool for the forward chemical genetic approach. Observation of the phenotypes changing is the initial step to find the hit, but the target of hir is unknown. We tried to decrease the cell numbers to find the detective limitation, and the 1 x 10^4 cell was allowed to observe the differentiation between the NC and PC (Table 1B.1).

Table 1B. 1 The peak areas of methylated HS disaccharide in the small amount of cell numbers of MPS II patient (PC) between the normal person (NC).

	Cell numbers (10^4)		
	0.5	**1**	**2**
NC	-	192 ± 24	136 ± 41
PC	220 ± 29	988 ± 96	1512 ± 15
Ratio	-	5.1	11

doi:10.6844/NCKU201900656

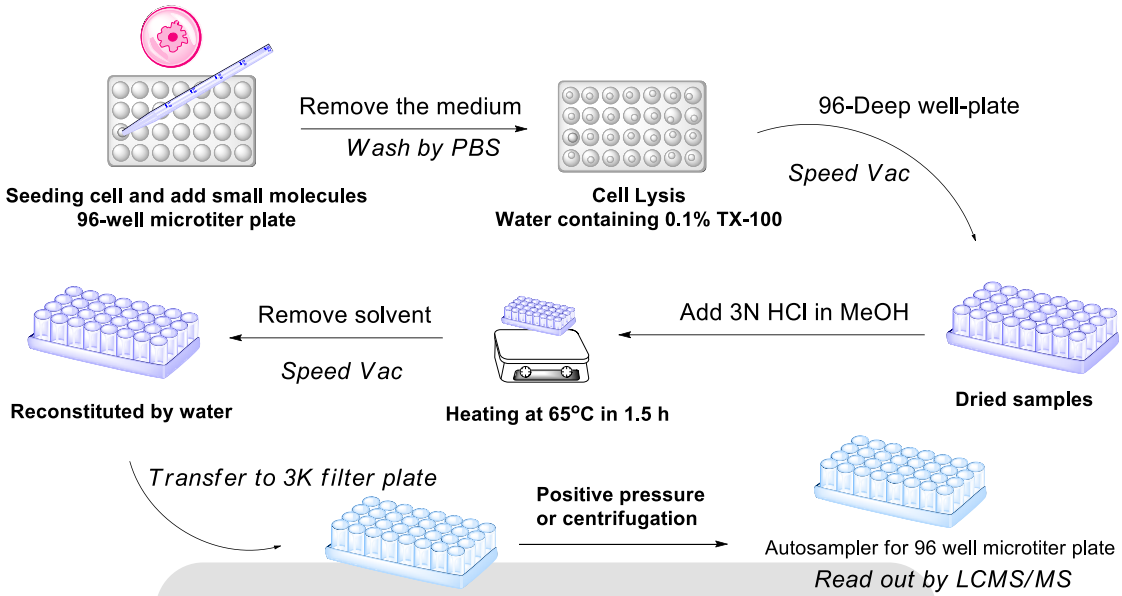

Figure 1B. 16 The protocol of rapid analysis for 96-well format in the cell-based assay

In the rapid analysis for small molecule evaluation, the 1 x 10^4 cell was seeded in the 96-well microplate, and the reaction of methanolysis was heated in the 96 deep-wall plates. When the reaction finished, the solvent was removed by the Speed Vac to get the dried sample and reconstituted by water. The sample would be filtered by 3K filter to remove the impurity. The detection was performed by the LCMS/MS to carried out the methylated HS disaccharide (Figure 1B. 16). From our results, the IDS and genistein were treated in the medium in 24h, and the results showed the amount of methylated HS disaccharide was decrease to be the positive results to prove the feasibility of this platform for rapid analysis (Figure 1B. 17). Although the assay platform was proved by the positive controls, IDS, and genistein, it also had some conditions and manipulations needed to be modified. Moreover, we hope to create the novel molecular library to proof of concept in the forward chemical genetic approach (See the appendix).

doi:10.6844/NCKU201900656

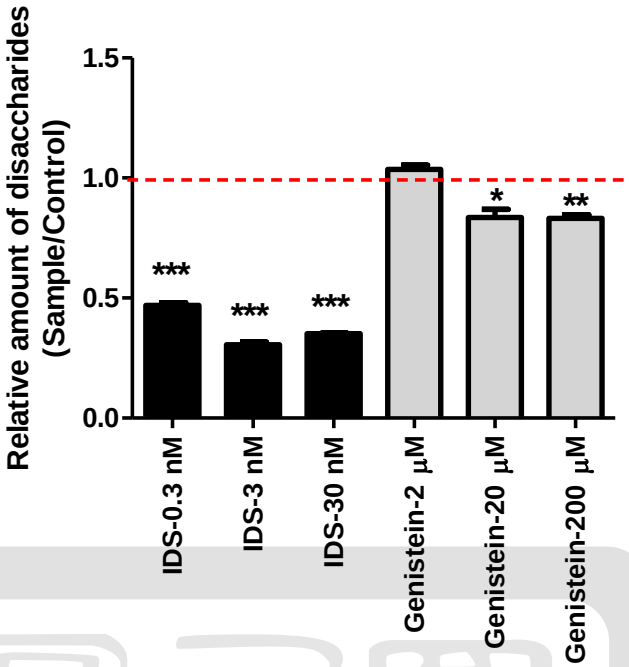

Figure 1B. 17 The relative amount of methylated HS disaccharide treated by IDS and genistein in MPS II cell for 24h with 96-well plate Control is the untreated cell sample. The results were presented as mean ± S.D. *P<0.05, **P<0.01 ***P<0.001 vs. control group.

1B.3 Sub-summary

We designed to establish the different approaches, Method I and Method II to analyze the difference of the amounts of heparan sulfate in the patient cell and normal cell. In Method I, we got some problems with the standard preparation by tag chemistry. Besides, the complexity of Method I was not only standard compound preparations but also the sample pretreatments. On the other hand, we successfully established the cell-based assay by Method II, which used the methanolysis of HS to generate the specific disaccharide fragments detected by LCMS/MS. By using Method II, the appropriate cell numbers are determined to differentiate the MPS II patient fibroblast and the normal person fibroblast, decrease the time of cell collection.

Moreover, the approach of methanolysis applied in the cell-based assay has not been reported to analyze the accumulated HS in the MPS patient. Method II described the

doi:10.6844/NCKU201900656

available assay platform for small molecules evaluation to observe the affected metabolic processing directly in the cell-based assay. On the other hand, we decided the mild and efficient condition (3N HCl, 65°C, 1.5 h) of methanolysis in the sample preparation. The IDS and genistein, as the positive controls were demonstrated by this assay platform to show the reduction of the GAG accumulation in the MPS II cell. Moreover, we established the rapid analysis for small molecule evaluation by 96-well microplate format. In the future, we hope to design the novel small molecule library will be evaluated to proof of concept.

doi:10.6844/NCKU201900656

Future perspectives of Chapter 1

In the drug discovery of LSDs therapy, MPS disorders have the biggest challenge to develop small molecules therapy, because of the assay platform is incomplete to screening the molecular libraries. The enzyme-based and the cell-based assay have established in our efforts. Currently, the small molecule library can be designed to analyze the binding of a compound and a protein, changes in the activity of a protein, or alterations to a cellular phenotype[77]. The targets in the biochemical assay are commonly used the purified materials to process in assays, called reverse chemical genetics. However, the phenotype demonstrated in assays that used the cell or model organisms is called forward chemical genetics. Herein, these established assay platforms for forward chemical screening and reverse chemical screening are available in our lab. Once the small molecular libraries are ready, these assay platforms will be used at the same time to screen out the potential hits for MPS therapy.

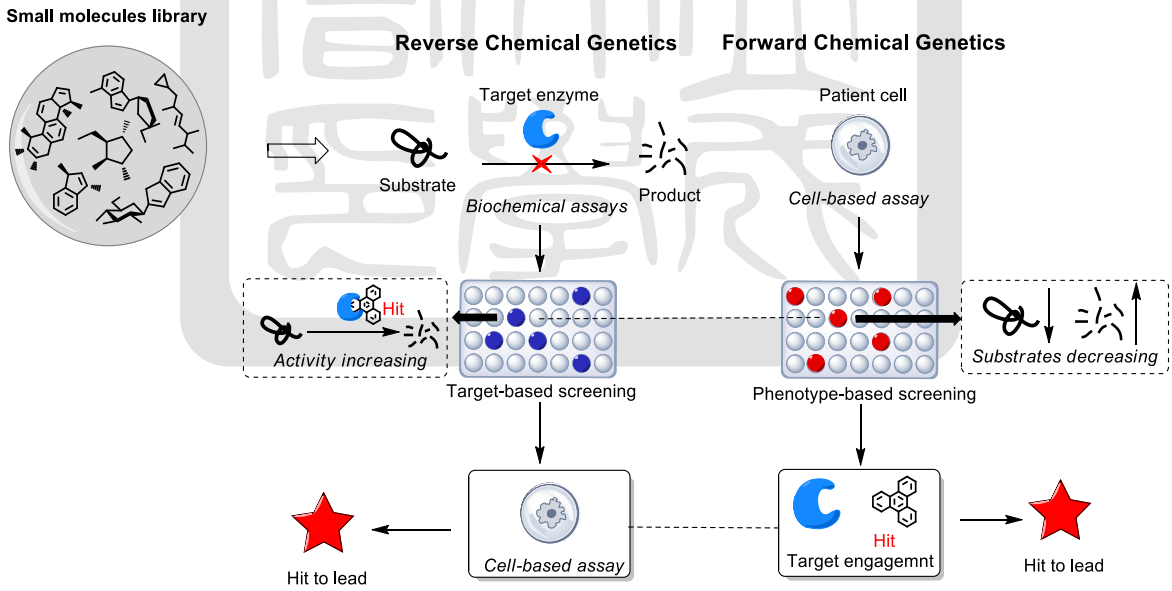

doi:10.6844/NCKU201900656

Chapter 2 Characterization and inhibition studies of human Golgi α-mannosidase II and lysosomal α-mannosidase with oligosaccharides-based substrates

2.1 Introduction

2.1.1 Glycoprotein biosynthesis

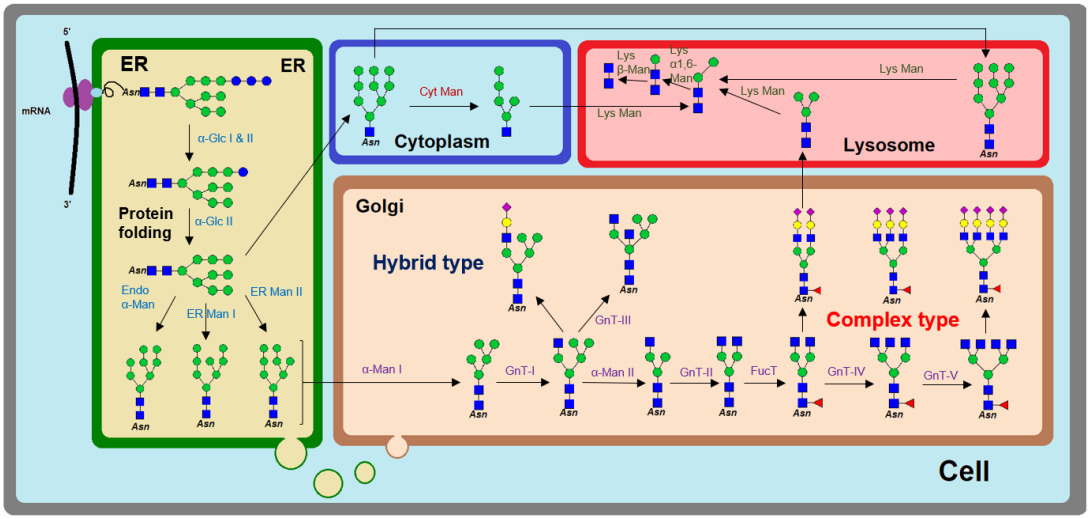

Figure 2. 1 Overall scheme of glycoprotein biosynthesis

Glycans are present as different types in the human body, such as glycoproteins, glycolipids, and proteoglycans. Glycans, including the large complex molecules and oligosaccharides, exist in various organelles such as Golgi, ER, lysosome, cytoplasm, nuclei, are also are found mostly on the cell surface and extracellular matrix (ECM) mostly. In recent years, glycobiology is getting more attention in cancer research because the process of glycans formation is associated with the pathogenic mechanisms of various cancer[78]. Glycosylation is kind of post-translational modification playing an important role in regulatory mechanism[79]. The glycosylated proteins are catalyzed by the functions of glycosyltransferases, which can add various complex carbohydrates to the sugar chains. Besides, aberrant glycosylation is associated with many physiological and pathological

doi:10.6844/NCKU201900656

events, including cell growth, migration, and tumor invasion[80, 81].

In the glycoprotein biosynthesis, the *N*-acetylglucosaminyltransferase-I (GnT-I) is a key enzyme in the development of multicellular organisms[82]. First, the high mannose type glycoprotein transported to the Golgi and demannosylated by the Golgi α-mannosidase II, forming the $Man_5GluNAc_2$, which is a substrate for GnT-I. Next, the GlcNAc residue is added on the $Man_5GluNAc_2$ by GnT-I and generates the $GlcNAcMan_5GlcNAc_2$, a substrate for GnT-II and α-mannosidase II. Golgi α-mannosidase II trims two terminal mannose residue to form the intermediate of $GlcNAcMan_3GlcNAc_2$, the precursor of complex type glycoproteins. On the contrary, the hybrid structures are generated by the action of GnT-III on the $GlcNAcMan_5GlcNAc_2$ (Figure 2.1).

2.1.2 The differentiated functions of *N*-acetylglucosaminyltransferases

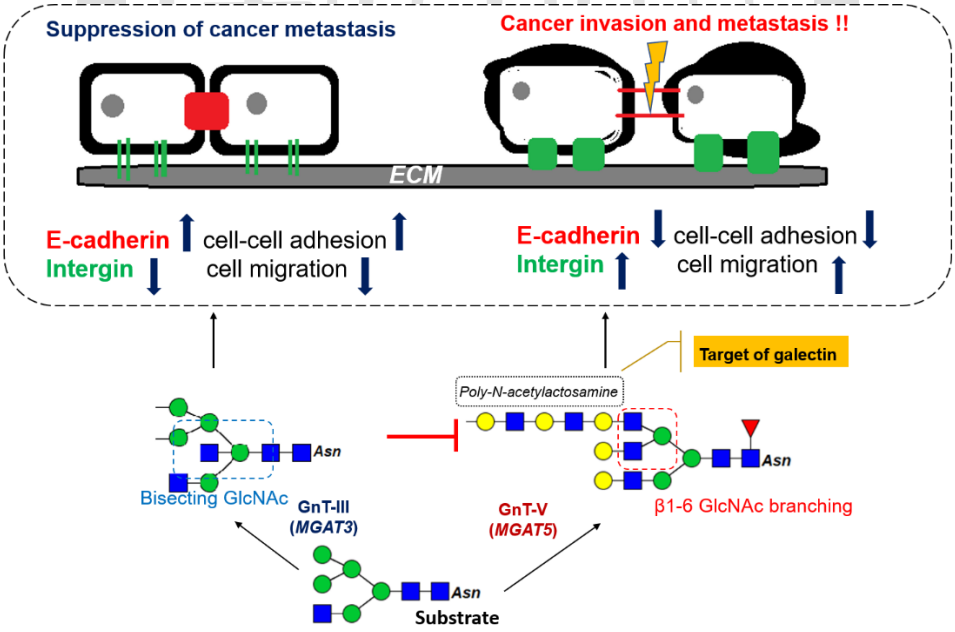

Figure 2. 2 The factors of cell metastasis by GnT-III and GnT-V

N-acetylglucosaminyltransferase-V (GnT-V), encoded by the *MGAT5* gene, is reported having a close relationship with cancer metastasis. GnT-V transfers the *N*-acetylglucosamine

doi:10.6844/NCKU201900656

(GlcNAc) from UDP-GlcNAc to the α-1,6-linked mannose of *N*-glycans to form the β1-6 GlcNAc branch which is over-expression in various cancers[83]. Mechanistically, the β1-6 G1cNAc branch glycans modification by GnT-V increases the binding affinity of galectin by several *N*-acetyllactosamine (LacNAc) residues and prolong the retention of growth receptors on the cell surface. On the other hand, GnT-III plays a key in role to suppressing the cancer metastasis by the synthesized bisecting GlcNAc linkage on the β-1,4-linked mannose of *N*-glycans to completely inhibit GnT-V activity. Furthermore, GnT-V and GnT-III were reported to regulate through the E-cadherin and integrin-mediated cell-cell communication in the development of cancer progression[84, 85]. The β-1,6-G1cNAc branch glycans modified by GnT-V promote the destabilization of E-cadherin, causing the cell-cell interaction decrease and enhance the cluster of integrin to increase the cell-ECM adhesion, resulting in cancer cell migration and tumor invasion[86]. Conversely, the bisecting glycans synthesized by GnT-III can stable the E-cadherin to enhance the cell-cell adhesion and decrease the cell-ECM adhesion by integrin down-regulation (Figure 2.2).

2.1.3 A commonly recognized drug target: Golgi α-mannosidase II

Though GnT-V is the most characterized cancer-associated enzyme in the malignant formation, no inhibitor has been reported. The known drug target, Golgi α-mannosidase II (GMII) is a class II retaining glycosyl hydrolase of the family (EC 3.2.1.114) and plays a major role in the mammalian *N*-glycosylation pathway and its inhibition influences the patterns of the *N*-linked oligosaccharide on the surface of the cancer cell which associates with the tumor progression and metastasis[87]. Swainsonine, a most potent inhibitor against mannosidase that removes α-1,3 and α-1,6 mannose from the $GlcNAcMan_5GlcNAc_2$ (Figure 2.3), causing the hybrid structure form. Moreover, swainsonine was investigated as an antitumor agent and showed good tolerability and low preclinical toxicity in clinical trials[78,

doi:10.6844/NCKU201900656

88-95

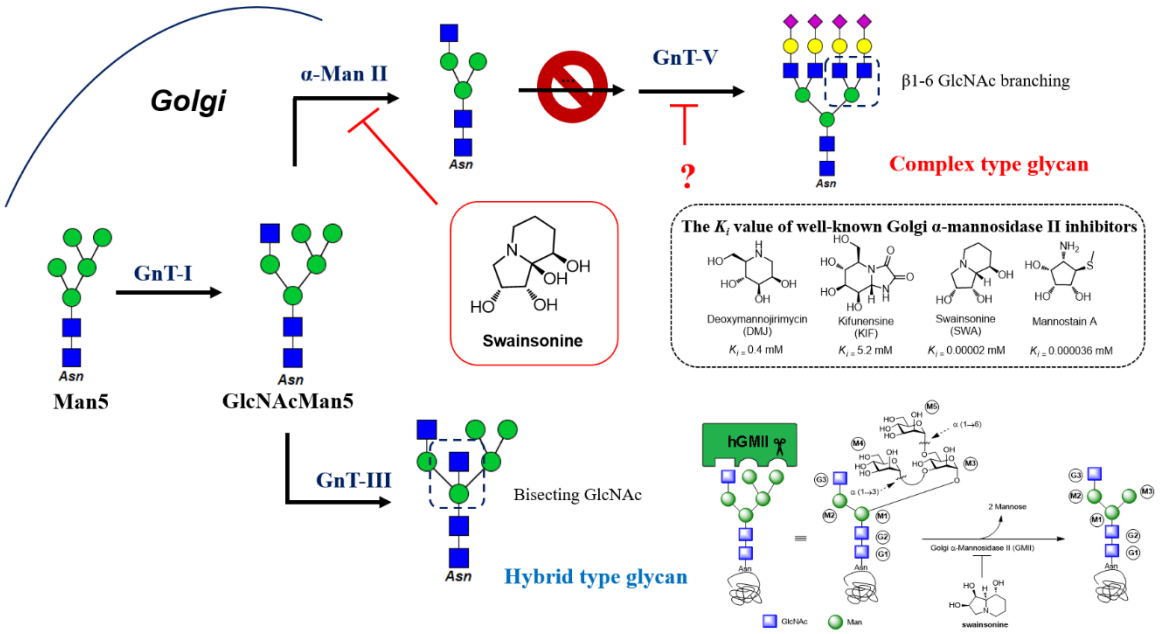

Figure 2. 3 The effect of the potent GMII inhibitor

Unfortunately, one difficulty in utilizing swainsonine toward cancer is that it suffers from a lack of selectivity. Swainsonine also associates with unwanted side effects such as co-inhibition of lysosomal-mannosidase (LM) (EC 3.2.1.24), causing the accumulation of high-mannose type oligosaccharides in lysosome that limits its clinical study. In phase I study, the accumulation of undegraded oligosaccharides of 5-days swainsonine-treated patient is higher than α-mannosidosis patient[96]. Due to the swainsonine is a toxin in locoweed for the livestock to cause the disease called locoism, which will affect the nervous system. Exactly, the neurological side effects due to swainsonine in the phase IB study may be related to repeating dosing over a prolonged[97]. However, a phase II clinical trial of GD0039 (Swainsonine) shown unfavorable results in 17 patients of renal carcinoma[98].

doi:10.6844/NCKU201900656

2.1.4 The binding pocket of Golgi mannosidase II

The crystal structure of *Drosophila melanogaster* Golgi mannosidase II has been reported, and the binding mode of natural oligosaccharides substrate is described (Figure 2.4). The whole binding pocket is called active site which has three regions include the catalytic site (Blue), holding site (Green), Anchor site (Red)[99]. In the catalytic site, the α-1,6 linked mannose (M5) is tightly bond with many hydrogen bonds and stacking interaction. The oxygens at C2 and C3 coordinate to zinc ion stable in the active site, which is the major binding position for the many GMII inhibitors including the swainsonine have studied. Another α-1,3 linked mannose (M4) is binding in the holding site, which is the key position that determines which mannose is cleavage first. The holding site in the GMII has not revealed any inhibitor binding it. Anchor site is for the required *N*-acetylglucosamine (G3) to stabilize the substrate for the hydrolysis reaction as well as increasing the affinity of linkages to be cleaved by GMII. Recently, the potential allosteric site[100] (yellow) of GMII using computational docking for the drug design is described. Because of the known catalytic site is complex and compact influenced by the hydrophilic and negatively charged residues. The potential allosteric site is more open compared to the active site because of the balanced distribution of negatively and positively charged residues.

doi:10.6844/NCKU201900656

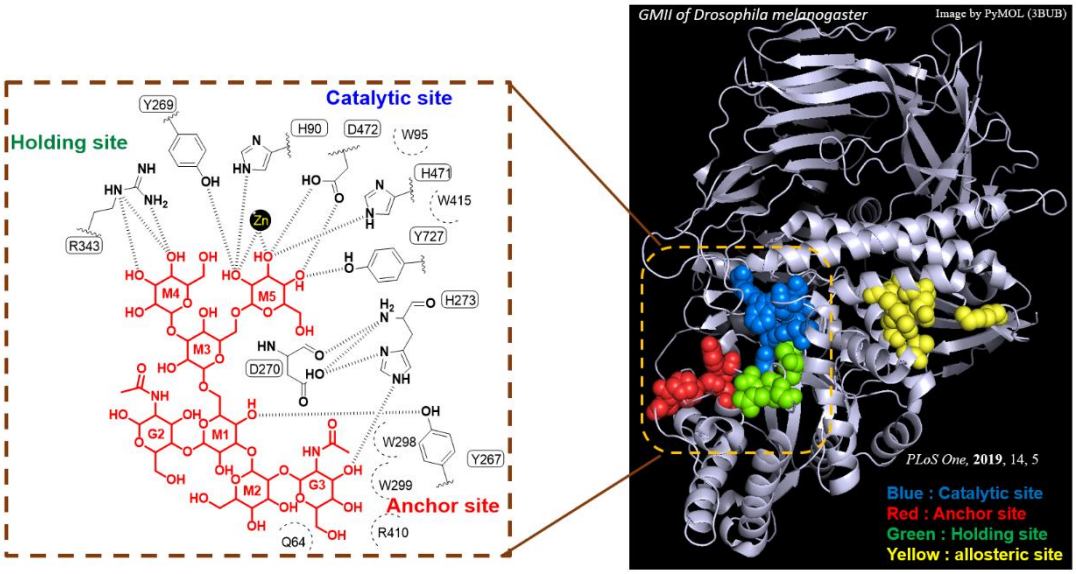

Figure 2. 4 The probable binding modes of GMII

2.1.5 The commercial substrate of preliminary screening

The fluorimetric enzyme assay is a common method to test the enzyme activity and the study of inhibitor (Figure 2.5). The commercial substrate, 4-Methylumbelliferyl α-D-mannopyranoside (4MU-Man) is a simplified substrate for the mannosidases. To fit the physiological condition, the different pH value buffers are used toward GMII and LM. Afterward, the condition is adjusted to 10.8 to read out the cleaved 4MU. The simplified 4MU-substrate assay is used in preliminary screening to find the potent inhibitor against Golgi- and lysosomal- mannosidase.

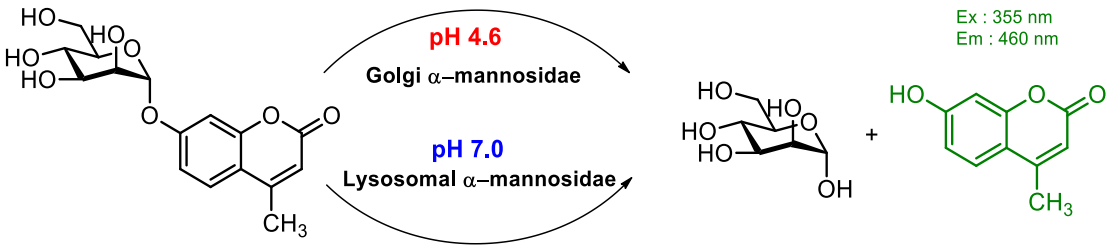

Figure 2. 5 The fluorimetric enzyme assay of mannosidase

doi:10.6844/NCKU201900656

2.1.6 Preliminary data in house

Our group has earlier reported our preliminary efforts toward the synthesis a series of aminomethyl pyrrolidines (ADMDP) as scaffolds to build diverse libraries for hGMII inhibition by using cyclic nitrone as key intermediate and parallel combinatorial chemistry. Although the potent inhibitors are filtered out, the property of selectivity isn't be discussed. Recently, the more potent hGMII inhibitor **7b-6c** is synthesized by "*Natural Product Inspired Combinatorial Chemistry*" and this hit is evaluated the potency of selectivity inhibition toward hLM and hGMII by 4MU-substrate assay (Figure 2. 6). The IC_{50} values of inhibitor **7b-6c** were determined to 13 μM (hLM) and 0.1 μM (hGMII) revealing an encouraging selectivity for hGMII (130 fold).

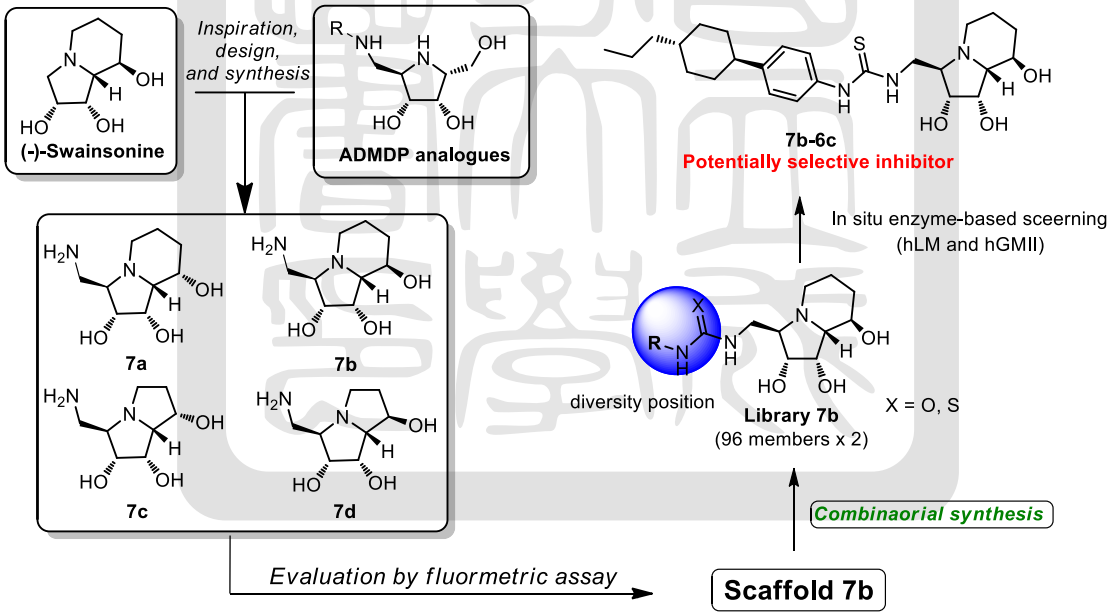

Figure 2. 6 Design novel scaffolds for selective inhibition of hGMII

doi:10.6844/NCKU201900656

2.1.7 Motivation

In our previous work, the potential selective inhibitor is screened out by the 4MU-substrate assay. With this preliminary information in hand, we will study binding mode of this potential compound by the enzyme kinetic assay. Based on the mechanism of GMII reaction, we are curious about the binding mode of the potential selective inhibitor (**7b-6c)** when using the natural substrate of GMII. To enhance the sensitivity, the chemical tag is used to prepare the real oligosaccharide-based substrates toward hGMII and hLM. On the other hand, the oligosaccharide-based substrate of hGMII is obtained by the chemoenzymatic synthesis. With these oligosaccharide-based substrates in hand, the assay conditions are established to characterize the property of potent mannosidase inhibitors. Herein, we will prepare the oligosaccharide-based substrate toward the hGMII and hLM. Furthermore, the assay platform will be established to mimic the real situation for bio-evaluation of small molecules by using the LC system to investigate the hGMll selective inhibition study more thoroughly (Figure 2.7).

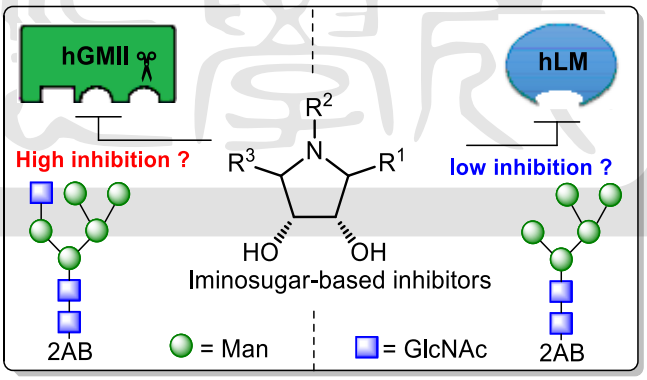

Figure 2. 7 The concept of the oligosaccharides-based substrate assay

doi:10.6844/NCKU201900656

2.2. Results and discussions

2.2.1 Preparation of the labeled oligosaccharide-based substrates

In oligosaccharides analyses, high-resolution techniques are essential because the lower sensitivity of oligosaccharides are difficult to detect by the LC system. Fluorescence labels are useful tools to monitor the extremely low concentrations of mono- or oligosaccharides involved in a biochemical process of interest. 2-Aminobenzamide (2AB) is a commonly used fluorescent probe attached to reducing end in the carbohydrate by reductive amination. Once the fluorescent probe tagged, the LC system is allowed to visualize the analysis (Figure 2.8).

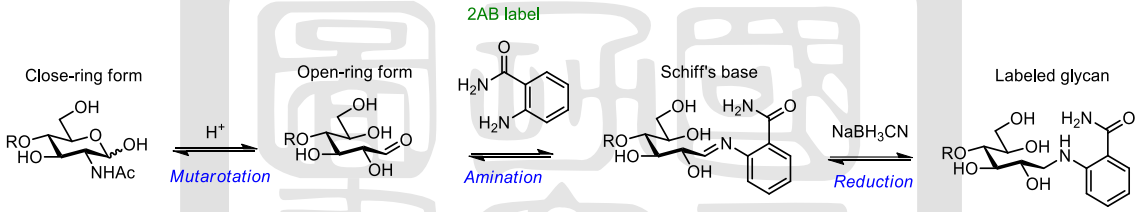

Figure 2. 8 Mechanism of 2AB labeling by reductive amination

The commercial oligosaccharides, Man5 ($Man_5GlcNAc_2$) is kind of high-mannose type oligosaccharides can be the substrate of hLM. By following the protocol of 2AB labeling, the tagged oligosaccharides called **O2AB-1** (Man5-2AB) is obtained successfully and clean up by the hydrophilic interaction chromatography solid phase extraction (HILIC SPE) (Scheme 2. 1).

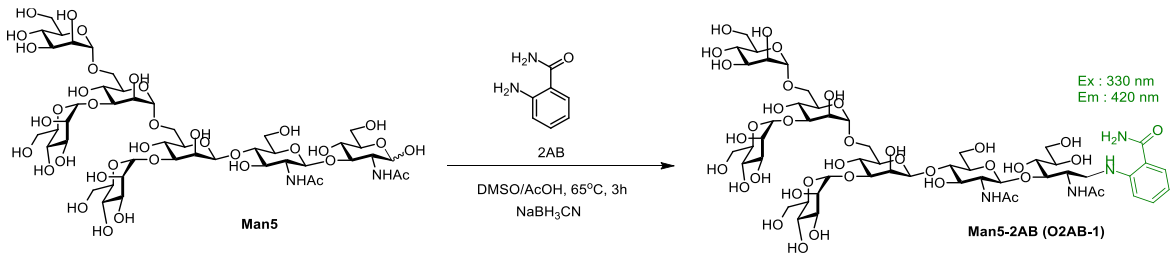

Scheme 2. 1 Preparation of labeled oligosaccharides **O2AB-1**

doi:10.6844/NCKU201900656

HILIC SPE is a skill to remove the impurities after the reaction of glycan labeling and enzyme-catalyzed synthesis. Hydrophilic interaction chromatography (HILIC) can improve the retention of highly polar species, such as carbohydrate and glycan which are not suited by the reversed-phase chromatography (Figure 2. 9). This method is a robust, reliable solution for clean up the sample from a complex mixture to ensure the analyte obtains successful results when protein treatment.

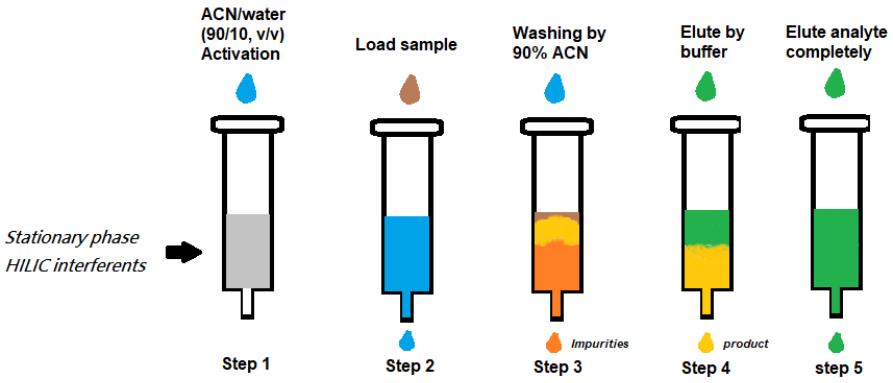

Figure 2. 9 The principle of HILIC SPE

2.2.2 Chemoenzymatic synthesis of hGMII substrate

The substrate of hGMII, $GlcNAcMan_5GlcMAc_2$ (GlcNAcMan5) was synthesized by the catalysis of GnT-I by using the Man5 as the substrate in the biosynthesis of glycoprotein. However, GlcNAcMan5 is not a commercially available, and the chemical oligosaccharide synthesis is present large difficulties about the size, branched, and the wide variety of monosaccharides and glycosidic linkages within their structures (Figure 2. 10). The strategy of natural source isolation is commonly used in the specific oligosaccharides, but the N-linked oligosaccharides are showed the multiple heterogeneous types in biological systems to lead the complicated isolated method. Furthermore, in the *Tolbert et al.* works, the GnT-I was purified from *E. coli* is used in the enzyme-catalyzed synthesis of GlcNAcMan5 and

doi:10.6844/NCKU201900656

conversion of the reaction is monitored by MALDI-TOF-MS[101]. The best advantage of enzyme-catalyzed synthesis of oligosaccharides is not requiring protecting groups to differentiate the hydroxy groups of saccharide in glycosylation reactions to achieve high stereoselectivity in the formation of glycosidic bonds and high conversion yields generally.

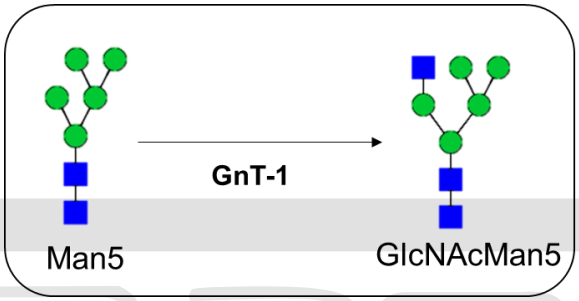

Figure 2. 10 The Man5 as a substrate of GnT-I to form the GlcNAcMan5

Based on this previous work, we used the **O2AB-1** treated by GnT-I and monitored the reaction process by the UPLC with fluorescence detector. The chemoenzymatic synthesis of labeled oligosaccharides, **O2AB-2**, was conducted at the 37ºC with the excess sugar donor UDP-GlcNAc in 24 h. The GnT-I was used to produce the labeled oligosaccharide **O2AB-2** allows the regioselective and stereoselective addition of a β1,2-N-acetylglucosamine onto the **O2AB-1** in a single step in the presence of the chemical tag (Scheme 2.2).

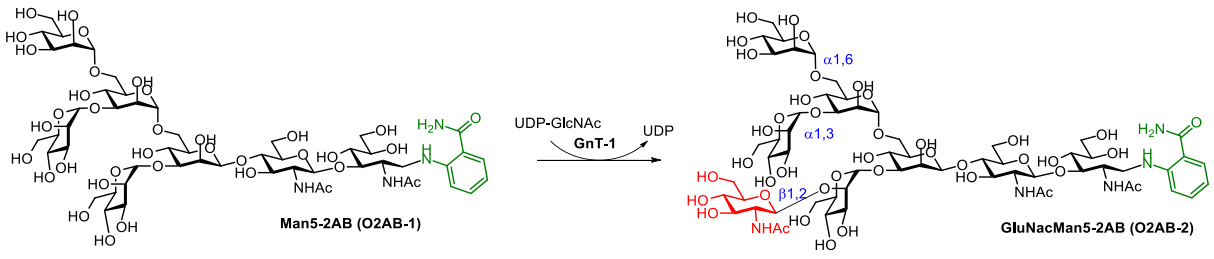

Scheme 2. 2 Chemoenzymatic synthesis of labeled oligosaccharides **O2AB-2**

To find optimized condition, different concentration of GnT-1 was tested. At first, the

doi:10.6844/NCKU201900656

conversion of 10 μM **O2AB-1** incubates with 1 μg/μL GnT-I is completely at the 37ºC in 24 h. Next, we try to decrease the concentration of GnT-I with the same conditions of substrate, temperature, and time. From the results, the 0.1 μg/μL GnT-I catalyze 50% **O2AB-1** to form the **O2AB-2** and the 0.3 μg/μL GnT-I is 80% in 24 h, and these conversions are not changed with 48 h monitoring by UPLC. The reaction is complete by the optimized condition of 0.5 μg/μL GnT-I incubate with 10μM at the 37ºC in 24 h (Figure 2.11). The mixture is clean up by HILIC SPE, and the final concentration of the **O2AB-2** is checked by the area ratio of internal standard, LNnT (50 pmol/μL). **O2AB-2** was obtained in 60% yield, and the mass of **O2AB-2** is detected by MALDI-TOF-MS.

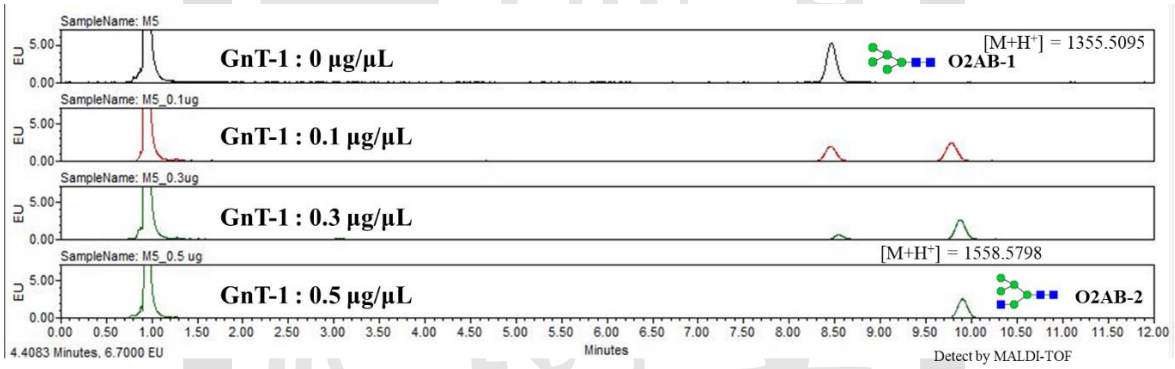

Figure 2. 11 The different concentrations of GnT-1 to optimize the condition

2.2.3 UPLC-based enzyme activity studies

With these oligosaccharides-based substrates, **O2AB-1**, **O2AB-2** in hand, the enzyme activities of hLM and hGMII could commence by UPLC system (Figure 2.12). To establish the assay platform, the suitable conditions of needed to be investigated. Observation of the remaining substrate to characterize the enzyme activity was required, therefore, the internal standard was essential to normalize to normalize the divergence of instrument and the operational error

doi:10.6844/NCKU201900656

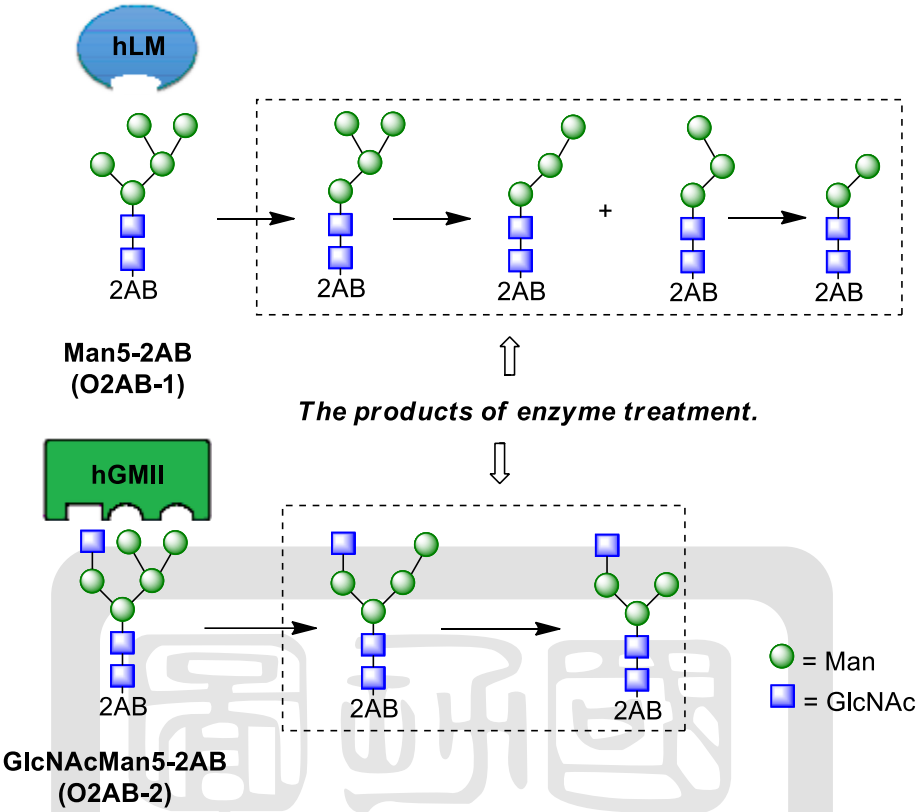

Figure 2. 12 The predicted products of the enzyme-treated by hLM and hGMII

At first, the LNnT (Lacto-N-neotetraose) was chosen to be the internal standard in the enzymatic reaction of **O2AB-1**. As a result, the LNnT is overlapped to the products of **O2AB-1** treated by hLM in UPLC analysis. Thus, we chose the internal standard, NA2, which has a longer retention time for substrate **O2AB-1** to avoid the overlapping. After optimization of the different concentrations of hLM treated, the condition of the 0.15 μg/μL hLM added in the 2.5 μM **O2AB-1** in the pH 4.6 citrate phosphate buffer incubated at 37ºC for 24 h was easy to analyze the changing of the residual substrate. The appeared peaks are the hLM-treating products of **O2AB-1** treated by hLM described by *Bryan et al*[102]. and were checked by MALDI-TOF-MS (Figure 2.13).

doi:10.6844/NCKU201900656

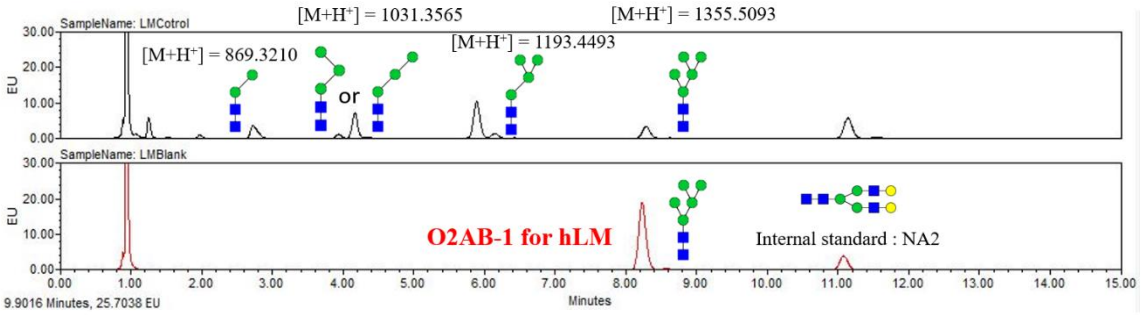

Figure 2. 13 Analysis of the digestion of **O2AB-1** by the hLM

Likewise, we used the LNnT as the internal standard in the reaction of the **O2AB-2** treated by hGMII. The optimized condition was the 2.5 μM **O2AB-2** treated by 5 ng/μL hGMII in the pH 7.0 phosphate buffer incubated at 37°C in 24 h. According to the hydrolyzed mechanism of mannosidase, described by *Rose et al.*[87], the first cleaved saccharide is the α1,6-linked mannose at the catalytic site, and the α1,3-linked mannose bound at the holding site is the second cleaved saccharide. From the results, we observed two peaks appear in the reaction of digestion of **O2AB-2** by hGMII, and the products are also checked by MALDI-TOF-MS (Figure 2.14).

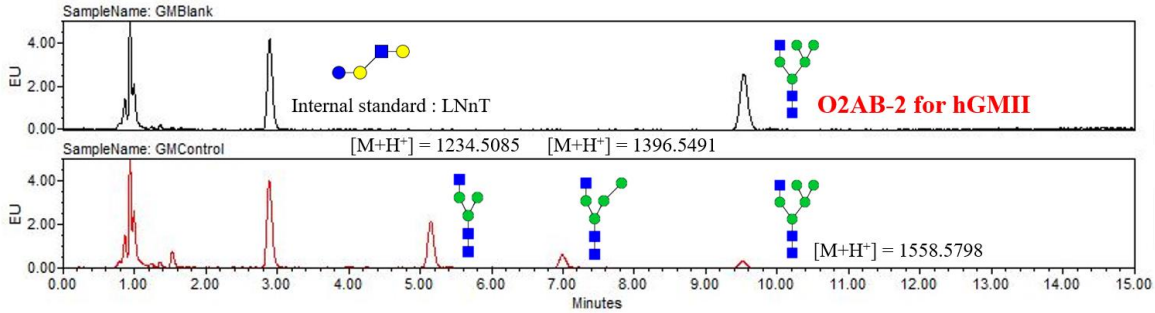

Figure 2. 14 Analysis of the digestion of **O2AB-2** by the hLM

In summary, the assay platform of the oligosaccharides-based substrate toward hGMII and hLM established to investigate the enzyme activity by UPLC. It's noteworthy that the centrifugation is a very important step before the sample injection to avoid the needle

doi:10.6844/NCKU201900656

blocking to influence the processing of analysis. In fact, we tried different concentrations of the enzyme to find the best condition to observe the percentage of the residual substrate, which calculated by the ratio of the internal standard (Figure 2.15). By the concept of enzyme inhibition, the peak area of the substrate will increase to show the property of potential inhibitors. Thus, the potential selective inhibitor 7b-6c screened out by 4-mu substrate assay will be used in this assay platform to prove the concept of characterization about the properties of selectivity and inhibition.

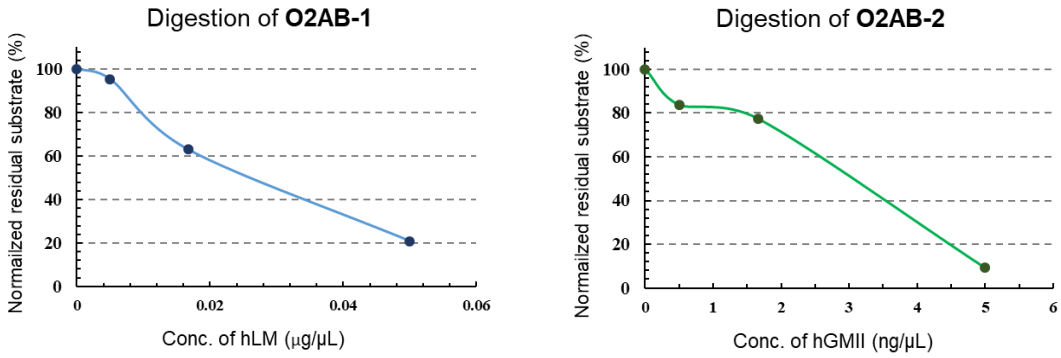

Figure 2. 15 Adjustment of the concentrations of hLM and hGMll digestion

2.2.4 Characterization of the potential inhibitor against hGMII by O2AB substrate

By the results of preliminary work, the IC_{50} value of **7b-6c** was 100 nM to challenge the selectivity and inhibition of O2AB substrate assay. At the same time, the swainsonine and the **1i-Ec** involved in the comparison of the selective inhibition[103]. Compound **1i-Ec** is the ADMDP analog, which is the potent competitive inhibitor described in the previous work (Figure 2.16). The property of inhibition of **1i-Ec** against hGMII has been shown, but the issue of selectivity toward the hLM and hGMII has not been investigated extensively.

doi:10.6844/NCKU201900656

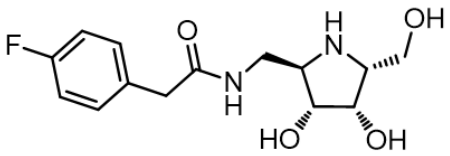

IC_{50} = 300 nM
Competitive inhibitor of
hGMII with 4MU-Man.

1i-Ec

Figure 2. 16 The potent hGMII inhibitor in previous works of our lab

Three compounds, **swainsonine**, **7b-6c** and **1i-Ec,** treated the same concentration 100nM in the reaction of hLM and hGMII catalyzed to observe the percentage of the residual substrate. Although swainsonine was the best inhibitor against hLM (68%) and hGMII (95%) in 100 nM, the selectivity between these two enzymes were poor. On the other hand, **1i-Ec** showed the worst results of inhibition and selectivity toward hLM and hGMII. Notably, **7b-6c** has a better inhibition against hGMII and showed the best selectivity toward hLM and hGMII (Figure 2.17). As a result, the O2AB substrate assay could be used in the characterization of selective inhibition against hGMII to further confirm the property of the potent small molecules in the real situation.

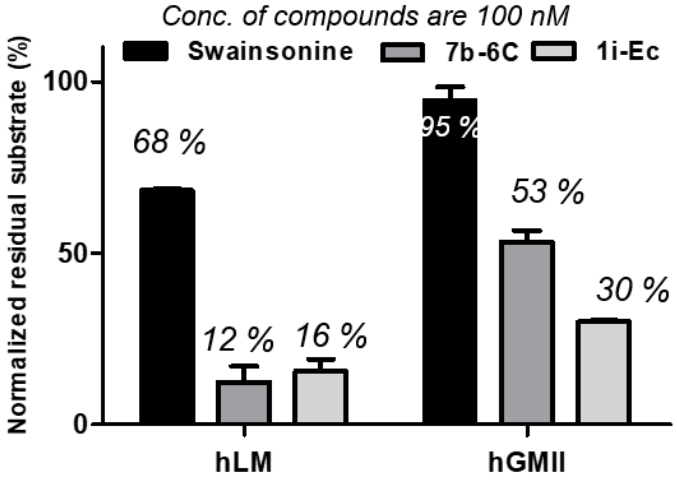

Figure 2. 17 The property of selective inhibition against hGMII by O2AB substrate assay

doi:10.6844/NCKU201900656

2.2.5 Comparison of the enzyme kinetic assay about the different substrates

Currently, we were curious about the results of different substrates used in the enzyme kinetic studies. The O2AB-substrate assay evaluates the IC_{50} value of **7b-6c** and swainsonine toward hGMII and hLM compared with the 4MU-substrate assay (Table 2.1). The inhibition results of 7b-6c were determined to be 10 μM (hLM) and 0.1 μM (hGMII), revealing an encouraging selectivity for hGMII (100 fold), but the selectivity was silmiar to the 4MU-substrate assay (130 fold). On the other hand, the selectivity of swainsonine in the O2AB-substrate assay (4.4 fold) is even worse than the 4MU-substrate assay (12.5 fold). The different results between the O2AB-substrate assay and 4MU-substrate assay were the important information of the differentiation about the real situation. The results described by O2AB-substrate assay could explain the swainsonine-induced high-mannose glycan accumulated in the lysosome is about the poor selectivity and high inhibition against hLM and hGMII. Fortunately, the compound **7b-6c** is remaining the best selectivity and better inhibition against the hGMII to prove the preliminary works about the molecule design and the library screening.

Table 2. 1 Inhibition studies in different substrate assays

Compound	**Inhibition activity (IC_{50} in μM)**		Selectivity index (hLM/hGMII)
	α-hLM (pH 4.6)	α-hGMII (pH 7.0)	
7b-6C	**10**[a]	**0.1**[a]	**100**[a]
	13[b]	**0.1**[b]	**130**[b]
Swainsonine	0.025[a]	0.005[a]	4.4[a]
	0.2[b]	0.016[b]	12.5[b]

[a]O2AB-substrate, [b]4MU-substrate

doi:10.6844/NCKU201900656

With the promising results of selective inhibition of 7b-6c against hGMII, the binding mode of **7b-6c** and hGMII using 4-MU substrate was investigated. Unexpectedly, from the Lineweaver-Burk plots of **7b-6c** inhibition of hGMII, **7b-6c** was found to inhibit the enzyme in a non-competitive manner with K_i value of 105 nM. On the other hand, the Michaelis-Menten equation also showed the different V_{max} to determine the **7b-6c** is the non-competitive inhibitor against hGMII (Figure 2.18).

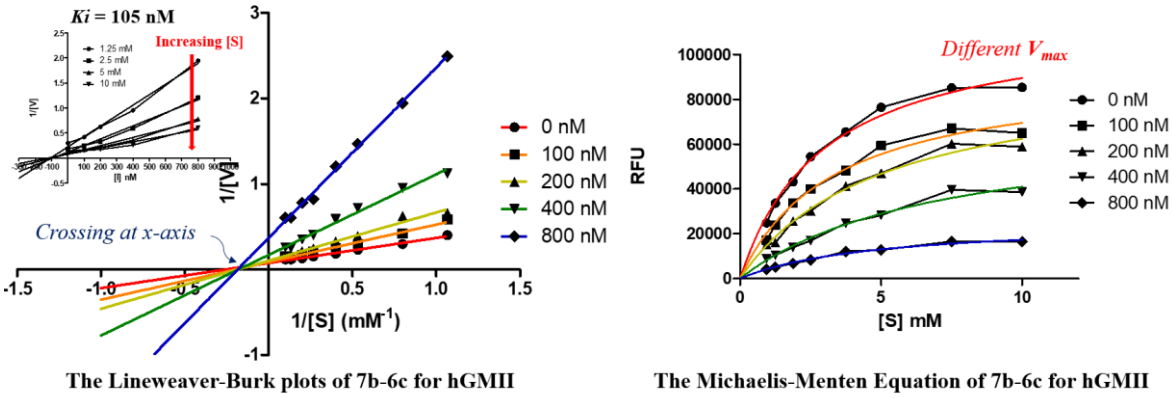

Figure 2. 18 Enzyme kinetic study of **7b-6c** by 4MU-substrate assay. The increasing concentrations of substrate were used to determine the Ki values and the data were plotted as 1/v versus 1/[S]

The kinetic analysis of 4MU-substrate assay indicated that **7b-6c** is bound to the other site, not the catalytic site so that 4MU-substrate can no longer fit there. Thus, O2AB-substrate assay was used to further display the interaction of 7b-6c with **hGMII** in mimicking a more realistic situation. Interestingly, the results of enzyme kinetic by using O2AB-substrate was a competitive manner with K_i value of 43 nM (Figure 2.19). Meanwhile, the different result showed by the kinetic analysis of O2AB-substrate assay that **7b-6c** is bound to the active site to compete with the oligosaccharides-based substrate. Although the result displayed the non-competitive manner by using 4MU-substrate, the **7b-6c** is not bound

doi:10.6844/NCKU201900656

to the allosteric site due to the results of O2AB-substrate assay. Even though the different binding modes described by 4MU-substrate and O2AB-substrate assay, the exact binding site of **7b-6c** will study by utilizing computational docking to understand about interactions between enzyme and inhibitor in detail.

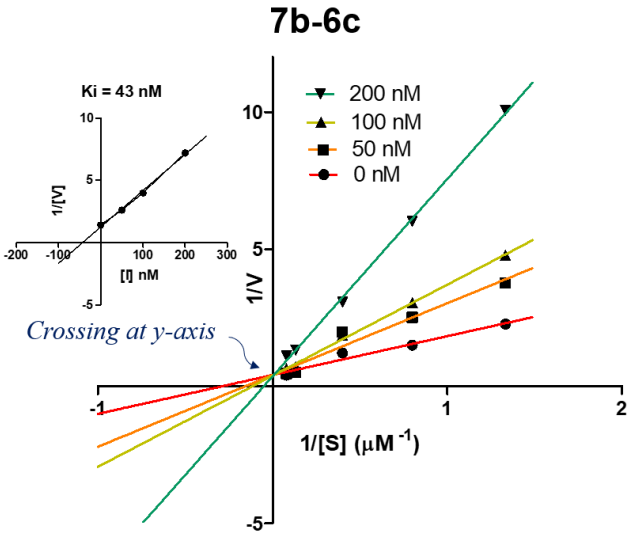

Figure 2. 19 Enzyme kinetic study of **7b-6c** by O2AB-substrate assay. The increasing concentrations of substrate were used to determine the Ki values and the data were plotted as 1/v versus 1/[S]

Future perspective

With the information of the enzyme kinetic analysis by different assay platforms, we are curious about the interactions between enzyme and inhibitor. The binding modes of **7b-6c** about the different enzyme kinetic results between the 4MU and O2AB-substrate will be studied by utilizing computational docking or co-crystal. By the way, the evaluation of the anti-cancer activity of **7b-6c** is on-going to challenge the potencies of the cell toxicity and cell metastasis. Moreover, we hope the potential selective inhibitor can reduce the accumulation of high mannose type glycans in the lysosome to improve the side effect to be the potential cancer therapeutic agent.

doi:10.6844/NCKU201900656

2.3. Sub-summary

We have successfully prepared the labeled oligosaccharide-based substrate by chemical tag, 2AB to enhance the sensitivity. The prepared **O2AB-1** as the substrate to treat the GnT-I obtained the **O2AB-2** as the substrate of hGMII by the chemoenzymatic synthesis in good yield. By using these oligosaccharide-based substrates, we successfully established the oligosaccharides-based substrate assay called O2AB-substrate assay to characterize the property of selective inhibition. Establishment of the O2AB-substrate assay is higher cost and time consuming compared with the 4MU-substrate, but the O2AB-substrate assay was an important experiment to characterize the potency of selective inhibitors. Moreover, the 4MU-substrate is suitable for the preliminary screening, and the O2AB-substrate assay is us mimicking the real condition of enzyme inhibition. Based on the preliminary works, the potential selective inhibitors against hGMII, **1i-Ec** and **7b-6c** are investigated by the O2AB-substrate assay to obtain the precise bio-evaluation. Swainsonine show it ability as the most potent inhibitor against hLM and hGMII, but show the poor selectivity to resulting in the accumulation of high-mannose type glycan. Compound **1i-Ec** has no significant potency toward the inhibition or selectivity; Moreover, **7b-6c** has a better inhibition against hGMll and the best selectivity toward hLM and hGMII (100-fold). Comparison with the 4MU-substrate assay, the selectivity of **7b-6c** is decreased slightly by O2AB-substrate assay, but the swainsonine is showed the lower selectivity in using oligosaccharide-based substrate. However, the artificial substrate (4MU-substrate) between the nature substrate (O 2AB-substrate) have different influences in the interaction of enzyme and inhibitor. The enzyme kinetic analysis by the different substrates showed the different binding mode toward the same inhibitor **7b-6c** against hGMII. By the interest results of the different binding modes, **7b-6c** presumably binds in the active site which is a complicated binding pocket for the oligosaccharide-based substrate, and not bind in the catalytic site and allosteric site. With

doi:10.6844/NCKU201900656

this information in hand, computational docking will be further utilized to demonstrate the binding mode of **7b-6c** in the condition of 4-MU or O2AB substrate in the future. Furthermore, the potential selective inhibitor against hGMII, **7b-6c** will challenge the anti-cancer activity and improve the accumulation of high-mannose-type glycans in the lysosome.

doi:10.6844/NCKU201900656

Chapter 3 Experimental Section

3.1 Abbreviation

(1) LSD : Lysosomal storage disease; (2) GAG : glycosaminoglycan; (3) ERT : Enzyme replacement therapy; (4) MPS : Mucopolysaccharidsis; (5) IDS : Iduronate-2-sulfatase; (6) IDUA : Iduronidase; (7) HS : Heparan sulfate; (8) DS : Dermatan sulfate; (9) CS : Chondroitin sulfate; (10) KS : Keratan sulfate; (11) GlcA : Glucuronic acid; (12) IdoA : Iduronic acid; (13) Glc : Glucose; (14) GlcN : Glucosamine; (15) GlcNAc : N-aectylglucosamine; (16) Xyl : Xylose; (17) Man : Mannose; (18) ZFN : Zinc-finger nucleases; (19) PC : Pharmacological chaperone; (20) 4MU : 4-Methylumbelliferone or 4-Methylumbelliferyl; (21) HSPG : Heparan sulfate proteoglycan; (22) HCl : Hydrochloric acid; (23) NaCl : Sodium chloride; (24) DAD : Diode-array detector; (25) HPLC : High performance liquid chromatography; (26) LC : Liquid chromatography; (27) LCMS/MS : Liquid chromatography tandem mass spectrometry; (28) NRE : Non-reducing end; (29) ABEE : p-aminobenzoic ethyl ester; (30) NAIM : 2,3-naphthalenediamine; (31) AcOH : Acetic acid; (32) I_2 : Iodine; (33) rt : room temperature; (34) 2AB : 2-Aminobenzamide; (35) $NaBH_3CN$: Sodium cyanoborohydride; (36) DMSO : Dimethyl sulfoxide; (37) PMP : 1-phenyl-3-methyl-5-pyrazolone; (38) NaOH : Sodium hydroxide; (39) Ac_2O : Acetic anhydride; (40) MeOH : Methanol; (41) NBS : N-Bromosuccinimide; (42) $CHCl_3$: Chloroform; (43) Bu_3SnH : Tributyltin hydride; (44) AIBN : Azodiisobutyronitrile; (45) THF : Tetrahydrofuran; (46) LiOH : Lithium hydroxide; (47) TLC : Thin-layer chromatography; (48) HRMS : High resolution mass spectrometry; (49) NMR : Nuclear magnetic resonance; (50) ECM : Extracellular matrix; (51) GnT : N-acetylglucosaminyltransferase; (52) UDP : Uridine diphosphate; (53) HILIC : Hydrophilic interaction liquid chromatography; (54) SPE : Solid phase extraction; (55) MALDI-TOF-MS : Matrix-assisted laser desorption/ ionization time of flight mass spectrometry: (56)

doi:10.6844/NCKU201900656

LNnT : Lacto-N-neotetraose; (57) UPLC : Ultra performance liquid chromatography; (58) NA2 : Galactosylated biantennary complex N-glycan

3.2 General information

All chemicals were obtained from commercial suppliers and used without further purification. Reactions were magnetically stirred and monitored by thin-layer chromatography on silica gel. Silica gel was used Merck Kiseslgel Si60 (40-63 μm). Thin-layer chromatography (TLC) was performed on glass plates coated to a thickness of 1 mm with Merck Kieselgel 60F254. NMR spectra were recorded on dilute solutions in $CDCl_3$, CD_3OD, DMSO-d_6, and D_2O on Bruker AVANCE 600 and AMX 400 spectrometers at ambient temperature. Chemical shifts are given in δ values, and coupling constant *J* are given in Hz. The splitting patterns are reported as s (singlet), d (doublet), t (triplet), q (quartet), m (multiplet), dd (double of doublets), dt (double of triplets), dq (double of quartets), br (board). High-resolution ESI mass spectra were recorded on a Bruker Daltonics spectrometer. Concentration refers to rotary evaporation.

doi:10.6844/NCKU201900656

3.3 Procedures of Chapter 1

Part A

Enzyme kinetic assay

The initial velocities of hydrolysis at 37 ºC were measured spectrophotometrically at various concentrations of 4-MU substrate at 355 nm excitation and 460 nm emission using multi-detection reader (SpectraMax M5, Molecular Device). The data obtained were fitted to the Michaelis–Menten equation using the GraphPad to determine the Km values and V_{max} values. The 5 μL 2 mM 4-methylumbelliferyl-α-L-iduronate 2-sulfate is 2x diluted by reaction buffer (0.1 M sodium acetate, pH 5.0, 10 mM lead Acetate and 0.02 % sodium azide) in the black-bottom 384-wells plate, and added 10 μl 0.5 μg/mL recombinant human iduronate-2-sulfatase (rhIDS) to each wells. The reaction mixtures were incubated at 37 ºC for 1 h, whereafter 10 μL 0.5 μg/mL recombinant human iduronidase in McIlvain's buffer (0.4 M sodium acetate and 0.2 M citric acid, pH 4.5) were added and the second incubation of 1h at 37 ºC was carried out. Reaction mixtures were terminated by the addition of 80 μL stop solution (0.4 M K_2CO_3, pH 10.6) and the fluorescence of 4-methylumbelliferone (4MU) was determined at 355 nm excitation and 460 nm emission.

Thermal shift assay

The stability of rhIDS was assessed using a modified fluorescence thermal stability assay on a Rotor-Gene system in acidic buffer (0.1 M sodium phosphate, 0.05 M citric acid, pH 4.6), neutral buffer (0.1 M sodium phosphate, pH 7.4) and basic buffer (0.1 M sodium phosphate, pH 8.5). Briefly, rhIDS (4 μg) was combined with 20x SYPRO Orange in a final reaction volume of 20 λ. A thermal gradient was applied to the plate at a rate of 1 °C per minute, during which time the fluorescence of SYPRO Orange was continuously monitored. The fluorescence intensity at each temperature was normalized to the maximum fluorescence

doi:10.6844/NCKU201900656

after complete thermal denaturation

In vitro stabilization of rhIDS activity

An assessment of the different pH values incubated with IDS against denaturation was performed by using Idursulfase (rhIDS). The 10λ 20 μg/mL rhIDS aliquots were incubated with acidic buffer (0.1 M sodium acetate, pH 4.6) and neutral buffer (0.1 M sodium acetate, pH 7.0) at 60 °C as a function of time in an attempt to heat-inactivate (denature) rhIDS. The samples were diluted into ten-fold volume of reaction buffer (0.1 M sodium acetate, pH 5.0, 10 mM lead Acetate and 0.02 % sodium azide). The 5μL samples was immediately incubated with 5μL substrate (0.5 mM 4-methylumbelliferyl-α-L-iduronate 2-sulfate)in black-bottom 384-wells plate for 1 h at 37°C, whereafter 10 μL 4 μg/mL recombinant human iduronidase in McIlvain's buffer (0.4 M sodium acetate and 0.2 M citric acid, pH 4.5) were added and the second incubation of 1h at 37 ºC was carried out. Reaction mixtures were terminated by the addition of 80 μL stop solution (0.4 M K_2CO_3, pH 10.6) and the fluorescence of 4-methylumbelliferone (4MU) was determined at 355 nm excitation and 460 nm emission. Enzyme activity was reported relative to the unheated enzyme.

Cell cultures

Human normal fibroblast (C015) and MPS (GM00615) patient fibroblast were cultured in DMEM (Dulbecco's modified Eagle's medium; Gibco) supplemented with 10% heat-inactivated FBS, 2 mM L-Glutamine, 1 mM sodium pyruvate and 1% Non-essential amino acids. All the cells used for biological evaluation was at 1-30 passage.

doi:10.6844/NCKU201900656

The procedure of intracellular enzyme activity assay for Normal fibroblast and patient fibroblast

MPS II patient fibroblast (GM00615) and Normal fibroblast (C015) were seeded in the sterile clear-bottom 24-wells plate at a number of 50000 cell / well and incubated at 37 ºC and 5% CO_2 for 24 h. The enzyme assay was performed: after being washed third times with PBS, the cells were homogenized in 30 λ 0.1% triton X 100 in pH 4.6 buffer (0.1 M sodium acetate) or 0.1% triton X 100 in pH 7.4 RIPA buffer (50 mM Tris-HCl, 50 mM NaCl). The 10 λ of samples were incubated at 37 ºC for 4 h with 20 λ 1.25 mM 4-methylumbelliferyl-α-L-iduronate 2-sulfate in reaction buffer (0.1 M sodium acetate, pH 5.0, 10 mM lead Acetate and 0.02 % sodium azide) for enzyme assay. Then, the 50 μL 4 μg/mL recombinant human iduronidase in McIlvain's buffer (0.4 M sodium acetate and 0.2 M citric acid, pH 4.5) were added and the second incubation of 24 h at 37 ºC was carried out. Reaction mixtures were terminated by the addition of 200 μL stop solution (0.4 M K_2CO_3, pH 10.6) in the black-bottom 96-wells plate and the fluorescence of 4-methylumbelliferone (4MU) was determined at 355 nm excitation and 460 nm emission. Raw fluorescence counts were background subtracted, as defined by counts from substrate solution only. A MicroBCA Protein Assay Kit was used to determine protein concentration. 4-methylumbelliferone (4-MU) standard curve ranging from 0 μmol/L to 200 μmol/L was run in the parallel day for the conversion of fluorescence data to absolute rhIDS activity expressed as nmol/mg protein per h.

doi:10.6844/NCKU201900656

The rhIDS activity enhancement assay in MPS II patient fibroblast with co-administration of Idursulfase and disaccharides derived from heparin

MPS II patient fibroblast (GM00615) were seeded in the sterile clear-bottom 24-wells plate at a number of 50000 cell / well and incubated at 37 ºC and 5% CO_2 for 24 h. The cells were then incubated with Idursulfase (3 nM) alone, compounds alone (30 nM **D2S0**, **D2S6**), or Idursulfase (3 nM) and **D2S0, D2S6** (30 nM) for 24 h. The cells were washed three times with growth medium, and then maintained in fresh growth medium at 37 ℃, 5% CO_2 for 24 h. The enzyme assay was performed: after being washed third times with PBS, the cells were homogenized in 30 λ 0.1% triton X 100 in pH 4.6 buffer (0.1 M sodium acetate). The 10 λ of samples were incubated at 37 ºC for 4 h with 20 λ 1.25 mM 4-methylumbelliferyl-α-L-iduronate 2-sulfate in reaction buffer (0.1 M sodium acetate, pH 5.0, 10 mM lead Acetate and 0.02 % sodium azide) for enzyme assay. Then, the 50 μL 4 μg/mL recombinant human iduronidase in McIlvain's buffer (0.4 M sodium acetate and 0.2 M citric acid, pH 4.5) were added and the second incubation of 24 h at 37 ºC was carried out. Reaction mixtures were terminated by the addition of 200 μL stop solution (0.4 M K_2CO_3, pH 10.6) in the black-bottom 96-wells plate and the fluorescence of 4-methylumbelliferone (4MU) was determined at 355 nm excitation and 460 nm emission. Raw fluorescence counts were background subtracted, as defined by counts from substrate solution only. A MicroBCA Protein Assay Kit was used to determine protein concentration. 4-methylumbelliferone (4-MU) standard curve ranging from 0 μmol/L to 200 μmol/L was run in the parallel day for the conversion of fluorescence data to absolute rhIDS activity expressed as nmol/mg protein per h.

doi:10.6844/NCKU201900656

HPLC-based assay of characterization of four disaccharides in the reaction treated by rhIDS from the disaccharide standards

Four disaccharide standards (**D2S0**, **D2S6**, **D0S0**, **D0S6**, 1 mM) were analyzed by HPLC equipped by analytical anion exchange column (LC-SAX1, 250mm, 4.6 mm, Supelco Co.) a constant flow rate of 1 ml/min. Solvent A was the water that adjusted to the pH 3.5 by 1N HCl, and solvent B was the 2M NaCl aqueous and also acidified to pH 3.5. After injection of 10 μL of samples, the 100% solvent A over 4 min, then the linear gradient of 50% B was applied in the following 40 min. Finally, 20 min of initial conditions was applied to reequilibrate the column for further analyses. Detection was carried out at 232 nm.

In the rhIDS-treated sample preparation, the **D2S0** or **D2S6** (1mM) are incubated with the 1 μg/mL rhIDS in a final reaction volume of 20 λ at 37 ºC for 2 h. Reaction mixtures were terminated by C4-tip (Merck Co. ZTC04S008) to remove the enzyme and inject 10 μL sample into the HPLC follow the condition described above.

The protocol of clean-up by C4-tip; the tip was equipped on the 20μL pipette and activated by drawing twice of acetonitrile, then equilibrated by drawing twice of 0.1 %TFA aqueous. Next, the C4-tip pipetting the sample several times to clean up the mixture, whereafter the C4-tip was regenerated by drawing twice of 0.1 %TFA aqueous to 50% acetonitrile in 0.1% TFA aqueous to 100% acetonitrile sequentially.

doi:10.6844/NCKU201900656

Part B

The HS methanolysis digestion in the cell-basd assay by LCMS/MS

The preparation of 3N HCl in methanol or methanol-d_4 were performed by dropwise of acetyl chloride (220 μL) into methanol or methanol-d_4 (1 mL) on ice. In the model reactions, the 500 μg heparan sulfate standard is added 500 μL 3N HCl in methanol, and 25 μL 2,2-dimethoxypropane which reduced the formation of side products at 65 ºC for 1.5 h. The mixtures were dried by nitrogen and reconstitution of 500 μL ammonium acetate (10 mM). The reconstituted fluids were filtrated and centrifuged by using a 3 kDa Amicon filter in 12,000 rpm for 30 minutes. After this, the sample is lyophilized overnight and ready for LC-MS/MS analysis. Separation of methylated HS products based on a ZIC-cHILIC (HPLC column 1mm x 15 cm i.d., 3 μm particle size, 100Å pore size). LCMS was achieved with a Agilent 1100 Series binary high-performance liquid chromatography pump (Agilent Technologies, Palo Alto,CA), and a Famos autosampler (LC Packings, San Francisco, CA). The mobile phase was prepared by mixing solvents **A**) water (100%; 0.1% formic acid) and **B**) acetonitrile (100%; 0.1% formic acid). The required composition was produced by mixing these solvents. In the beginning, the gradient consisted of 2% **A** for 2.0 min, and then it was linearly converted to a gradient of 98% **A** over 11 min. Then, 98% **A** was kept for 2 min to clean the column, and then the column was equilibrated back to initial conditions with 2% **A** for 5 min. The mobile phase was pumped at a flow rate of 0.1 mL/min. The sample was reconstituted by 60 μL DMSO and the sample injection volume was 5 μL. MS spectra of the methylated HS products were obtained with a Velos Pro dual-pressure linear ion trap mass spectrometer from Thermo Fisher Scientific (San Jose, CA, US). The Velos Pro LTQ mass spectrometer was operated in positive mode. The sample was eluted into the mass spectrometer by using an online electrospray ionization source. All spectra were acquired in the mass range m/z 200–1500. For MS/MS experiments, the precursor ion was

doi:10.6844/NCKU201900656

selected (m/z = 390.2 or 384.2 to 161.9) within a selected mass window of 5 Da and the setting of collision energy is 35%. The data were analyzed by using the analysis software Xcalibur 2.2.

In the preparation of cell samples, the different amounts of normal fibroblast and MPS II fibroblast are lyzed by the beads crusher in 2000 rpm for 10 min. The cell samples are lyophilized overnight, then the 200 μL 3N HCl in methanol and 10 μL 2,2-dimethoxypropane at 65 ºC for 1.5 h and the mixtures were dried by nitrogen and reconstitution of 500 μL ammonium acetate (10 mM). The reconstituted fluids were filtrated and centrifuged by using a 3 kDa Amicon filter in 12,000 rpm for 30 minutes. After this, the sample is lyophilized overnight and ready for LC-MS/MS analysis.

In the rapid analysis of small molecule evaluation, the $1x\ 10^4$ MPS II patient fibroblast (GM00615) was seeded in the sterile clear-bottom 96-wells plate at a number of 10000 cell / well and incubated at 37 ºC and 5% CO_2 for 24 h. Then, the cells were then incubated with Idursulfase (0.3-30 nM), genistein (2 μM – 200 μM) for 24 h. The assay was performed: Remove the medium, then washed third times with PBS and the cells were homogenized in 100 μl water containing 0.1% triton X in 1 h on the plate shaker. The cell lysates were transferred to the 96-deep-well plate and dried by the Speed Vac or lyophilizer, then the 100 μL 3N HCl in methanol and 5 μL 2,2-dimethoxypropane at 65 ºC for 1.5 h and the mixtures were dried by Speed Vac (50 torrs, 40ºC, 1h) and reconstitution of 100 μL ammonium acetate (10 mM). The reconstituted fluids were filtrated and centrifuged by using a 3 kDa Amicon filter in 12,000 rpm for 30 minutes. After this, the sample is lyophilized overnight and ready for LC-MS/MS analysis.

doi:10.6844/NCKU201900656

3.4 Preparation and characterization of compounds Chapter 1

General procedure for preparation of PMP-labeled compound

Preparation of compound 1'

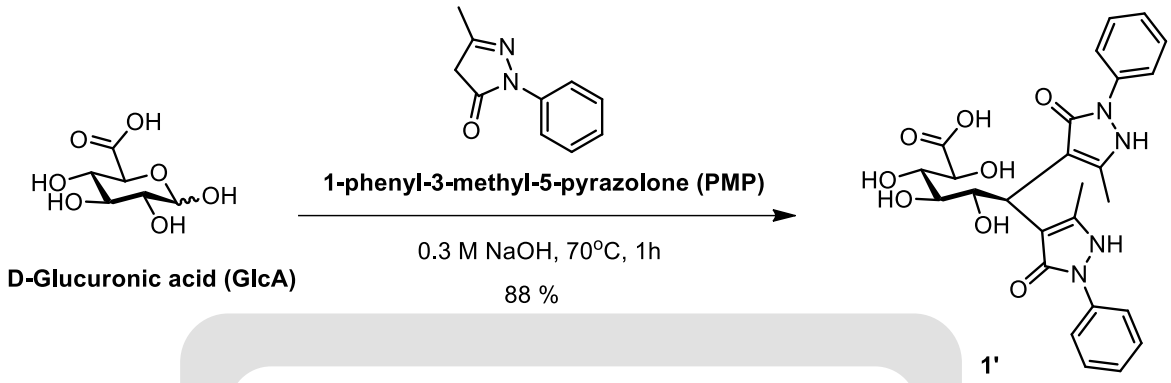

A mixture of D-Glucuronic acid (200 mg, 1.0 mmol) in 0.3 M NaOH aqueous (10 mL) was added 0.5 M methanolic solution of PMP (10 ml) at 70°C for 1h. The reaction was neutralized with 3 M HCl aqueous (300 μL), and concentrated. The residue was purified by flash column chromatography (silica gel, chloroform/methanol/water, 40/10/1, v/v) to give compound **1'** as a brown solid (462 mg, 88%). ^{1}H NMR (600 MHz, DMSO-d_6) δ 7.83 (dd, 4H, J = 8.2, 11.5 Hz), 7.34 (m, 4H), 7.09 (dd, 2H, J = 7.6, 10.2 Hz), 4.42 (d, 1H, J = 9.7 Hz), 3.78 (d, 1H, J = 7.2 Hz), 3.64 (d, 1H, J = 9.7 Hz), 3.57 (d, 1H, J = 7.2 Hz), 3.55 (s, 1H), 2.13 (s, 3H), 2.12 (s, 3H). ^{13}C NMR (150 MHz, DMSO-d_6) δ 175.2, 158.0, 156.6, 147.1, 146.6, 139.8, 139.5, 128.5, 128.4, 123.7, 123.6, 119.5, 119.4, 102.3, 101.5, 75.9, 72.9, 71.1, 68.1, 33.1, 12.7, 12.6. HRMS calcd for $[C_{26}H_{28}N_4O_8+H]^+$ 525.1980, found 525.1977.

doi:10.6844/NCKU201900656

Preparation of compound 2'

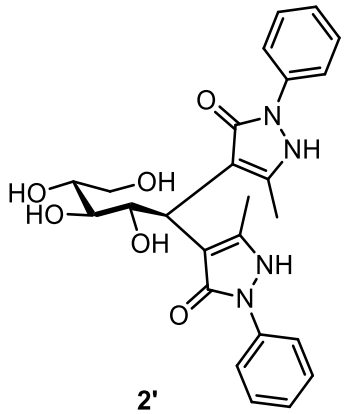

2'

The preparation was accorded on General procedure. D-Xylose (200 mg, 1.3 nnmol) was used to give compound **2'** as a brown solid (530 mg, 85%). ^{1}H NMR (600 MHz, MeOD) δ 7.57 (dd, 4H, *J* =8.0, 8.4 Hz), 7.35 (q, 4H, *J* = 8.0 Hz), 7.18 (q, 2H, *J* = 7.5 Hz), 4.64 (d, 1H, *J* = 10.1 Hz), 3.97 (d, 1H, *J* = 10.1 Hz), 3.76 (t, 1H, *J* = 5.3 Hz), 3.63 (dd, 1H, *J* = 4.6, 11.3 Hz), 3.52 (dd, 1H, *J* = 6.3, 11.3 Hz), 3.47 (d, 1H, *J* = 4.5 Hz), 2.27 (s, 3H), 2.26 (s, 3H). ^{13}C NMR (150 MHz, MeOD) δ 160.0, 158.1, 148.8, 148.5, 138.5, 138.1, 130.0, 129.9, 127.5, 127.4, 123.0, 122.9, 105.5, 104.3, 75.5, 71.7, 71.6, 64.0, 58.3, 49.9, 34.4, 18.4, 12.0, 11.6. HRMS calcd for $[C_{25}H_{28}N_4O_6+H]^+$ 481.2082, found 481.2077.

Preparation of compound 3'

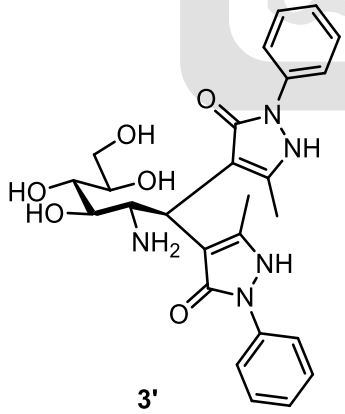

3'

The preparation was accorded on General procedure. D-Glucosamine hydrochloride (200 mg, 0.9 nnmol) was used to give compound **3'** as a yellow solid (366 mg, 80%). ^{1}H NMR

doi:10.6844/NCKU201900656

(600 MHz, MeOD) δ 7.73 (d, 2H, J = 8.2 Hz), 7.69 (d, 2H, J = 8.1 Hz), 7.39 (t, 4H, J = 7.8 Hz), 7.20 (q, 2H, J = 7.2 Hz), 4.20 (d, 1H, J = 5.9 Hz), 4.07, (s, 1H), 4.00 (d, 1H, J = 8.8 Hz), 3.73 (d, 1H, J = 12.0 Hz), 3.67, (m, 1H), 3.61 (d, 1H, J = 12.0 Hz), 2.20 (s, 6H). ^{13}C NMR (150 MHz, MeOD) δ 159.6, 158.9, 148.9, 148.5, 140.4, 139.9, 129.7, 129.7, 126.6, 126.3, 123.0, 122.9, 102.0, 99.1, 74.8, 72.8, 67.9, 64.5, 57.4, 32.5, 12.6, 12.5 HRMS calcd for $[C_{26}H_{31}N_5O_8+H]^+$ 510.2347, found 510.2348.

Overall scheme of preparation of L-IdoA

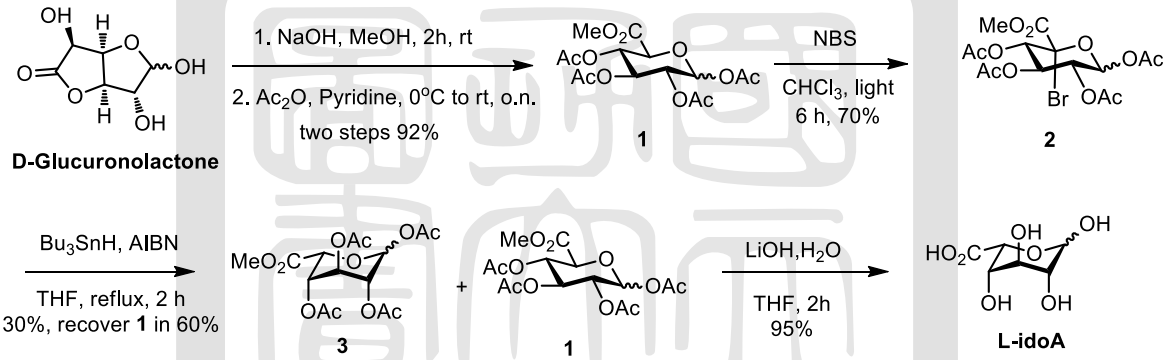

Preparation of compound 1

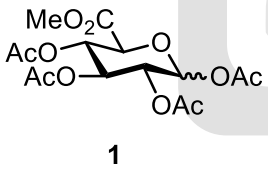

1

D-glucuronolactone (50.0 g, 283.9 mmol) and NaOH (120 mg, 0.01 equiv) in MeOH (350 mL) was stirred at room temperature for 2 h. The reaction was neutralized with HOAc (300 μL), and then MeOH was removed in vacuo. The residue was added pyridine (370 mL, 16 equiv) and Ac_2O (214 mL, 8 equiv) at 0 ºC and stirred overnight. After evaporation in vacuo, the residue was purified by flash column chromatography (silica gel, hexanes/ethyl acetate 1/1, v/v) to give **1** as a white solid (98.2 g, 92%). The beta form can be obtained from

doi:10.6844/NCKU201900656

recrystallization in hot ethanol to get (45.1 g). Beta form: ^{1}H NMR (600 MHz, $CDCl_3$) δ 5.76 (d, 1H, *J* = 7.8 Hz), 5.30 (dd, 1H, *J* = 9.0, 9.3 Hz), 5.24 (dd, 1H, *J* = 9.3, 9.5 Hz), 5.14 (dd, 1H, *J* = 7.8, 9.0 Hz), 4.17 (d, 1H, *J* = 9.5 Hz), 3.74 (s, 3H), 2.11 (s, 3H), 2.03 (s, 6H), 2.02 (s, 3H); ^{13}C NMR (150 MHz,$CDCl_3$) δ 170.2, 169.7, 169.4, 169.0, 167.0, 91.6, 73.2, 72.0, 70.3, 69.1, 53.3, 21.0, 20.8, 20.7. HRMS calcd for $[C_{15}H_{20}O_{11}+Na]^+$ 399.0910, found 399.0898.

Preparation of compound 2

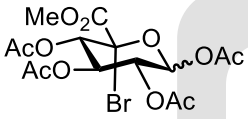

2

A mixture of **1** (10.0 g, 26.6 mmol) and NBS (18.9 g, 4 equiv) in dry $CHCl_3$ (90 mL) was stirred for 1.5 h under irradiation with one 250W tungsten light blub. The reaction was quenched with 10% aqueous $Na_2S_2O_3$. The organic layer was washed with 10% aqueous $Na_2S_2O_3$, brine, dried over anhydrous $MgSO_4$, and concentrated. The residue was purified by flash column chromatography (silica gel, hexanes/ethyl acetate, 3/1, v/v) to to give **2** as a yellow solid (8.5 g, 70%). Beta form: ^{1}H NMR (600 MHz, $CDCl_3$) δ 6.23 (d, 1H, *J* = 8.7 Hz), 5.48 (t, 1H, *J* = 9.5 Hz), 5.27 (d, 1H, *J* = 9.5 Hz), 5.19 (dd, 1H, *J* = 8.7, 9.5 Hz), 3.79 (s, 3H), 2.09 (s, 3H), 2.04 (s, 3H), 2.00 (s, 3H), 1.97 (s, 3H); ^{13}C NMR (150 MHz, $CDCl_3$) δ 169.5, 169.0, 168.9, 168.2, 164.2, 90.8, 88.9, 70.7, 69.8, 69.1, 54.1, 20.6, 20.5, 20.4× 2.HRMS calcd for $[C_{15}H_{19}BrO_{11}+Na]^+$ 477.0001, found 477.0003.

doi:10.6844/NCKU201900656

Preparation of compound 3

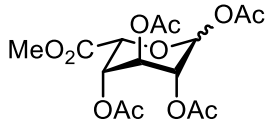

3

A mixture of **2** (8.7 g, 19.2 mmol), tributyltin hydride (44 mL, 2.5 equiv) and AIBN (723 mg, 0.23 equiv) in dry THF (64 mL) was refluxed for 45 min. After cooling and evaporation in vacuo, and the residue was treated with EtOAc and aqueous KF for 20 min. The mixture was filtered through Celite, the filtrate was concentrated, and purified by flash column chromatography (silica gel, toluene/ethyl acetate, 2/1, v/v) to give **3** (2.2 g, 30%) and **1** (4.3 g, 60%) as a white solid. Alpha form: ^{1}H NMR (600 MHz, $CDCl_3$) δ 6.24 (d, 1H, J = 1.4 Hz), 5.14 (t, 1H, J = 3 Hz), 5.11 (t, 1H, J = 3.8 Hz), 4.84 (d, 1H, J = 2.7 Hz), 4.83 (t, 1H, J = 2.7 Hz), 3.76 (s, 3H), 2.10 (s, 3H), 2.08 (s, 3H), 2.07 (s, 3H), 2.05 (s, 3H); 13C NMR (150 MHz, CDCl3) δ 169.5, 169.2, 168.7, 168.2, 167.8, 90.5, 68.3, 66.8, 66.2, 65.8, 52.9, 20., 20.8 × 2, 20.7. HRMS calcd for $[C_{15}H_{20}O_{11}+Na]^+$ 399.0801, found 399.0898.

Preparation of L-idoA

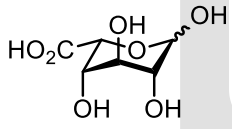

L-idoA

A mixture of **3** (400 mg, 1 mmol) in THF (5 mL) was added LiOH (2M aqeous solution, 500 μL, 1 equiv) at 0 ºC and was stirred for 2 h. The reaction was adjusted pH value to approximately 7 by adding DOWEX 50WX8-200 ion-exchange resin. The mixture was filtered, the filtrate was concentrated and purified by column chromatography (silica gel, *n*-propanol/water, 5/1. v/v) to give **L-idoA** as a yellow solid (184 mg, 95%). NMR analysis indicates that the compound exists as a mixture of anomers of both pyranose and furanose in D2O. Beta form pyranose: ^{1}H NMR (600 MHz, D_2O) δ 5.05 (d, 1H, J = 1.5 Hz), 4.33 (s,

doi:10.6844/NCKU201900656

1H), 4.12 (t, 1H, J = 3.3 Hz), 3.91 (m, 1H), 3.66 (m, 1H). ^{13}C NMR (150 MHz, D_2O) δ 176.4, 92.9, 75.0, 70.7, 69.4, 69.2. alpha form pyranose: ^{1}H NMR (600 MHz, D_2O) δ 4.94 (d, 1H, J = 6.3 Hz), 4.42 (d, 1H J = 6.3 Hz), 3.78 (dd, 1H, J = 5.0, 8.0 Hz), 3.62 (t, 1H, J = 8.0 Hz), 3.35 (dd, 1H, J = 6.3, 8.0 Hz). ^{13}C NMR (150 MHz, D_2O) δ 176.2, 93.9, 75.0, 71.2,70.9, 70.8. HRMS calcd for $[C_6H_9O_7]^-$ 193.0343, found 193.0353.

doi:10.6844/NCKU201900656

3.5 Procedures of Chapter 2

Enzyme kinetic assay by 4MU-substrate

Compound **7b-6c** was diluted to give the various final concentrations, mixed with different concentrations of 4-Methylumbelliferyl α-D-mannopyranoside (4MU-Man) as substrate and human Golgi α-mannosidase II in pH 7.0 potassium phosphate buffer, then assay was carried out at 37ºC for 2 h. Reaction mixtures were terminated by the addition of 200 μL stop solution (0.4 M K_2CO_3, pH 10.6) in the black-bottom 96-wells plate and the fluorescence of 4-methylumbelliferone (4MU) was determined at 355 nm excitation and 460 nm emission. The data obtained were fitted to the Michaelis–Menten equation using the GraphPad to determine the Km values and V_{max} values, and further to determine the IC_{50} and K_i. The assays performed in black button 384-wells of the microtiter plates.

UPLC-based enzyme activity

Compounds were diluted to give the final concentration of 100 nM, mixed with O2AB-1 or OAB-2 as substrates and human lysosomal α-mannosidase in pH 4.6 buffer (0.1M sodium phosphate, 0.05M citric acid) and human Golgi α-mannosidase in pH 7.0 buffer (0.1 M potassium phosphate), then assay was carried out at 37 ºC for 24 h. Reaction mixtures were terminated by C4-tip (Merck Co. ZTC04S008) to remove the enzyme and mixed with 20 μL acetonitrile to centrifugation in 12,000 rpm for 10 minutes. The sample was injected 10 μL into the UPLC for analysis. Inhibition was performed as a relative ratio of peak areas to the internal standard. The active compounds were selected and further tested at a lower concentration to determine their IC_{50} values and K_i values.

Released glycans were analyzed by Waters Acquity UPLC equipped with Acquity UPLC Glycan BEH Amide column (2.1 mm x 150 mm, 1.7 μm) with the flow rate of 0.4 ml/min.

doi:10.6844/NCKU201900656

Solvent A was the 0.1 M ammonium formate buffer in pH 4.5 and solvent B was the 100% acetonitrile. After injection of 10 μL of samples, the 30% solvent A over 2 min, then the linear gradient of 80% solvent B was applied in the following 20 min. Finally, 5 min of initial conditions was applied to reequilibrate the column for further analyses, ,and detected by the fluorescence of 2-Aminobenzamide (2AB) was determined at 330 nm excitation and 420 nm emission.

3.6 Preparation and characterization of compounds Chapter 2

Preparation of O2AB-1

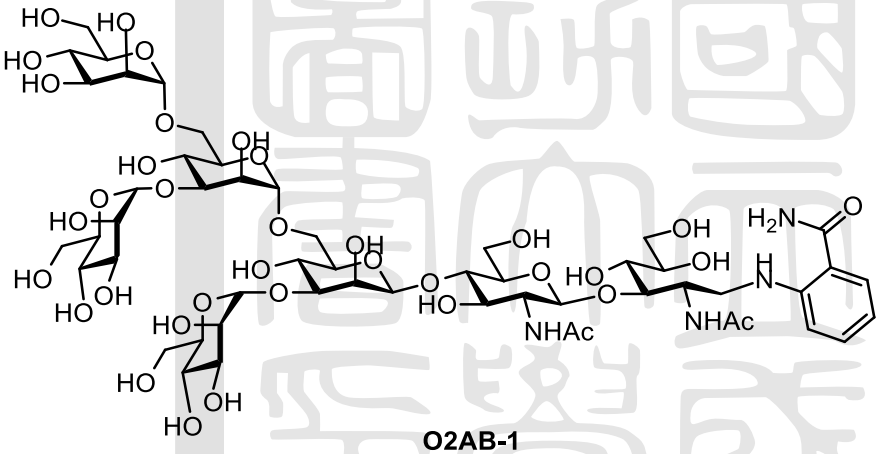

O2AB-1

A mixture of 1 mg Glyko® oligomannose 5 (Man5) in the reaction solution composed of acetic acid (15 μL) and DMSO (35 μL) was added 2-AB (2.5 mg) and $NaBH_3CN$ (3 mg) at 65°C for 3 h. The reaction mixtures were cleaned up by HILIC cartridge, then lyophilized overnight to reconstituted by water to give the final concentration of 50 μM. MALDI-TOF-MS calcd for $[C_{53}H_{86}N_4O_{36}+H]^+$ 1355.5095, found 1355.5093.

doi:10.6844/NCKU201900656

Chemoenzymatic synthesis of O2AB-2

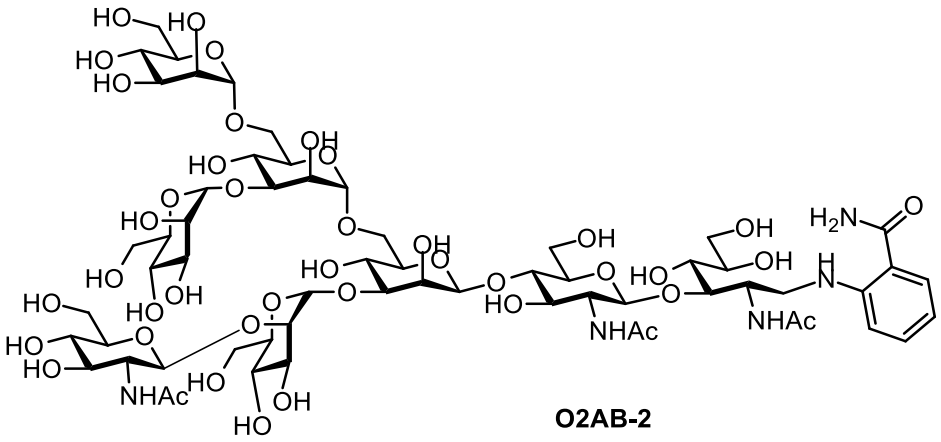

O2AB-2

A mixture of 50 μM **O2AB-1** solution (25 μL) in the reaction buffer (20 mM Hepes, 150 mM NaCl, 20 mM $MnCl_2$, pH 7.5) composed of 1 mM UDP-GluNAc (75 μL) was added the enzyme, 0.5 μg/μL GnT-I (25 μL) and incubated at 37°C for 24 h. The reaction was monitored by UPLC, and the reaction mixtures were cleaned up by HILIC cartridge, then lyophilized overnight to reconstituted by water to gave the final concentration of 50 μM. The yield was 60 % calculated by the ratio of peak areas to the internal standard, LNnT. MALDI-TOF-MS calcd for $[C_{61}H_{99}N_5O_{41}+Na]^+$ 1580.5708, found 1580.5692.

MALDI-TOF mass analysis.

For mass spectrum analysis, we mixed 1 μL of sample with 1 μl matrix solution consisting of 2, 5-dihydroxybenzoic acid (50 nmol/μL in 50% ACN). Then 1 μl of the resulting mixture was spotted onto the MALDI stainless steel sample plate and allowed to air dry at room temperature. Measurements were performed on an Ultraflex II MALDI-TOF/TOF mass spectrometer (Bruker Daltonik GmbH, Bremen, Germany). Mass spectra were obtained in the range of mass to charge ratio (*m*/*z*) from 10,000 to 30,000 with linear mode.

doi:10.6844/NCKU201900656

References

1. Dardis, A.; Buratti, E., Impact, Characterization, and Rescue of Pre-mRNA Splicing Mutations in Lysosomal Storage Disorders. *Genes (Basel)* **2018,** *9* (2).
2. Parenti, G.; Pignata, C.; Vajro, P.; Salerno, M., New strategies for the treatment of lysosomal storage diseases (review). *Int J Mol Med* **2013,** *31* (1), 11-20.
3. Coutinho, M. F.; Lacerda, L.; Alves, S., Glycosaminoglycan storage disorders: a review. *Biochem Res Int* **2012,** *2012*, 471325.
4. Chan, M. J.; Liao, H. C.; Gelb, M. H.; Chuang, C. K.; Liu, M. Y.; Chen, H. J.; Kao, S. M.; Lin, H. Y.; Huang, Y. H.; Kumar, A. B.; Chennamaneni, N. K.; Pendem, N.; Lin, S. P.; Chiang, C. C., Taiwan National Newborn Screening Program by Tandem Mass Spectrometry for Mucopolysaccharidoses Types I, II, and VI. *J Pediatr* **2019,** *205*, 176-182.
5. Lin, H. Y.; Lin, S. P.; Chuang, C. K.; Niu, D. M.; Chen, M. R.; Tsai, F. J.; Chao, M. C.; Chiu, P. C.; Lin, S. J.; Tsai, L. P.; Hwu, W. L.; Lin, J. L., Incidence of the mucopolysaccharidoses in Taiwan, 1984-2004. *Am J Med Genet A* **2009,** *149A* (5), 960-4.
6. Chang, J. H.; Lin, S. P.; Lin, S. C.; Tseng, K. L.; Li, C. L.; Chuang, C. K.; Lee-Chen, G. J., Expression studies of mutations underlying Taiwanese Hunter syndrome (mucopolysaccharidosis type II). *Hum Genet* **2005,** *116* (3), 160-6.
7. Gandhi, N. S.; Mancera, R. L., The structure of glycosaminoglycans and their interactions with proteins. *Chem Biol Drug Des* **2008,** *72* (6), 455-82.
8. Sarrazin, S.; Lamanna, W. C.; Esko, J. D., Heparan sulfate proteoglycans. *Cold Spring Harb Perspect Biol* **2011,** *3* (7).
9. Sanderson, R. D.; Elkin, M.; Rapraeger, A. C.; Ilan, N.; Vlodavsky, I., Heparanase regulation of cancer, autophagy and inflammation: new mechanisms and targets for therapy. *FEBS J* **2017,** *284* (1), 42-55.
10. Concolino, D.; Sestito, S.; Ceravolo, F.; Grisolia, M.; Pascale, E.; Pensabene, L., Profile of idursulfase for the treatment of Hunter syndrome. *Research and Reports in Endocrine Disorders* **2015**.
11. Demydchuk, M.; Hill, C. H.; Zhou, A.; Bunkoczi, G.; Stein, P. E.; Marchesan, D.; Deane, J. E.; Read, R. J., Insights into Hunter syndrome from the structure of iduronate-2-sulfatase. *Nat Commun* **2017,** *8*, 15786.
12. Hsieh, P. H.; Thieker, D. F.; Guerrini, M.; Woods, R. J.; Liu, J., Uncovering the Relationship between Sulphation Patterns and Conformation of Iduronic Acid in Heparan Sulphate. *Sci Rep* **2016,** *6*, 29602.
13. Dierks, T.; Schlotawa, L.; Frese, M. A.; Radhakrishnan, K.; von Figura, K.;

doi:10.6844/NCKU201900656

Schmidt, B., Molecular basis of multiple sulfatase deficiency, mucolipidosis II/III and Niemann-Pick C1 disease - Lysosomal storage disorders caused by defects of non-lysosomal proteins. *Biochim Biophys Acta* **2009,** *1793* (4), 710-25.

14. Lampe, C.; Bosserhoff, A. K.; Burton, B. K.; Giugliani, R.; de Souza, C. F.; Bittar, C.; Muschol, N.; Olson, R.; Mendelsohn, N. J., Long-term experience with enzyme replacement therapy (ERT) in MPS II patients with a severe phenotype: an international case series. *J Inherit Metab Dis* **2014,** *37* (5), 823-9.
15. Muenzer, J.; Wraith, J. E.; Beck, M.; Giugliani, R.; Harmatz, P.; Eng, C. M.; Vellodi, A.; Martin, R.; Ramaswami, U.; Gucsavas-Calikoglu, M.; Vijayaraghavan, S.; Wendt, S.; Puga, A.; Ulbrich, B.; Shinawi, M.; Cleary, M.; Piper, D.; Conway, A. M.; Kimura, A., A phase II/III clinical study of enzyme replacement therapy with idursulfase in mucopolysaccharidosis II (Hunter syndrome). *Genetics in Medicine* **2006,** *8* (8), 465-473.
16. Muenzer, J.; Gucsavas-Calikoglu, M.; McCandless, S. E.; Schuetz, T. J.; Kimura, A., A phase I/II clinical trial of enzyme replacement therapy in mucopolysaccharidosis II (Hunter syndrome). *Mol Genet Metab* **2007,** *90* (3), 329-37.
17. Safary, A.; Akbarzadeh Khiavi, M.; Mousavi, R.; Barar, J.; Rafi, M. A., Enzyme replacement therapies: what is the best option? *Bioimpacts* **2018,** *8* (3), 153-157.
18. Valayannopoulos, V.; Wijburg, F. A., Therapy for the mucopolysaccharidoses. *Rheumatology (Oxford)* **2011,** *50 Suppl 5*, v49-59.
19. Whiteman, D. A.; Kimura, A., Development of idursulfase therapy for mucopolysaccharidosis type II (Hunter syndrome): the past, the present and the future. *Drug Des Devel Ther* **2017,** *11*, 2467-2480.
20. Laoharawee, K.; DeKelver, R. C.; Podetz-Pedersen, K. M.; Rohde, M.; Sproul, S.; Nguyen, H. O.; Nguyen, T.; St Martin, S. J.; Ou, L.; Tom, S.; Radeke, R.; Meyer, K. E.; Holmes, M. C.; Whitley, C. B.; Wechsler, T.; McIvor, R. S., Dose-Dependent Prevention of Metabolic and Neurologic Disease in Murine MPS II by ZFN-Mediated In Vivo Genome Editing. *Mol Ther* **2018,** *26* (4), 1127-1136.
21. Boyd, R. E.; Lee, G.; Rybczynski, P.; Benjamin, E. R.; Khanna, R.; Wustman, B. A.; Valenzano, K. J., Pharmacological chaperones as therapeutics for lysosomal storage diseases. *J Med Chem* **2013,** *56* (7), 2705-25.
22. Pereira, D. M.; Valentao, P.; Andrade, P. B., Tuning protein folding in lysosomal storage diseases: the chemistry behind pharmacological chaperones. *Chem Sci* **2018,** *9* (7), 1740-1752.
23. Parenti, G., Treating lysosomal storage diseases with pharmacological chaperones: from concept to clinics. *EMBO Mol Med* **2009,** *1* (5), 268-79.
24. Benjamin, E. R.; Khanna, R.; Schilling, A.; Flanagan, J. J.; Pellegrino, L. J.;

doi:10.6844/NCKU201900656

Brignol, N.; Lun, Y.; Guillen, D.; Ranes, B. E.; Frascella, M.; Soska, R.; Feng, J.; Dungan, L.; Young, B.; Lockhart, D. J.; Valenzano, K. J., Co-administration with the pharmacological chaperone AT1001 increases recombinant human alpha-galactosidase A tissue uptake and improves substrate reduction in Fabry mice. *Mol Ther* **2012,** *20* (4), 717-26.

25. Cheng, W. C.; Wang, J. H.; Li, H. Y.; Lu, S. J.; Hu, J. M.; Yun, W. Y.; Chiu, C. H.; Yang, W. B.; Chien, Y. H.; Hwu, W. L., Bioevaluation of sixteen ADMDP stereoisomers toward alpha-galactosidase A: Development of a new pharmacological chaperone for the treatment of Fabry disease and potential enhancement of enzyme replacement therapy efficiency. *Eur J Med Chem* **2016,** *123*, 14-20.
26. Cheng, W. C.; Wang, J. H.; Yun, W. Y.; Li, H. Y.; Hu, J. M., Rapid preparation of (3R,4S,5R) polyhydroxylated pyrrolidine-based libraries to discover a pharmacological chaperone for treatment of Fabry disease. *Eur J Med Chem* **2017,** *126*, 1-6.
27. Li, H. Y.; Lee, J. D.; Chen, C. W.; Sun, Y. C.; Cheng, W. C., Synthesis of (3S,4S,5S)-trihydroxylpiperidine derivatives as enzyme stabilizers to improve therapeutic enzyme activity in Fabry patient cell lines. *Eur J Med Chem* **2018,** *144*, 626-634.
28. Cheng, W. C.; Weng, C. Y.; Yun, W. Y.; Chang, S. Y.; Lin, Y. C.; Tsai, F. J.; Huang, F. Y.; Chen, Y. R., Rapid modifications of N-substitution in iminosugars: development of new beta-glucocerebrosidase inhibitors and pharmacological chaperones for Gaucher disease. *Bioorg Med Chem* **2013,** *21* (17), 5021-8.
29. Schalli, M.; Weber, P.; Tysoe, C.; Pabst, B. M.; Thonhofer, M.; Paschke, E.; Stutz, A. E.; Tschernutter, M.; Windischhofer, W.; Withers, S. G., A new type of pharmacological chaperone for GM1-gangliosidosis related human lysosomal beta-galactosidase: N-Substituted 5-amino-1-hydroxymethyl-cyclopentanetriols. *Bioorg Med Chem Lett* **2017,** *27* (15), 3431-3435.
30. Porto, C.; Cardone, M.; Fontana, F.; Rossi, B.; Tuzzi, M. R.; Tarallo, A.; Barone, M. V.; Andria, G.; Parenti, G., The pharmacological chaperone N-butyldeoxynojirimycin enhances enzyme replacement therapy in Pompe disease fibroblasts. *Mol Ther* **2009,** *17* (6), 964-71.
31. Muntze, J.; Gensler, D.; Maniuc, O.; Liu, D.; Cairns, T.; Oder, D.; Hu, K.; Lorenz, K.; Frantz, S.; Wanner, C.; Nordbeck, P., Oral Chaperone Therapy Migalastat for Treating Fabry Disease: Enzymatic Response and Serum Biomarker Changes After 1 Year. *Clin Pharmacol Ther* **2019,** *105* (5), 1224-1233.
32. Hoshina, H.; Shimada, Y.; Higuchi, T.; Kobayashi, H.; Ida, H.; Ohashi, T., Chaperone effect of sulfated disaccharide from heparin on mutant iduronate-2-sulfatase in mucopolysaccharidosis type II. *Mol Genet Metab* **2018,** *123* (2), 118-122.

doi:10.6844/NCKU201900656

33. Kim, Y. S.; Thanawiroon, C.; Bazin, H. G.; Kerns, R. J.; Linhard, R. J., Enzymatic preparation of heparin disaccharides as building blocks in glycosaminoglycan synthesis. *Prep Biochem Biotechnol* **2001,** *31* (2), 113-24.
34. Khanna, R.; Flanagan, J. J.; Feng, J.; Soska, R.; Frascella, M.; Pellegrino, L. J.; Lun, Y.; Guillen, D.; Lockhart, D. J.; Valenzano, K. J., The pharmacological chaperone AT2220 increases recombinant human acid alpha-glucosidase uptake and glycogen reduction in a mouse model of Pompe disease. *PLoS One* **2012,** *7* (7), e40776.
35. Xu, S.; Lun, Y.; Brignol, N.; Hamler, R.; Schilling, A.; Frascella, M.; Sullivan, S.; Boyd, R. E.; Chang, K.; Soska, R.; Garcia, A.; Feng, J.; Yasukawa, H.; Shardlow, C.; Churchill, A.; Ketkar, A.; Robertson, N.; Miyamoto, M.; Mihara, K.; Benjamin, E. R.; Lockhart, D. J.; Hirato, T.; Fowles, S.; Valenzano, K. J.; Khanna, R., Coformulation of a Novel Human alpha-Galactosidase A With the Pharmacological Chaperone AT1001 Leads to Improved Substrate Reduction in Fabry Mice. *Mol Ther* **2015,** *23* (7), 1169-1181.
36. Azadeh, M.; Pan, L.; Qiu, Y.; Boado, R., A Rapid Two-Step Iduronate-2-Sulfatatse Enzymatic Activity Assay for MPSII Pharmacokinetic Assessment. *JIMD Rep* **2018,** *38*, 89-95.
37. Dean, C. J.; Bockmann, M. R.; Hopwood, J. J.; Brooks, D. A.; Meikle, P. J., Detection of mucopolysaccharidosis type II by measurement of iduronate-2-sulfatase in dried blood spots and plasma samples. *Clin Chem* **2006,** *52* (4), 643-9.
38. Voznyi, Y. V.; Keulemans, J. L. M.; van Diggelen, O. P., A fluorimetric enzyme assay for the diagnosis of MPS II (Hunter disease). *Journal of Inherited Metabolic Disease* **2001,** *24* (6), 675-680.
39. Cheng, W. C.; Lin, C. K.; Li, H. Y.; Chang, Y. C.; Lu, S. J.; Chen, Y. S.; Chang, S. Y., A combinatorial approach towards the synthesis of non-hydrolysable triazole-iduronic acid hybrid inhibitors of human alpha-l-iduronidase: discovery of enzyme stabilizers for the potential treatment of MPSI. *Chem Commun (Camb)* **2018,** *54* (21), 2647-2650.
40. Seabrook, S. A.; Newman, J., High-throughput thermal scanning for protein stability: making a good technique more robust. *ACS Comb Sci* **2013,** *15* (8), 387-92.
41. Wong, J. J.; Wright, S. K.; Ghozalli, I.; Mehra, R.; Furuya, K.; Katayama, D. S., Simultaneous High-Throughput Conformational and Colloidal Stability Screening Using a Fluorescent Molecular Rotor Dye, 4-(4-(Dimethylamino)styryl)-N-Methylpyridinium Iodide (DASPMI). *J Biomol Screen* **2016,** *21* (8), 842-50.
42. Tolun, A. A.; Graham, C.; Shi, Q.; Sista, R. S.; Wang, T.; Eckhardt, A. E.; Pamula, V. K.; Millington, D. S.; Bali, D. S., A novel fluorometric enzyme analysis method for Hunter syndrome using dried blood spots. *Mol Genet Metab* **2012,** *105* (3),

doi:10.6844/NCKU201900656

519-21.
43. Lawrence, R.; Brown, J. R.; Lorey, F.; Dickson, P. I.; Crawford, B. E.; Esko, J. D., Glycan-based biomarkers for mucopolysaccharidoses. *Mol Genet Metab* **2014,** *111* (2), 73-83.
44. De Pasquale, V.; Sarogni, P.; Pistorio, V.; Cerulo, G.; Paladino, S.; Pavone, L. M., Targeting Heparan Sulfate Proteoglycans as a Novel Therapeutic Strategy for Mucopolysaccharidoses. *Mol Ther Methods Clin Dev* **2018,** *10*, 8-16.
45. Shimada, T.; Kelly, J.; LaMarr, W. A.; van Vlies, N.; Yasuda, E.; Mason, R. W.; Mackenzie, W.; Kubaski, F.; Giugliani, R.; Chinen, Y.; Yamaguchi, S.; Suzuki, Y.; Orii, K. E.; Fukao, T.; Orii, T.; Tomatsu, S., Novel heparan sulfate assay by using automated high-throughput mass spectrometry: Application to monitoring and screening for mucopolysaccharidoses. *Mol Genet Metab* **2014,** *113* (1-2), 92-9.
46. Tomatsu, S.; Gutierrez, M. A.; Ishimaru, T.; Pena, O. M.; Montano, A. M.; Maeda, H.; Velez-Castrillon, S.; Nishioka, T.; Fachel, A. A.; Cooper, A.; Thornley, M.; Wraith, E.; Barrera, L. A.; Laybauer, L. S.; Giugliani, R.; Schwartz, I. V.; Frenking, G. S.; Beck, M.; Kircher, S. G.; Paschke, E.; Yamaguchi, S.; Ullrich, K.; Isogai, K.; Suzuki, Y.; Orii, T.; Noguchi, A., Heparan sulfate levels in mucopolysaccharidoses and mucolipidoses. *J Inherit Metab Dis* **2005,** *28* (5), 743-57.
47. Wolff, J. J.; Chi, L.; Linhardt, R. J.; Amster, I. J., Distinguishing glucuronic from iduronic acid in glycosaminoglycan tetrasaccharides by using electron detachment dissociation. *Anal Chem* **2007,** *79* (5), 2015-22.
48. 50. Oguma, T.; Tomatsu, S.; Montano, A. M.; Okazaki, O., Analytical method for the determination of disaccharides derived from keratan, heparan, and dermatan sulfates in human serum and plasma by high-performance liquid chromatography/turbo ionspray ionization tandem mass spectrometry. *Anal Biochem* **2007,** *368* (1), 79-86.
49. Mashima, R.; Sakai, E.; Tanaka, M.; Kosuga, M.; Okuyama, T., The levels of urinary glycosaminoglycans of patients with attenuated and severe type of mucopolysaccharidosis II determined by liquid chromatography-tandem mass spectrometry. *Mol Genet Metab Rep* **2016,** *7*, 87-91.
50. Osago, H.; Shibata, T.; Hara, N.; Kuwata, S.; Kono, M.; Uchio, Y.; Tsuchiya, M., Quantitative analysis of glycosaminoglycans, chondroitin/dermatan sulfate, hyaluronic acid, heparan sulfate, and keratan sulfate by liquid chromatography-electrospray ionization-tandem mass spectrometry. *Anal Biochem* **2014,** *467*, 62-74.
51. Cao, J.; Wen, C.; Lu, J.; Teng, N.; Song, S.; Zhu, B., Characterization of acidic polysaccharides from the mollusks through acid hydrolysis. *Carbohydr Polym* **2015,** *130*, 268-74.

doi:10.6844/NCKU201900656

52. Auray-Blais, C.; Bherer, P.; Gagnon, R.; Young, S. P.; Zhang, H. H.; An, Y.; Clarke, J. T.; Millington, D. S., Efficient analysis of urinary glycosaminoglycans by LC-MS/MS in mucopolysaccharidoses type I, II and VI. *Mol Genet Metab* **2011,** *102* (1), 49-56.
53. Forni, G.; Malvagia, S.; Funghini, S.; Scolamiero, E.; Mura, M.; Della Bona, M.; Villanelli, F.; Damiano, R.; la Marca, G., LC-MS/MS method for simultaneous quantification of heparan sulfate and dermatan sulfate in urine by butanolysis derivatization. *Clin Chim Acta* **2019,** *488*, 98-103.
54. Tanaka, N.; Kida, S.; Kinoshita, M.; Morimoto, H.; Shibasaki, T.; Tachibana, K.; Yamamoto, R., Evaluation of cerebrospinal fluid heparan sulfate as a biomarker of neuropathology in a murine model of mucopolysaccharidosis type II using high-sensitivity LC/MS/MS. *Mol Genet Metab* **2018,** *125* (1-2), 53-58.
55. Trim, P. J.; Hopwood, J. J.; Snel, M. F., Butanolysis derivatization: improved sensitivity in LC-MS/MS quantitation of heparan sulfate in urine from mucopolysaccharidosis patients. *Anal Chem* **2015,** *87* (18), 9243-50.
56. Li, G.; Li, L.; Tian, F.; Zhang, L.; Xue, C.; Linhardt, R. J., Glycosaminoglycanomics of cultured cells using a rapid and sensitive LC-MS/MS approach. *ACS Chem Biol* **2015,** *10* (5), 1303-10.
57. Chuang, C.-K.; Lin, H.-Y.; Wang, T.-J.; Tsai, C.-C.; Liu, H.-L.; Lin, S.-P., A modified liquid chromatography/tandem mass spectrometry method for predominant disaccharide units of urinary glycosaminoglycans in patients with mucopolysaccharidoses. *Orphanet Journal of Rare Diseases* **2014,** *9* (1), 135.
58. Zhang, H.; Young, S. P.; Auray-Blais, C.; Orchard, P. J.; Tolar, J.; Millington, D. S., Analysis of glycosaminoglycans in cerebrospinal fluid from patients with mucopolysaccharidoses by isotope-dilution ultra-performance liquid chromatography-tandem mass spectrometry. *Clin Chem* **2011,** *57* (7), 1005-12.
59. He, Q. Q.; Trim, P. J.; Snel, M. F.; Hopwood, J. J.; Ferro, V., Synthesis and mass spectrometric analysis of disaccharides from methanolysis of heparan sulfate. *Org Biomol Chem* **2018,** *16* (45), 8791-8803.
60. Lawrence, R.; Brown, J. R.; Al-Mafraji, K.; Lamanna, W. C.; Beitel, J. R.; Boons, G. J.; Esko, J. D.; Crawford, B. E., Disease-specific non-reducing end carbohydrate biomarkers for mucopolysaccharidoses. *Nat Chem Biol* **2012,** *8* (2), 197-204.
61. Lawrence, R.; Olson, S. K.; Steele, R. E.; Wang, L.; Warrior, R.; Cummings, R. D.; Esko, J. D., Evolutionary differences in glycosaminoglycan fine structure detected by quantitative glycan reductive isotope labeling. *J Biol Chem* **2008,** *283* (48), 33674-84.

doi:10.6844/NCKU201900656

62. Shimada, Y.; Wakabayashi, T.; Akiyama, K.; Hoshina, H.; Higuchi, T.; Kobayashi, H.; Eto, Y.; Ida, H.; Ohashi, T., A method for measuring disease-specific iduronic acid from the non-reducing end of glycosaminoglycan in mucopolysaccharidosis type II mice. *Mol Genet Metab* **2016,** *117* (2), 140-3.
63. Harvey, D. J., Derivatization of carbohydrates for analysis by chromatography; electrophoresis and mass spectrometry. *J Chromatogr B Analyt Technol Biomed Life Sci* **2011,** *879* (17-18), 1196-225.
64. Ruhaak, L. R.; Zauner, G.; Huhn, C.; Bruggink, C.; Deelder, A. M.; Wuhrer, M., Glycan labeling strategies and their use in identification and quantification. *Anal Bioanal Chem* **2010,** *397* (8), 3457-81.
65. Deakin, J. A.; Lyon, M., A simplified and sensitive fluorescent method for disaccharide analysis of both heparan sulfate and chondroitin/dermatan sulfates from biological samples. *Glycobiology* **2008,** *18* (6), 483-91.
66. Lin, C.; Lai, P.-T.; Liao, S. K.-S.; Hung, W.-T.; Yang, W.-B.; Fang, J.-M., Using Molecular Iodine in Direct Oxidative Condensation of Aldoses with Diamines: An Improved Synthesis of Aldo-benzimidazoles and Aldo-naphthimidazoles for Carbohydrate Analysis. *The Journal of Organic Chemistry* **2008,** *73* (10), 3848-3853.
67. France, R. R.; Cumpstey, I.; Butters, T. D.; Fairbanks, A. J.; Wormald, M. R., Fluorescence labelling of carbohydrates with 2-aminobenzamide (2AB). *Tetrahedron: Asymmetry* **2000,** *11* (24), 4985-4994.
68. Honda, S.; Akao, E.; Suzuki, S.; Okuda, M.; Kakehi, K.; Nakamura, J., High-performance liquid chromatography of reducing carbohydrates as strongly ultraviolet-absorbing and electrochemically sensitive 1-phenyl-3-methyl5-pyrazolone derivatives. *Analytical Biochemistry* **1989,** *180* (2), 351-357.
69. Wegrzyn, G.; Jakobkiewicz-Banecka, J.; Gabig-Ciminska, M.; Piotrowska, E.; Narajczyk, M.; Kloska, A.; Malinowska, M.; Dziedzic, D.; Golebiewska, I.; Moskot, M.; Wegrzyn, A., Genistein: a natural isoflavone with a potential for treatment of genetic diseases. *Biochem Soc Trans* **2010,** *38* (2), 695-701.
70. Jakobkiewicz-Banecka, J.; Piotrowska, E.; Narajczyk, M.; Baranska, S.; Wegrzyn, G., Genistein-mediated inhibition of glycosaminoglycan synthesis, which corrects storage in cells of patients suffering from mucopolysaccharidoses, acts by influencing an epidermal growth factor-dependent pathway. *J Biomed Sci* **2009,** *16*, 26.
71. Moskot, M.; Montefusco, S.; Jakobkiewicz-Banecka, J.; Mozolewski, P.; Wegrzyn, A.; Di Bernardo, D.; Wegrzyn, G.; Medina, D. L.; Ballabio, A.; Gabig-Ciminska, M., The phytoestrogen genistein modulates lysosomal metabolism and transcription factor EB (TFEB) activation. *J Biol Chem* **2014,** *289* (24), 17054-69.
72. Piotrowska, E.; Jakobkiewicz-Banecka, J.; Baranska, S.; Tylki-Szymanska, A.;

doi:10.6844/NCKU201900656

Czartoryska, B.; Wegrzyn, A.; Wegrzyn, G., Genistein-mediated inhibition of glycosaminoglycan synthesis as a basis for gene expression-targeted isoflavone therapy for mucopolysaccharidoses. *Eur J Hum Genet* **2006,** *14* (7), 846-52.

73. Friso, A.; Tomanin, R.; Salvalaio, M.; Scarpa, M., Genistein reduces glycosaminoglycan levels in a mouse model of mucopolysaccharidosis type II. *Br J Pharmacol* **2010,** *159* (5), 1082-91.
74. Kingma, S. D.; Wagemans, T.; L, I. J.; Seppen, J.; Gijbels, M. J.; Wijburg, F. A.; van Vlies, N., Adverse Effects of Genistein in a Mucopolysaccharidosis Type I Mouse Model. *JIMD Rep* **2015,** *23*, 77-83.
75. Markossian, S.; Ang, K. K.; Wilson, C. G.; Arkin, M. R., Small-Molecule Screening for Genetic Diseases. *Annu Rev Genomics Hum Genet* **2018,** *19*, 263-288.
76. Vasconcelos-Dos-Santos, A.; Oliveira, I. A.; Lucena, M. C.; Mantuano, N. R.; Whelan, S. A.; Dias, W. B.; Todeschini, A. R., Biosynthetic Machinery Involved in Aberrant Glycosylation: Promising Targets for Developing of Drugs Against Cancer. *Front Oncol* **2015,** *5*, 138.
77. Magalhaes, A.; Duarte, H. O.; Reis, C. A., Aberrant Glycosylation in Cancer: A Novel Molecular Mechanism Controlling Metastasis. *Cancer Cell* **2017,** *31* (6), 733-735.
78. Josic, D.; Martinovic, T.; Pavelic, K., Glycosylation and metastases. *Electrophoresis* **2019,** *40* (1), 140-150.
79. Pinho, S. S.; Reis, C. A., Glycosylation in cancer: mechanisms and clinical implications. *Nat Rev Cancer* **2015,** *15* (9), 540-55.
80. Nishiu, J.; Kioka, N.; Fukada, T.; Sakai, H.; Komano, T., Characterization of RatN-Acetylglucosaminyltransferase I Expressed inEsherichia coli. *Bioscience, Biotechnology, and Biochemistry* **2014,** *59* (9), 1750-1752.
81. Nagae, M.; Kizuka, Y.; Mihara, E.; Kitago, Y.; Hanashima, S.; Ito, Y.; Takagi, J.; Taniguchi, N.; Yamaguchi, Y., Structure and mechanism of cancer-associated N-acetylglucosaminyltransferase-V. *Nat Commun* **2018,** *9* (1), 3380.
82. Zhao, Y.; Nakagawa, T.; Itoh, S.; Inamori, K.; Isaji, T.; Kariya, Y.; Kondo, A.; Miyoshi, E.; Miyazaki, K.; Kawasaki, N.; Taniguchi, N.; Gu, J., N-acetylglucosaminyltransferase III antagonizes the effect of N-acetylglucosaminyltransferase V on alpha3beta1 integrin-mediated cell migration. *J Biol Chem* **2006,** *281* (43), 32122-30.
83. Carvalho, S.; Catarino, T. A.; Dias, A. M.; Kato, M.; Almeida, A.; Hessling, B.; Figueiredo, J.; Gartner, F.; Sanches, J. M.; Ruppert, T.; Miyoshi, E.; Pierce, M.; Carneiro, F.; Kolarich, D.; Seruca, R.; Yamaguchi, Y.; Taniguchi, N.; Reis, C. A.; Pinho, S. S., Preventing E-cadherin aberrant N-glycosylation at Asn-554 improves its critical function in gastric cancer. *Oncogene* **2016,** *35* (13), 1619-31.

doi:10.6844/NCKU201900656

84. Zhao, Y. Y.; Takahashi, M.; Gu, J. G.; Miyoshi, E.; Matsumoto, A.; Kitazume, S.; Taniguchi, N., Functional roles of N-glycans in cell signaling and cell adhesion in cancer. *Cancer Sci* **2008,** *99* (7), 1304-10.
85. Rose, D. R., Structure, mechanism and inhibition of Golgi alpha-mannosidase II. *Curr Opin Struct Biol* **2012,** *22* (5), 558-62.
86. Sun, J. Y.; Zhu, M. Z.; Wang, S. W.; Miao, S.; Xie, Y. H.; Wang, J. B., Inhibition of the growth of human gastric carcinoma in vivo and in vitro by swainsonine. *Phytomedicine* **2007,** *14* (5), 353-9.
87. Gerber-Lemaire, S.; Juillerat-Jeanneret, L., Studies toward New Anti-Cancer Strategies Based on α-Mannosidase Inhibition. *CHIMIA International Journal for Chemistry* **2010,** *64* (9), 634-639.
88. Li, Z.; Huang, Y.; Dong, F.; Li, W.; Ding, L.; Yu, G.; Xu, D.; Yang, Y.; Xu, X.; Tong, D., Swainsonine promotes apoptosis in human oesophageal squamous cell carcinoma cells in vitro and in vivo through activation of mitochondrial pathway. *Journal of Biosciences* **2012,** *37* (S1), 1005-1016.
89. Ma, J.; Wang, L.; Li, J.; Zhang, G.; Tao, H.; Li, X.; Sun, D.; Hu, Y., Swainsonine Inhibits Invasion and the EMT Process in Esophageal Carcinoma Cells by Targeting Twist1. *Oncol Res* **2018,** *26* (8), 1207-1213.
90. Silveira, C. R. F.; Cipelli, M.; Manzine, C.; Rabelo-Santos, S. H.; Zeferino, L. C.; Rodriguez Rodriguez, G.; de Assis, J. B.; Hebster, S.; Bernadinelli, I.; Laginha, F.; Boccardo, E.; Villa, L. L.; Termini, L.; Lepique, A. P., Swainsonine, an alpha-mannosidase inhibitor, may worsen cervical cancer progression through the increase in myeloid derived suppressor cells population. *PLoS One* **2019,** *14* (3), e0213184.
91. Sun, J. Y.; Yang, H.; Miao, S.; Li, J. P.; Wang, S. W.; Zhu, M. Z.; Xie, Y. H.; Wang, J. B.; Liu, Z.; Yang, Q., Suppressive effects of swainsonine on C6 glioma cell in vitro and in vivo. *Phytomedicine* **2009,** *16* (11), 1070-4.
92. Sun, L.; Jin, X.; Xie, L.; Xu, G.; Cui, Y.; Chen, Z., Swainsonine represses glioma cell proliferation, migration and invasion by reduction of miR-92a expression. *BMC Cancer* **2019,** *19* (1), 247.
93. You, N.; Liu, W.; Wang, T.; Ji, R.; Wang, X.; Gong, Z.; Dou, K.; Tao, K., Swainsonine inhibits growth and potentiates the cytotoxic effect of paclitaxel in hepatocellular carcinoma in vitro and in vivo. *Oncol Rep* **2012,** *28* (6), 2091-100.
94. E Goss, P.; Baptiste, J.; Fernandes, B.; Baker, M.; Dennis, J., *A Phase I Study of Swainsonine in Patients with Advanced Malignancies1*. 1994; Vol. 54, p 1450-7.
95. E Goss, P.; L Reid, C.; Bailey, D.; Dennis, J., *Phase IB clinical trial of oligosaccharide processing inhibitor swainsonine in patients with advanced malignancies*. 1997; Vol. 3, p 1077-86.

doi:10.6844/NCKU201900656

96. Shaheen, P. E.; Stadler, W.; Elson, P.; Knox, J.; Winquist, E.; Bukowski, R. M., Phase II study of the efficacy and safety of oral GD0039 in patients with locally advanced or metastatic renal cell carcinoma. *Investigational New Drugs* **2005,** *23* (6), 577-581.
97. Shah, N.; Kuntz, D. A.; Rose, D. R., Golgi alpha-mannosidase II cleaves two sugars sequentially in the same catalytic site. *Proceedings of the National Academy of Sciences of the United States of America* **2008,** *105* (28), 9570-9575.
98. Irsheid, L.; Wehler, T.; Borek, C.; Kiefer, W.; Brenk, R.; Ortiz-Soto, M. E.; Seibel, J.; Schirmeister, T., Identification of a potential allosteric site of Golgi alpha-mannosidase II using computer-aided drug design. *PLoS One* **2019,** *14* (5), e0216132.
99. Chen, R.; Pawlicki, M. A.; Hamilton, B. S.; Tolbert, T. J., Enzyme-Catalyzed Synthesis of a Hybrid N-Linked Oligosaccharide using N-Acetylglucosaminyltransferase I. *Advanced Synthesis & Catalysis* **2008,** *350* (11-12), 1689-1695.
100. Daher, S.; de gasperi, R.; Daniel, P.; Hall, N.; D Warren, C.; Winchester, B., *The Substrate-Specificity of Human Lysosomal α-D-Mannosidase in Relation to Genetic α-Mannosidosis*. 1991; Vol. 277 (Pt 3), p 743-51.
101. Cheng, W.-C.; Guo, C.-W.; Lin, C.-K.; Jiang, Y.-R., Synthesis and Inhibition Study of Bicyclic Iminosugar-Based Alkaloids, Scaffolds, and Libraries towards Glucosidase. *Israel Journal of Chemistry* **2015,** *55* (3-4), 403-411.

doi:10.6844/NCKU201900656

Appendix

doi:10.6844/NCKU201900656

LSDs	Approved ERT and Brand name	Average of elimination half-life
MPS I (Hurler syn.)	Laronidase (Aldurazyme™)/ 2003-FDA, EMA	90- 210 min
MPS II (Hunter syn.)	Idursulfase (Elaprase™)/ 2006-FDA; 2007-EMA	20-60 min
MPS IVA (Morquio A syn.)	Elosulfase Alfa (Vimzim™)/ 2014-FDA	10-60 min
MPS VI (Marateaux-Lamy syn.)	Galsulfase (Naglazyme™)/ 2005-FDA; 2006-EMA	10-30 min
Fabry disease	Agalsidase α (Fabrazyme™)/ 2001-EMA	80-120 min
	Agalsidase β (Replagal™)/ 2003-FDA, EMA	80-120 min
Pompe disease	Aglucosidase (Myozyme™)/ 2006-FDA, EMA	120-180 min
	Aglucosidase (Lumizyme™)/ 2010-FDA	130-160 min
Gaucher disease	Aglucerase (Ceredase™)/ 1991-FDA	4-10 min
	Imiglucerase (Cerezyme™)/ 1994-FDA; 1997-EMA	4-10 min
	Velaglucerase (VPRIV™)/ 2010-FDA, EMA	5-12 min
	Taliglucerase (Elelyso™)/ 2012-FDA	20-30 min

Table of the elimination half-time for approved protein drugs

doi:10.6844/NCKU201900656

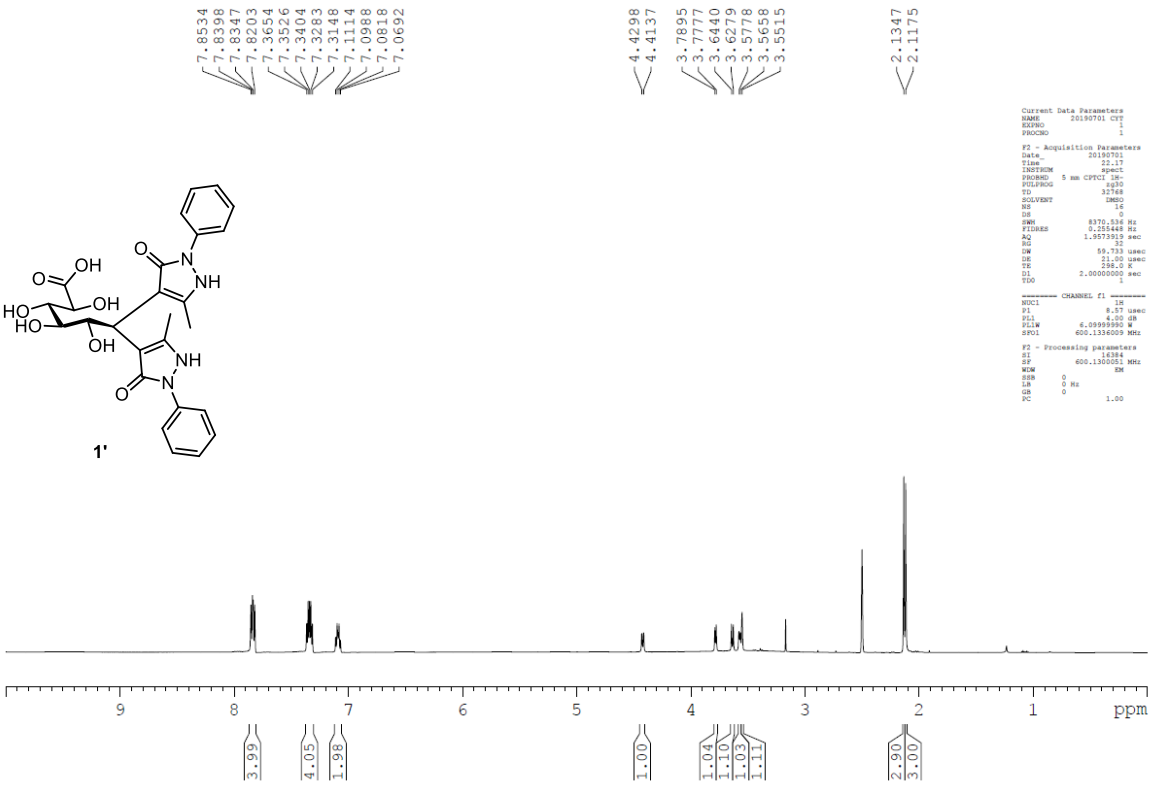

^{1}H NMR Spectra of compound **1'** (600 MHz, DMSO-d_6)

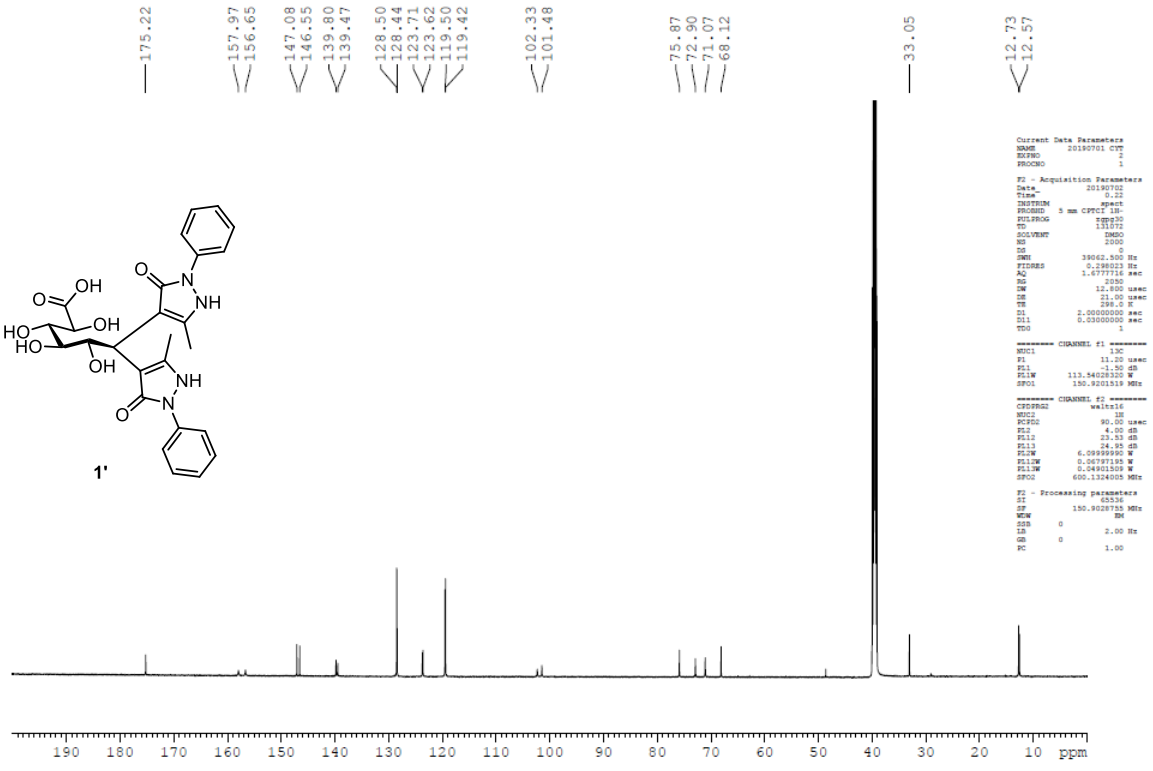

^{13}C NMR Spectra of compound **1'** (600 MHz, DMSO-d_6)

doi:10.6844/NCKU201900656

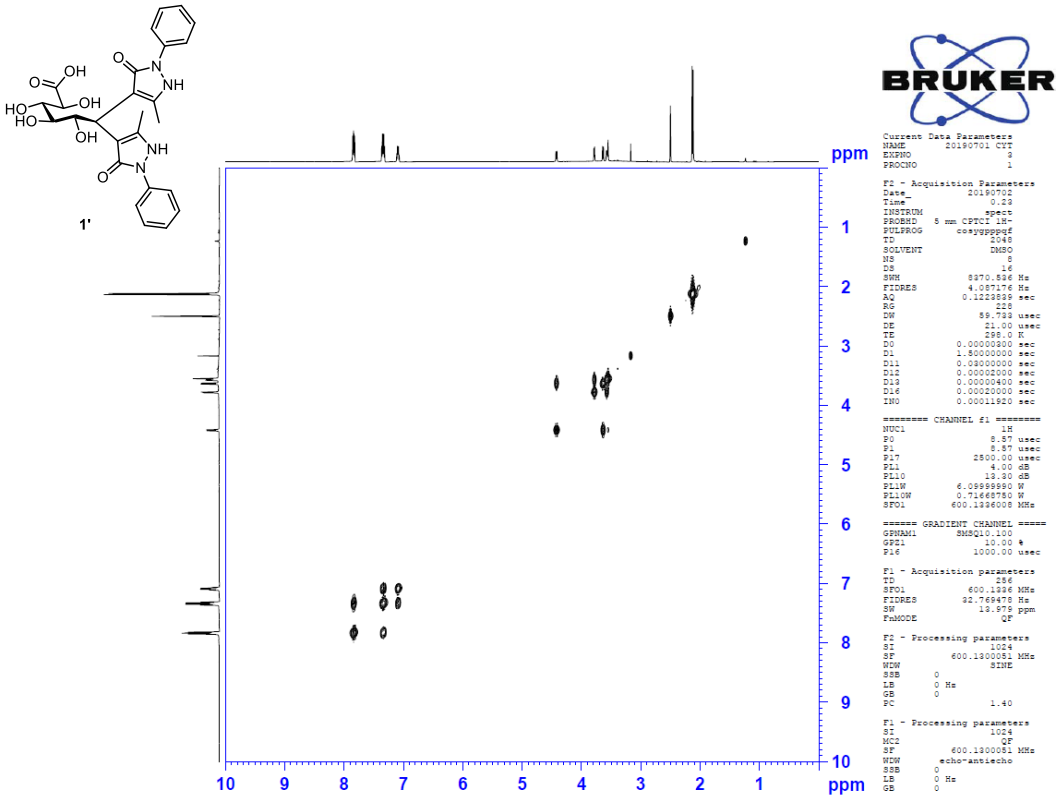

COSY Spectra of compound **1'** (600 MHz, DMSO-d_6)

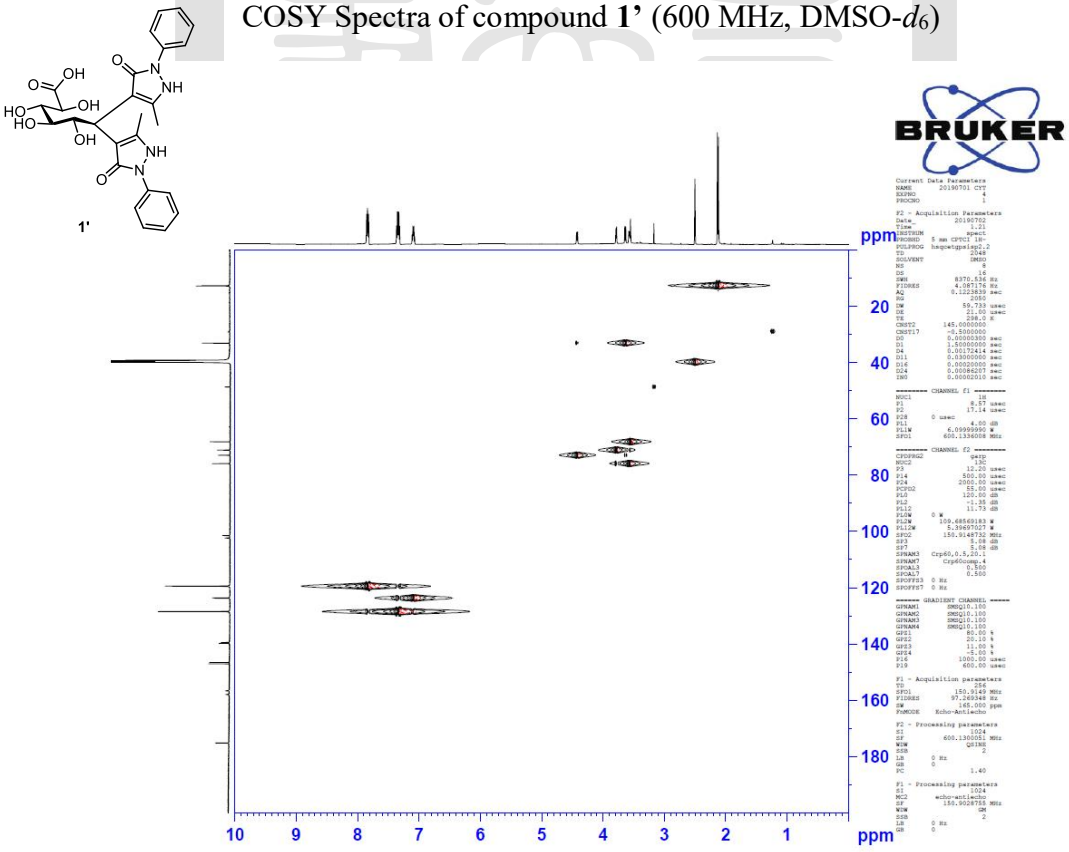

HSQC Spectra of compound **1'** (600 MHz, DMSO-d_6)

doi:10.6844/NCKU201900656

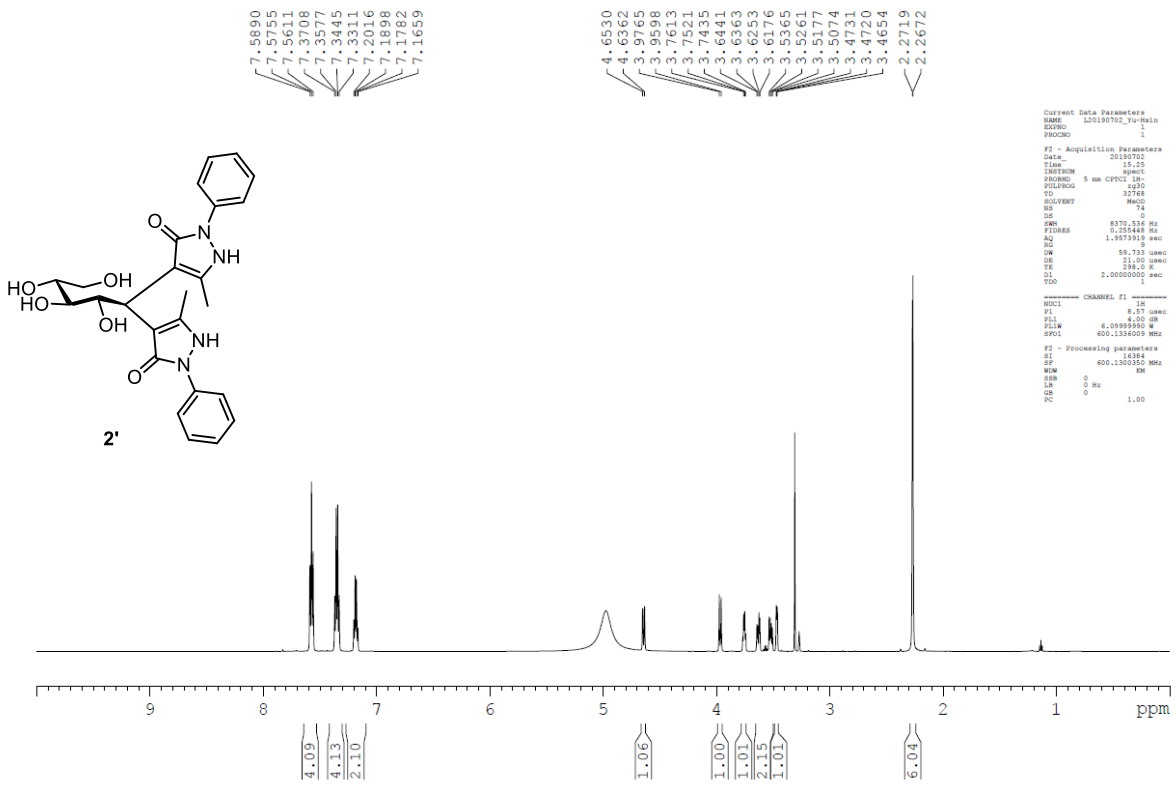

^{1}H NMR Spectra of compound **2'** (600 MHz, MeOD)

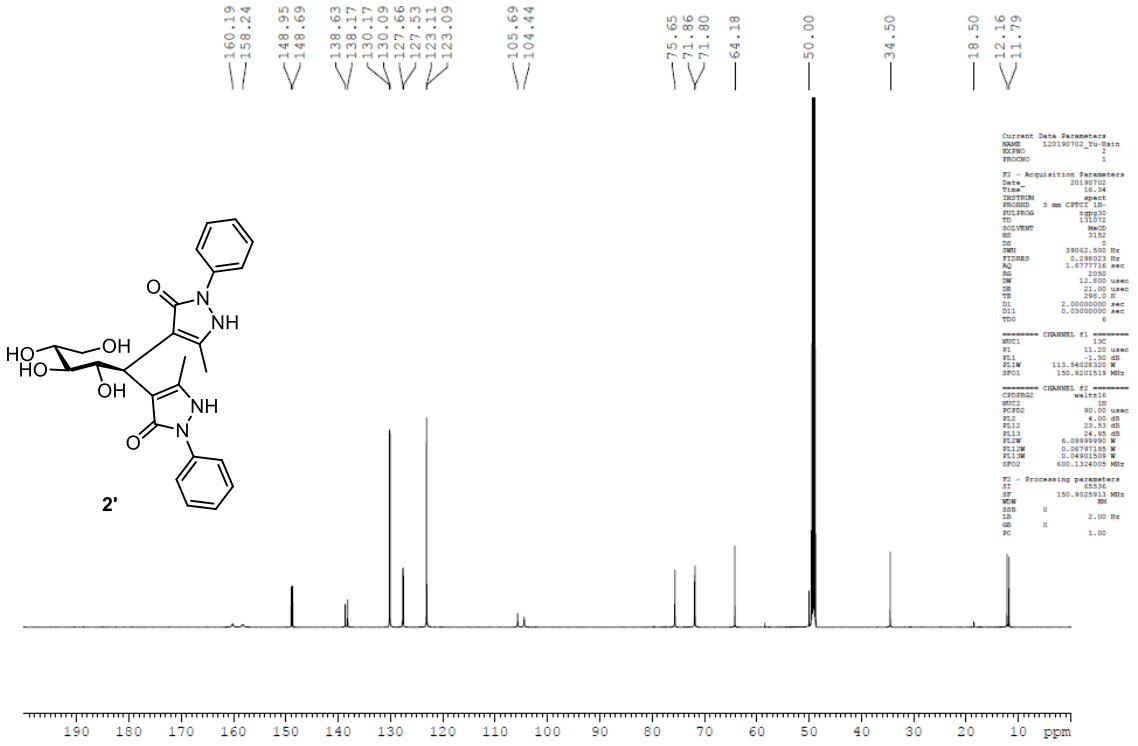

^{13}C NMR Spectra of compound **2'** (600 MHz, MeOD)

doi:10.6844/NCKU201900656

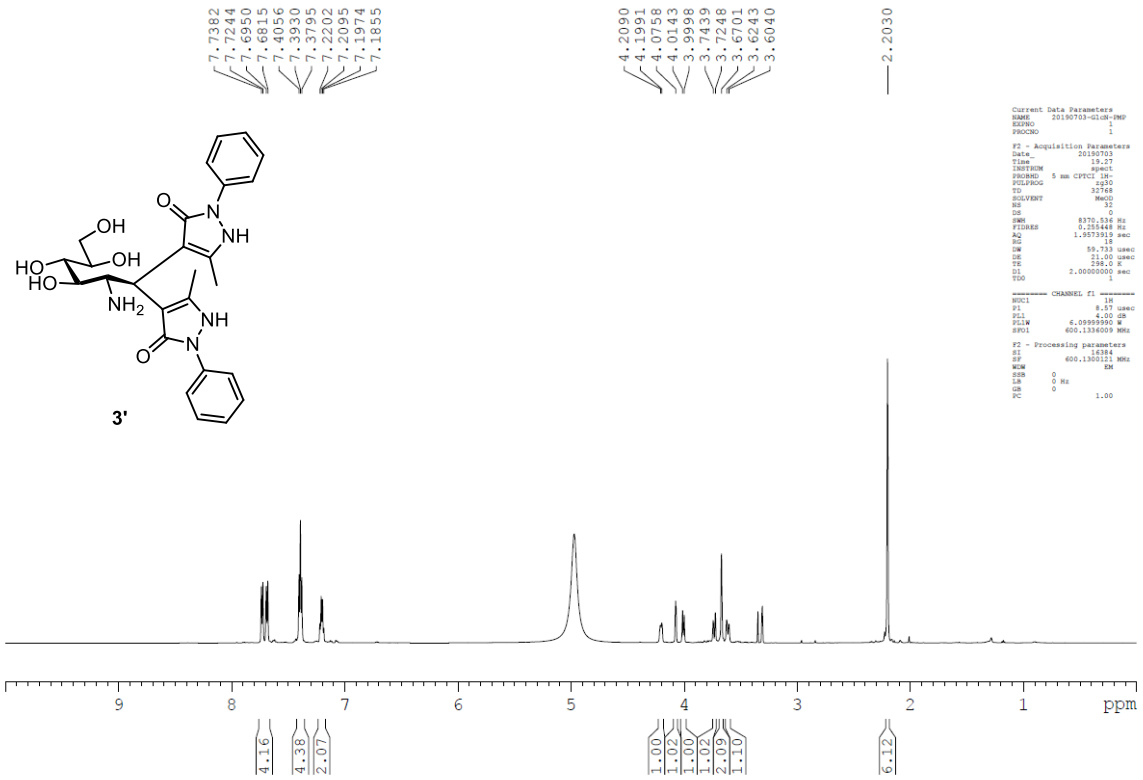

^{1}H NMR Spectra of compound **3'** (600 MHz, MeOD)

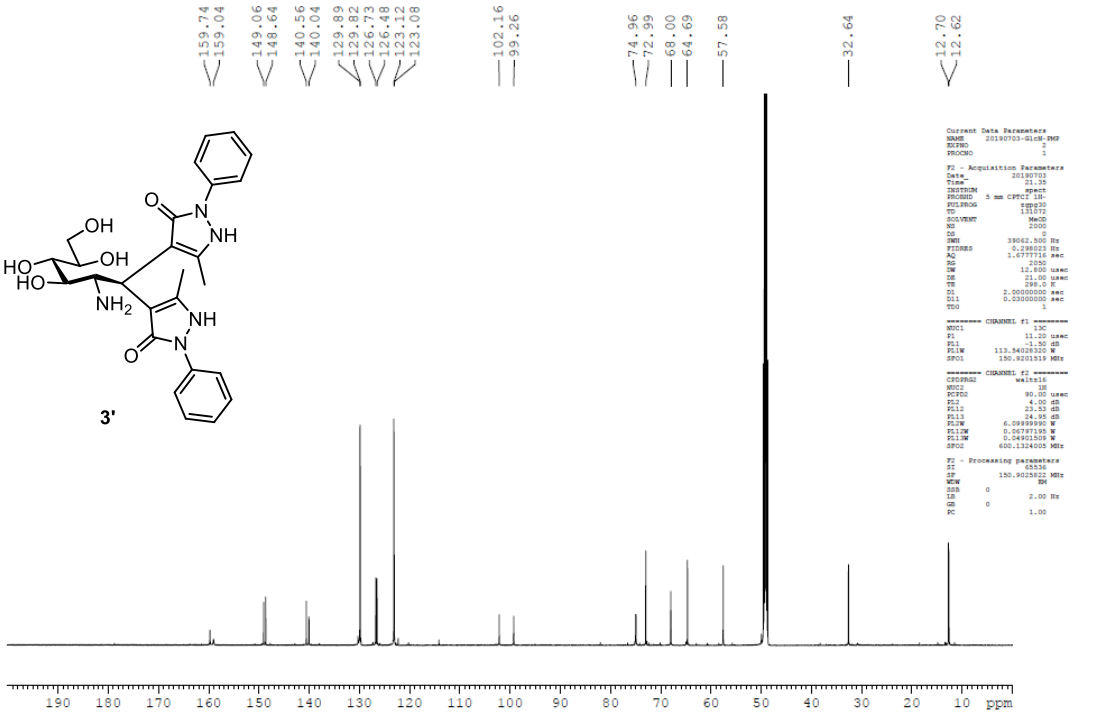

^{13}C NMR Spectra of compound **3'** (600 MHz, MeOD)

doi:10.6844/NCKU201900656

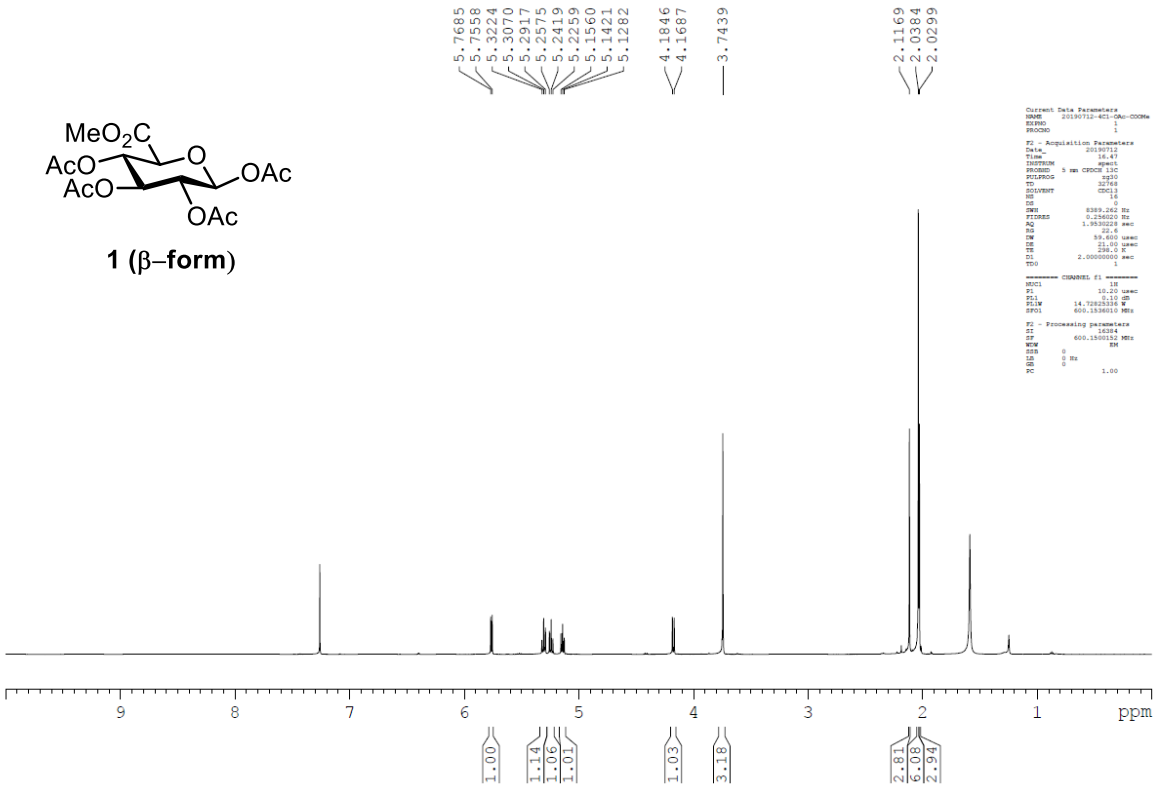

^{1}H NMR Spectra of compound **1** (600 MHz, $CDCl_3$)

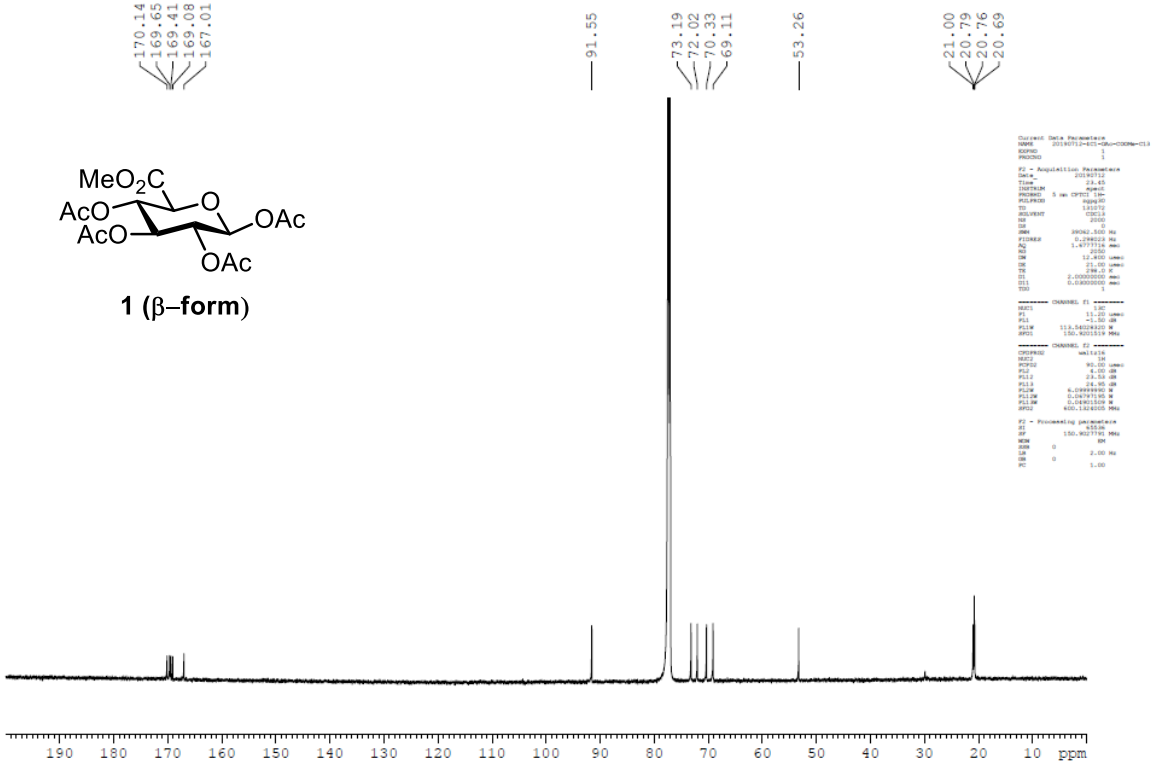

^{13}C NMR Spectra of compound **1** (600 MHz, $CDCl_3$)

doi:10.6844/NCKU201900656

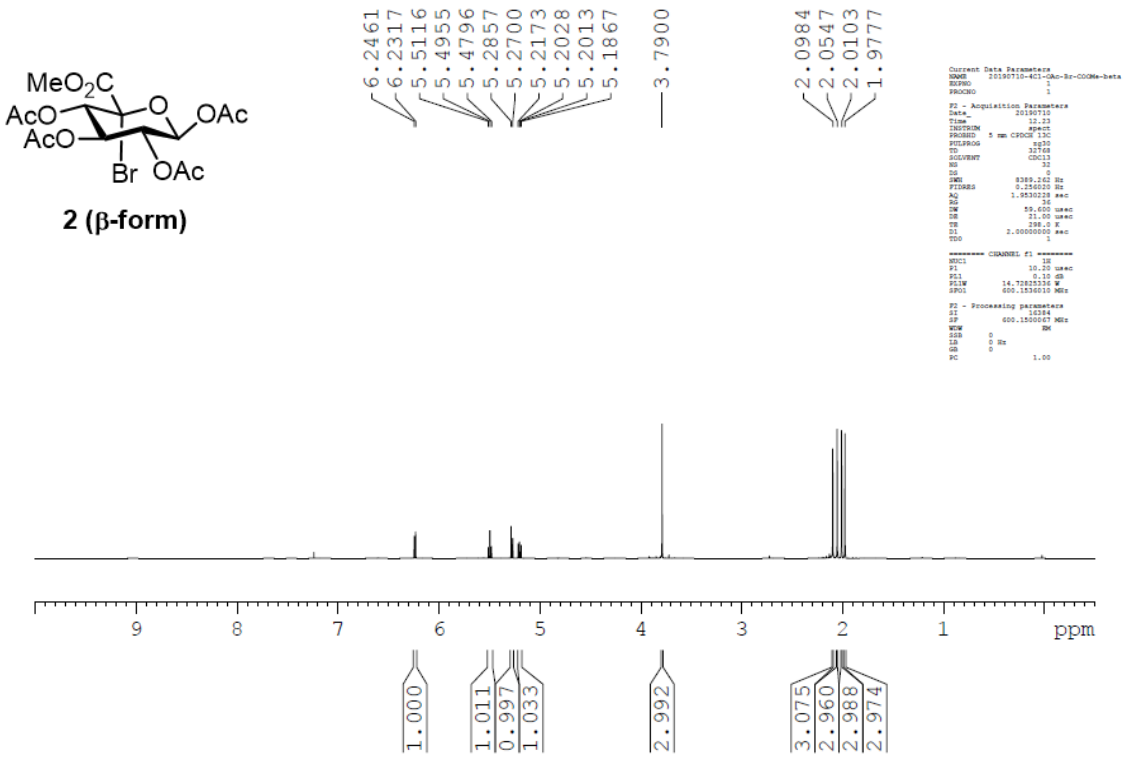

^{1}H NMR Spectra of compound **2** (600 MHz, $CDCl_3$)

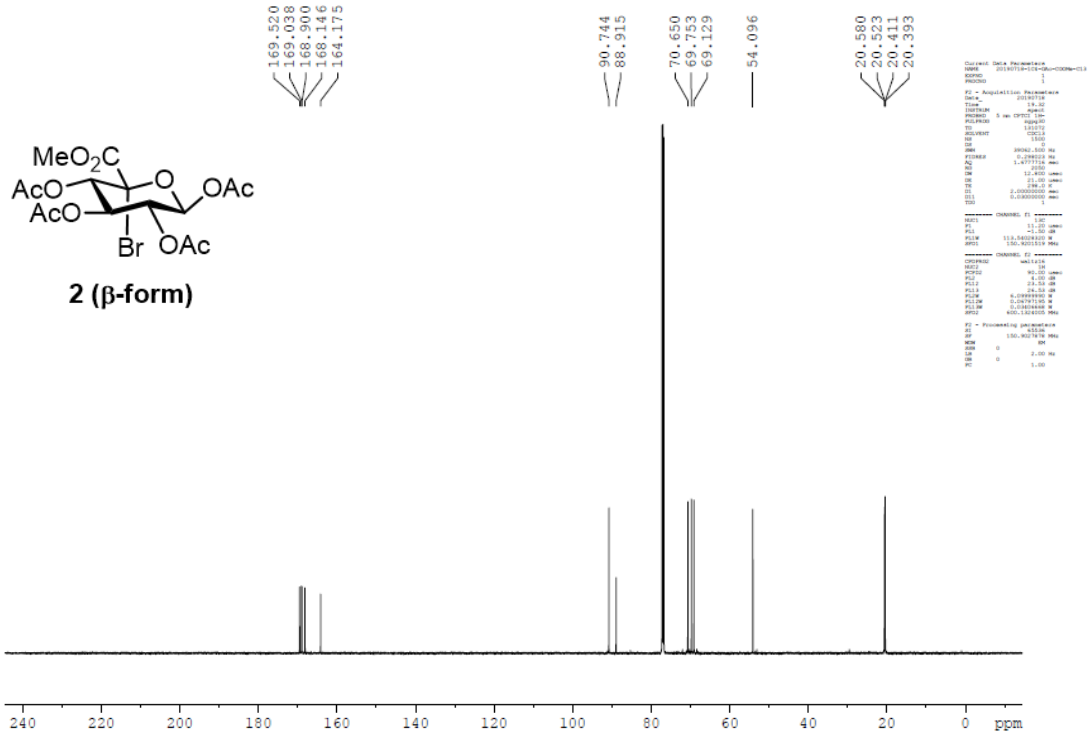

^{13}C NMR Spectra of compound **2** (600 MHz, $CDCl_3$)

doi:10.6844/NCKU201900656

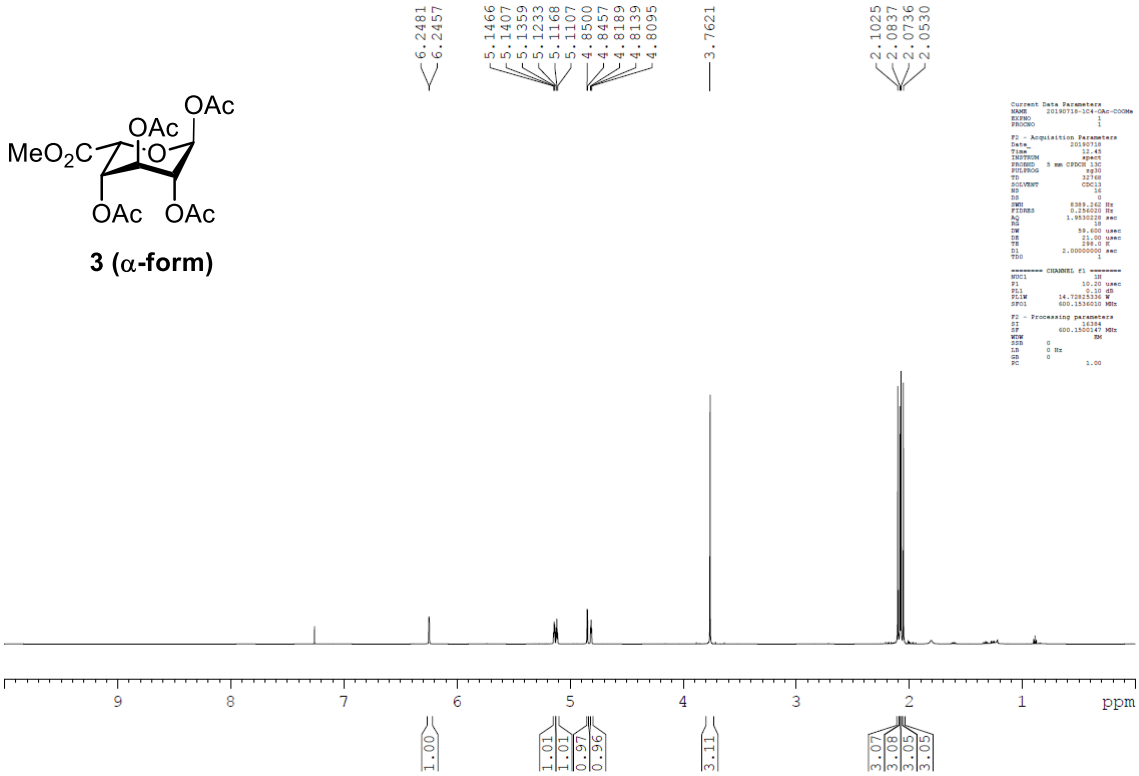

^{1}H NMR Spectra of compound **3** (600 MHz, $CDCl_3$)

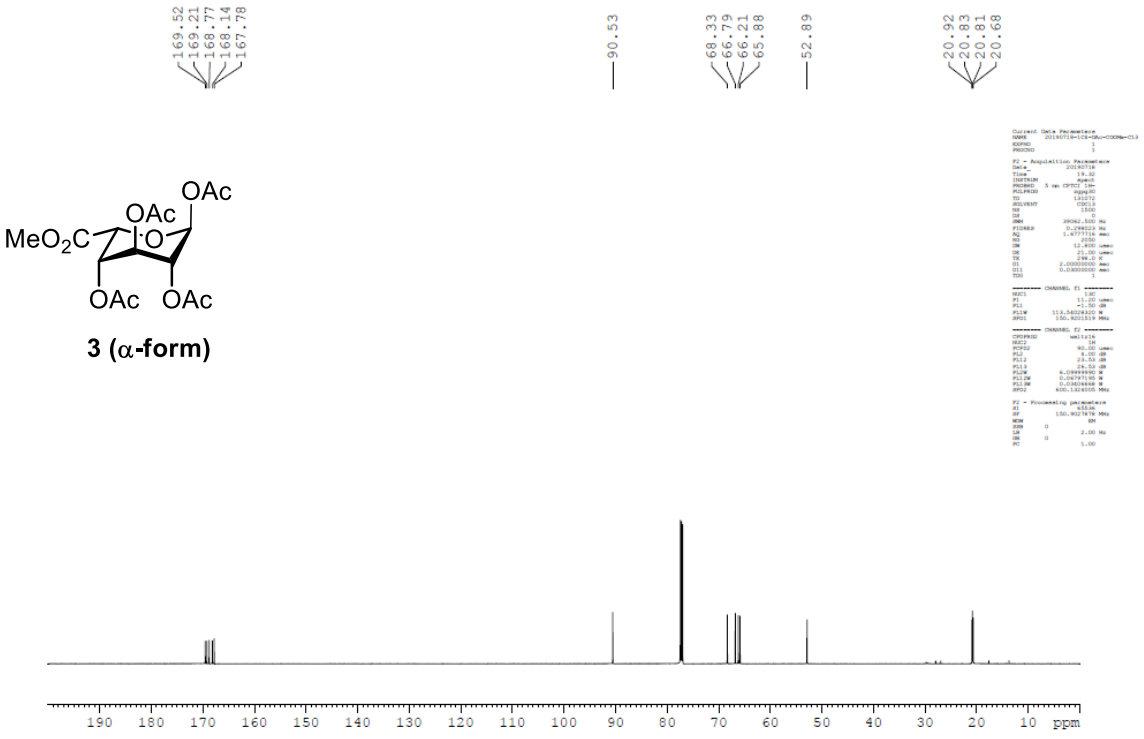

^{13}C NMR Spectra of compound **3** (600 MHz, $CDCl_3$)

doi:10.6844/NCKU201900656

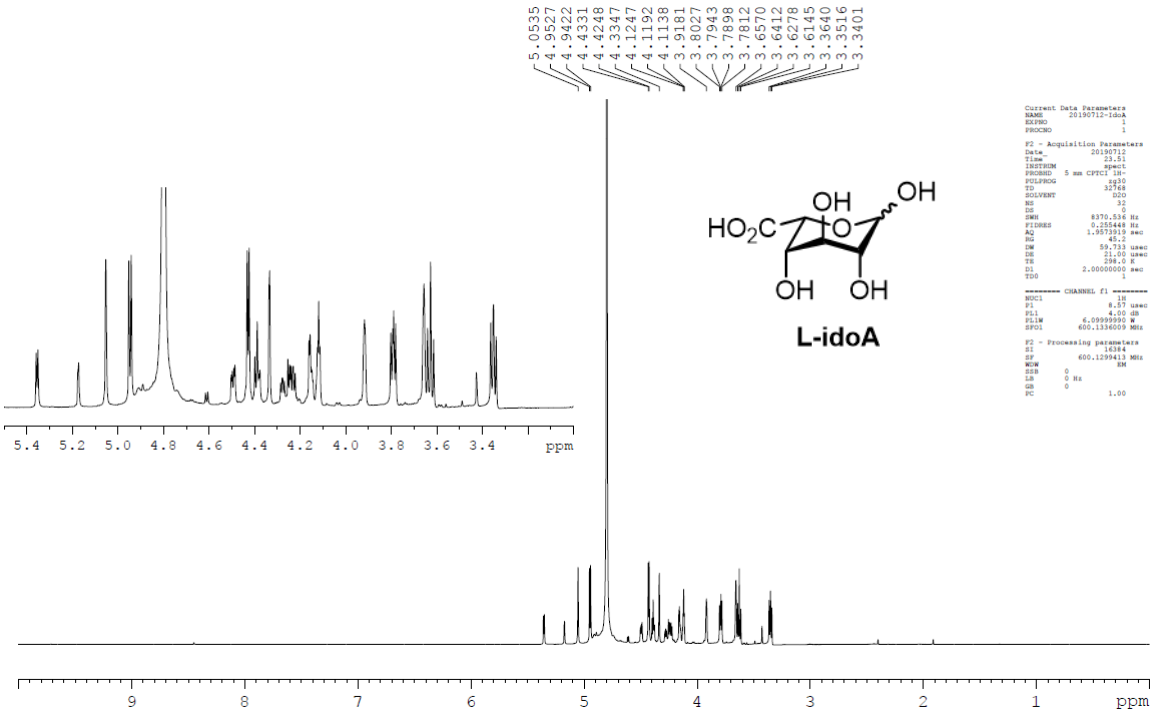

^{1}H NMR Spectra of L-idoA (600 MHz, D_2O)

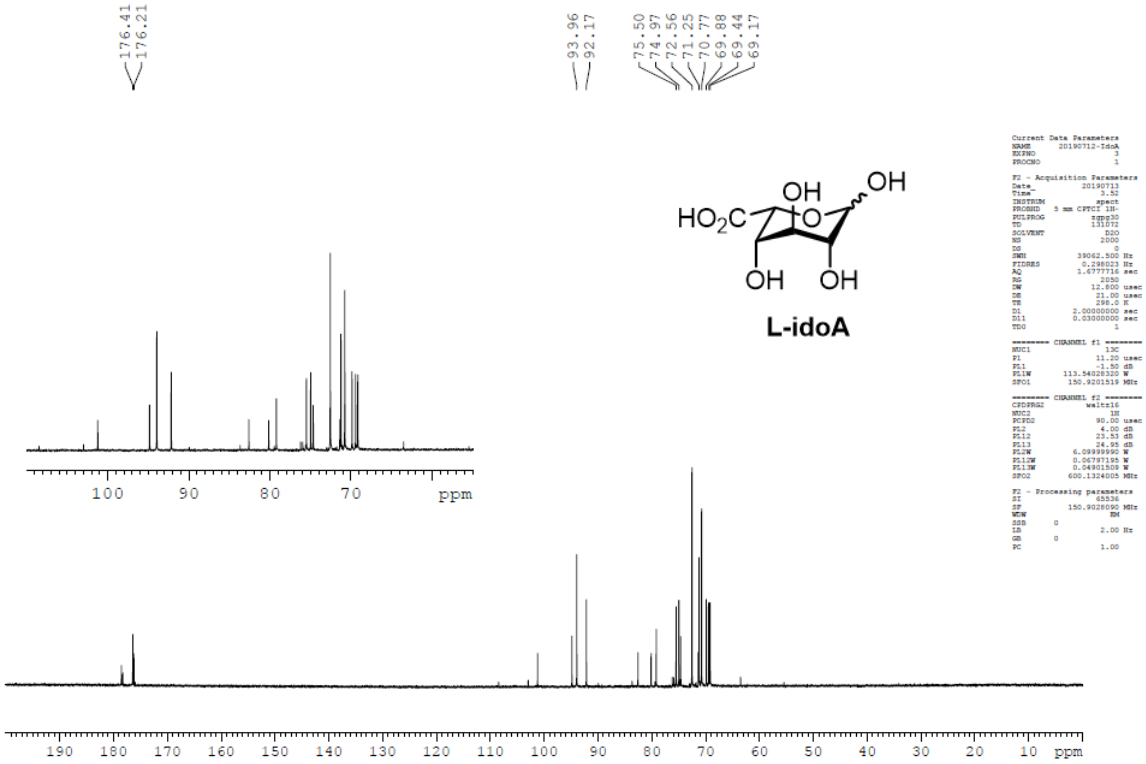

^{13}C NMR Spectra of L-idoA (600 MHz, D_2O)

doi:10.6844/NCKU201900656

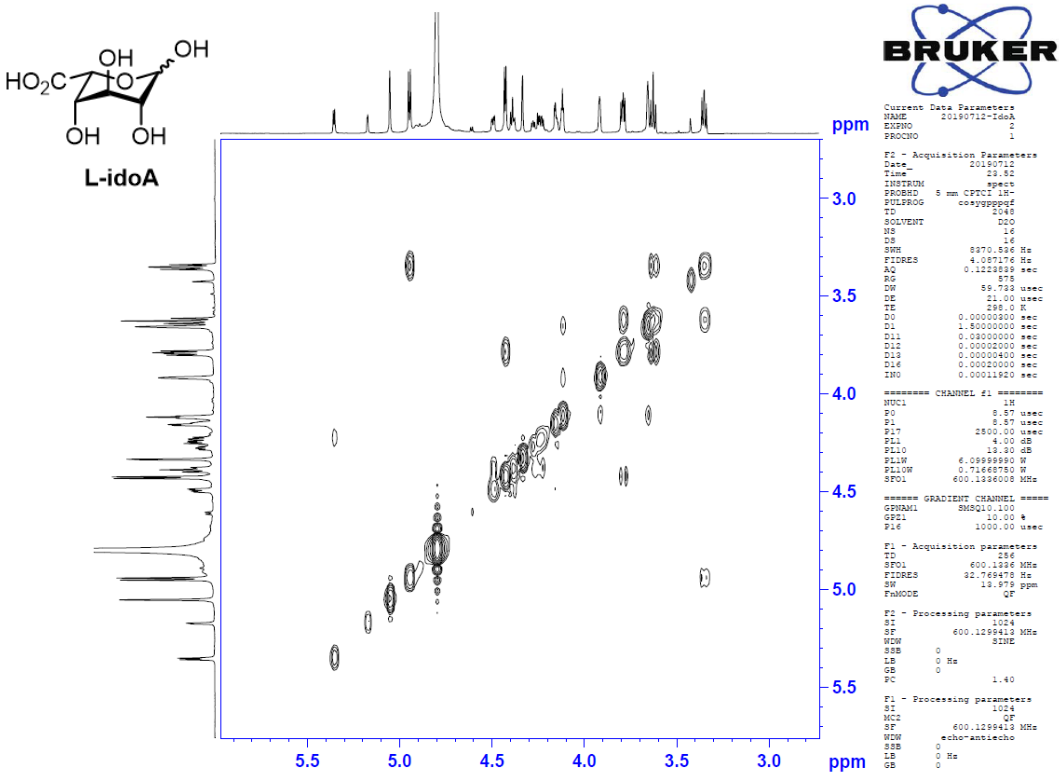

COSY Spectra of L-idoA (600 MHz, D_2O)

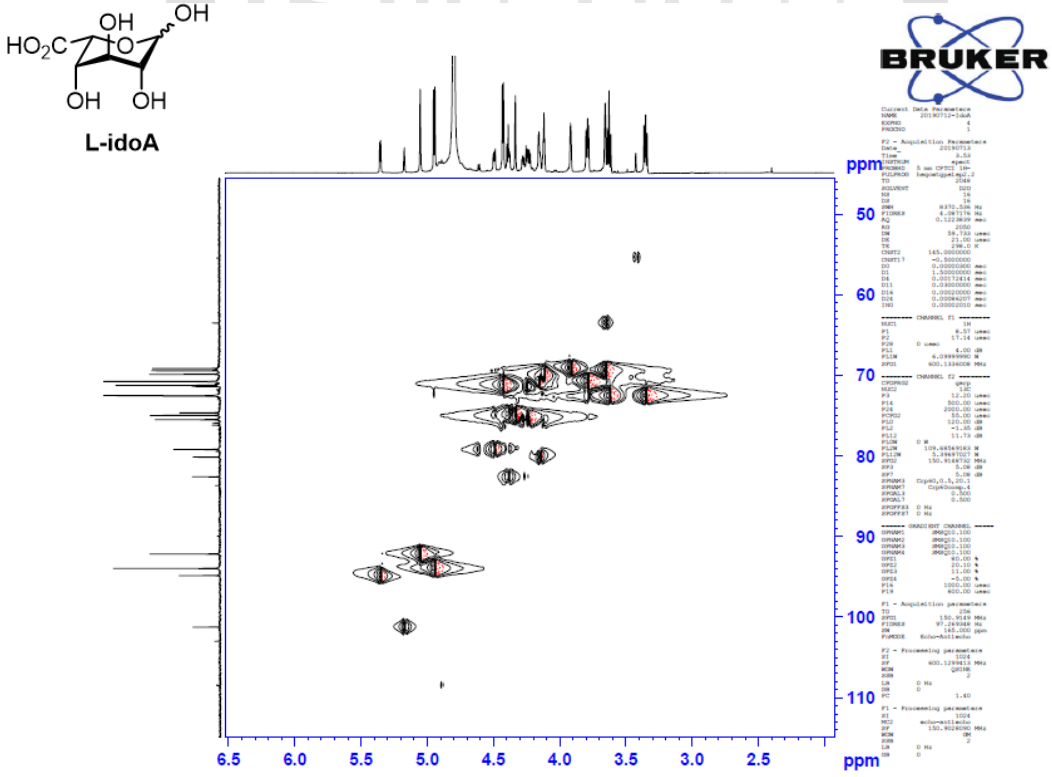

doi:10.6844/NCKU201900656

HSQC Spectra of L-idoA (600 MHz, D_2O)

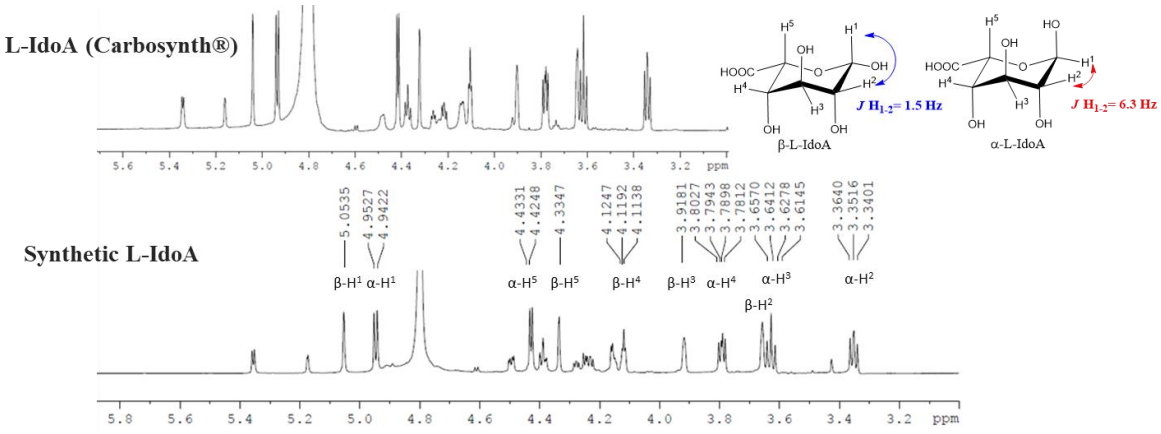

NMR spectra comparison of synthetic and commercial (Carbosynth®) L-idoA

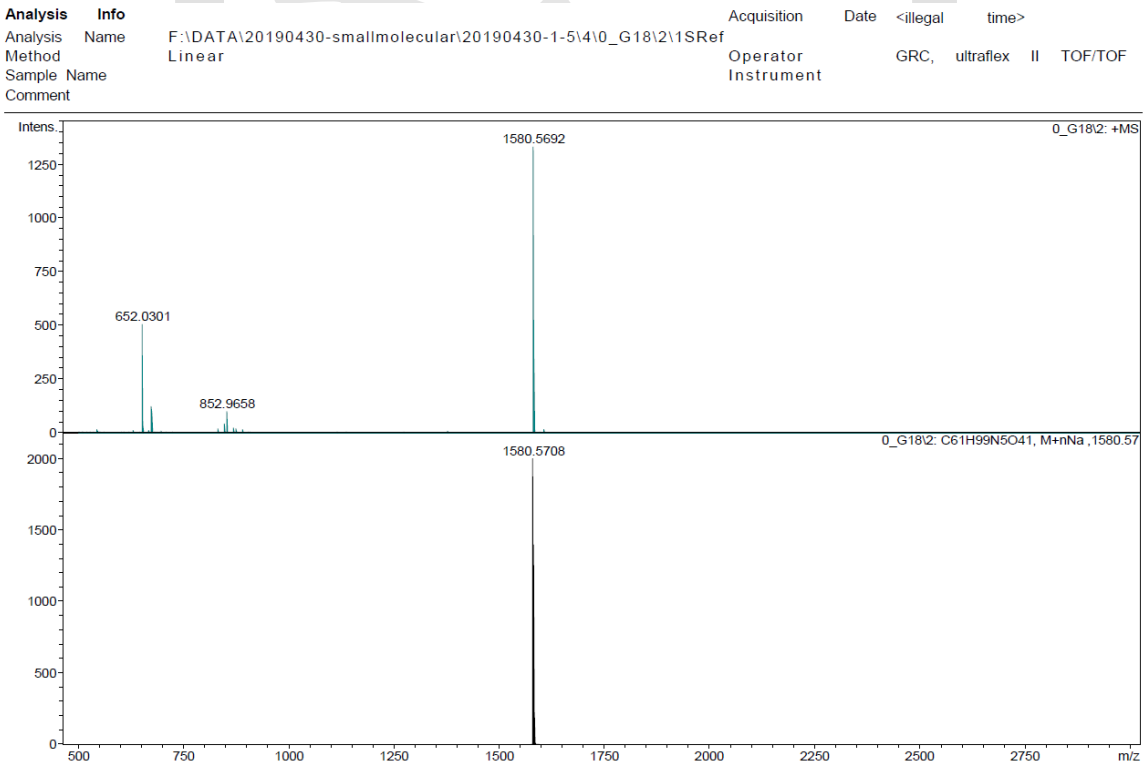

MALDI-TOF-MS spectrum of **O2AB-2** calcd for $[C_{61}H_{99}N_5O_{41}+Na]^+$ 1580.5708, found 1580.5692.

doi:10.6844/NCKU201900656

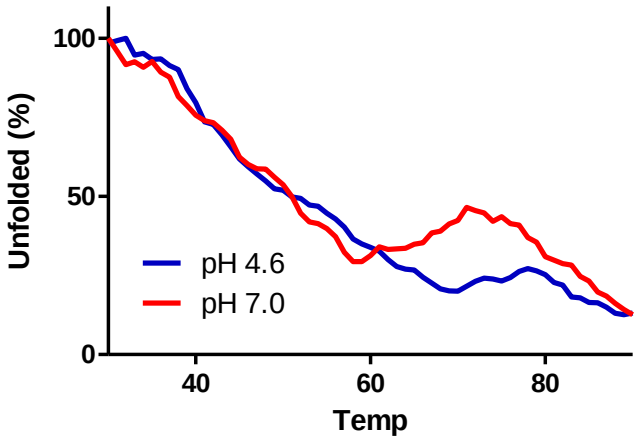

The *Tm* of IDS in the various pH conditions in thermal shift assay by DASPMI

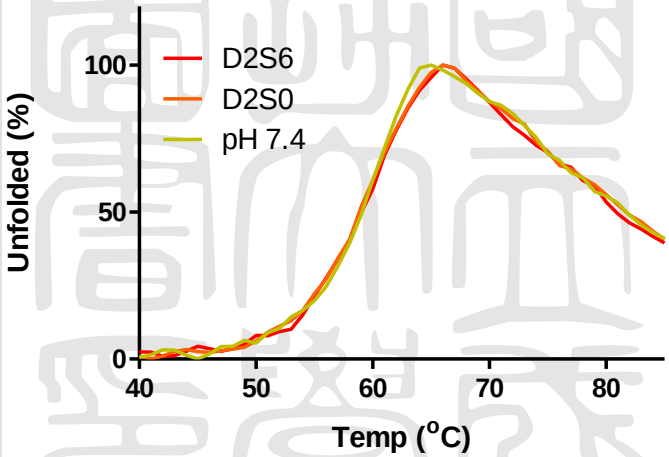

Thermal stability scans of rhIDS in the absence and presence of D2S6 or D2S0 (100 μM) at pH 7.4

Compound	*Tm* (°C)
pH 7.4	59.1
D2S6 (100 μM)	59.0
D2S0 (100 μM)	58.8

doi:10.6844/NCKU201900656

	Cell numbers (10^6)				
	0.05	**0.1**	**0.2**	**0.5**	**1**
NC	174 ± 4	1148 ± 60	1005 ± 40	1449 ± 66	2656 ± 120
PC	6030 ± 121	10122 ± 4067	46367 ± 10361	158808 ± 701	433929 ± 29534
Ratio	35	8.8	46	110	163

The ratio of peak areas in the patient cell and the normal cell

doi:10.6844/NCKU201900656

Development of new molecular scaffolds and libraries of small molecules as enzyme stabilizers on IDS in MPS II

MPS II has the highest incidence in all the mucopolysaccharidoses and the expensive cost about the enzyme drug is a heavy burden for patient's families in Taiwan. Therefore, it is an important issue about how to cost down the treatment of ERT for MPS II but there is no reference on the enzyme stabilizers for MPS II at present. In previous work, our laboratory has reported the studies of design and synthesis the enzyme stabilizers for MPS I. We will take this experience as a reference to design and synthesis the novel enzyme stabilizer for MPS II. Whatever, we plan to design and synthesize new scaffolds inspired by natural substrate, 2-O-sulfo-α-L-iduronic acid. By using the diversity-oriented synthesis approach will be applied to increase the highly diverse substituent to improve potency and selectivity toward IDS. Besides, the assay platform will be improved to screening potential small molecules for IDS stabilizers (Figure A).

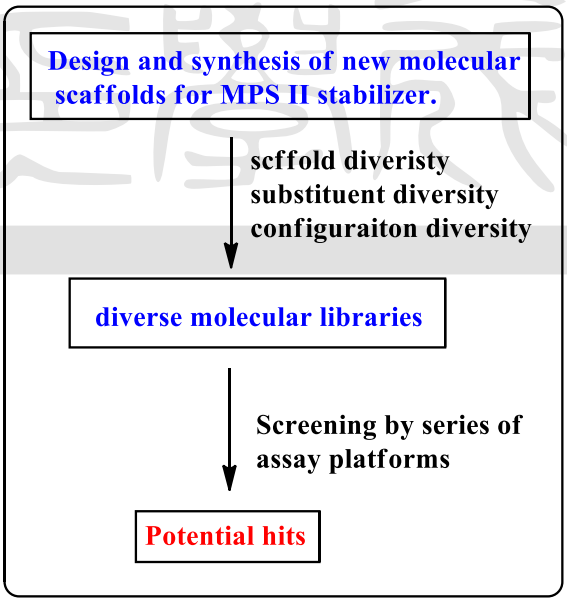

Figure A. The methods of studies IDS stabilizers

doi:10.6844/NCKU201900656

The substrates of IDS

Iduronate-2-sulfatase is a lysosomal enzyme to degrading the heparan sulfate (HS) and dermatan sulfate (DS). Both are negatively charged linear polysaccharides composed of repeating disaccharides with variable sulfation levels. The structure of HS consists of the iduronic acid (IdoA), and N-acetylglucosamine (GluNAc), and the DS are iduronic acid (IdoA) and N-acetylgalactosamine (GalNAc). The specific structure of IdoA in HS and DS is the first substrate to involving the degrading pathway of GAGs. There are three conformations of IdoA in the natural substrates (Figure B), chair forms ($^1C_4$ 、$^4C_1$) and skew boat ($^2S_0$). The distributions of conformation in the normal condition have been reported, the $^1C_4$ form is the major contributor to the conformational equilibrium.

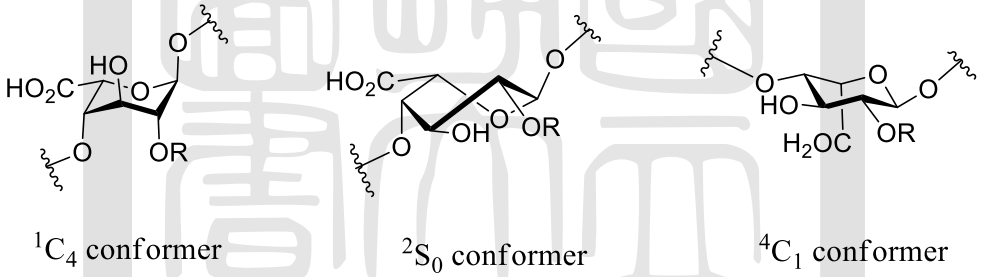

$^1C_4$ conformer $^2S_0$ conformer $^4C_1$ conformer

Figure B The conformers of IdoA

Molecular modification of iduronic acid

In previous work, our laboratory developed the methods of preparing the substituent-diverse, triazole–iduronic acid hybrid molecules by click reaction as the enzyme stabilizers for the potential treatment for MPS I.

doi:10.6844/NCKU201900656

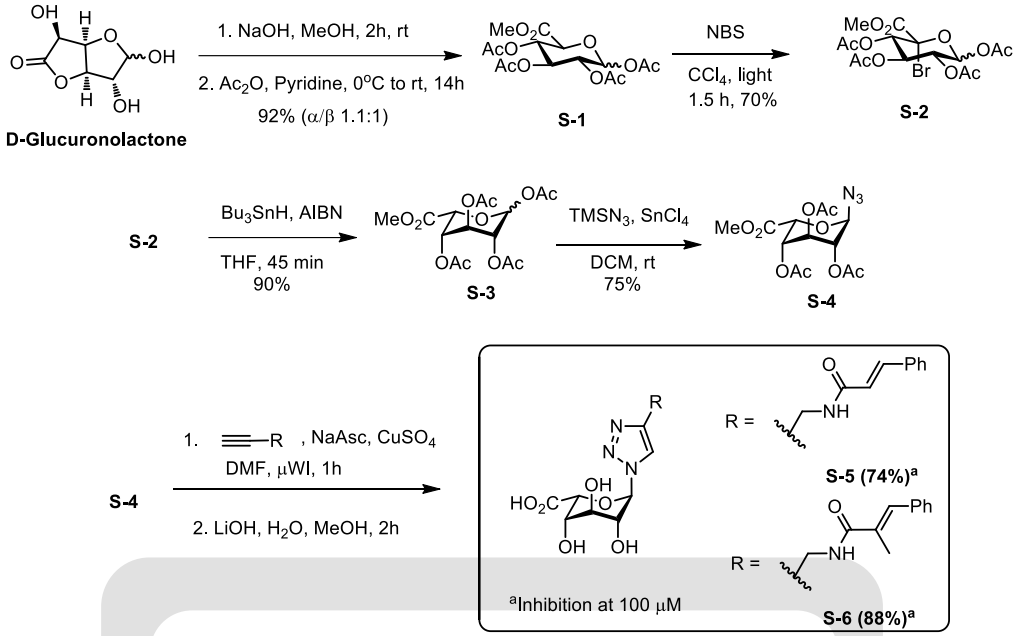

Scheme A. Synthetic route for the preparation of triazole–iduronic acid hybrid molecules as enzyme stabilizers (**S-5** and **S-6**) for MPS I

S-4 was prepared starting from D-glucuronolactone (Scheme A). Methanolysis of **S-4** followed by peracetylation gave a mixture of α- and β-anomers of **S-1**. Bromination of these at the C5 position under photo-induced radical conditions using N-bromosuccinimide gave **S-2** (70%). Next, **S-2** was treated with tributyltin hydride and azobisisobutyronitrile (AIBN) in boiling THF, which gave a separable mixture of **S-3** and **S-1** (**S-3**/ **S-1** = 1/2) in 90% yield. Based on NMR analysis and literature reports, **S-3** was confirmed to be a $^{1}C_{4}$ conformer because of the smaller coupling constants of $J^{4,5}$ and $J^{4,3}$ (2.4 and 3.6 Hz, respectively) observed. Treatment of **S-3** with $TMSN_3/SnCl_4$ gave the α-azide intermediate **S-4** in 75% yield. Afterward, **S-4** will treatment with N-acyl alkyne library in the presence of sodium ascorbate (NaAsc) gave rise to a click reaction, which was followed by deprotection to afford the potential molecules **S-5** (74% inhibition at 100 μM) and **S-6** (88% inhibition at 100 μM). The ability of **S-5** and **S-6** to affect IDUA stability were investigated. The ability of these molecules to protect the enzyme from heat-induced inactivation was also evaluated. In a control experiment without treating molecules, the IDUA activity was found to decrease

doi:10.6844/NCKU201900656

below 5% of the initial value after 120 min of incubation at 48 ℃. Upon treatment with **S-5** or **S-6**, this enzyme activity still remains around 60% at 500 mM.

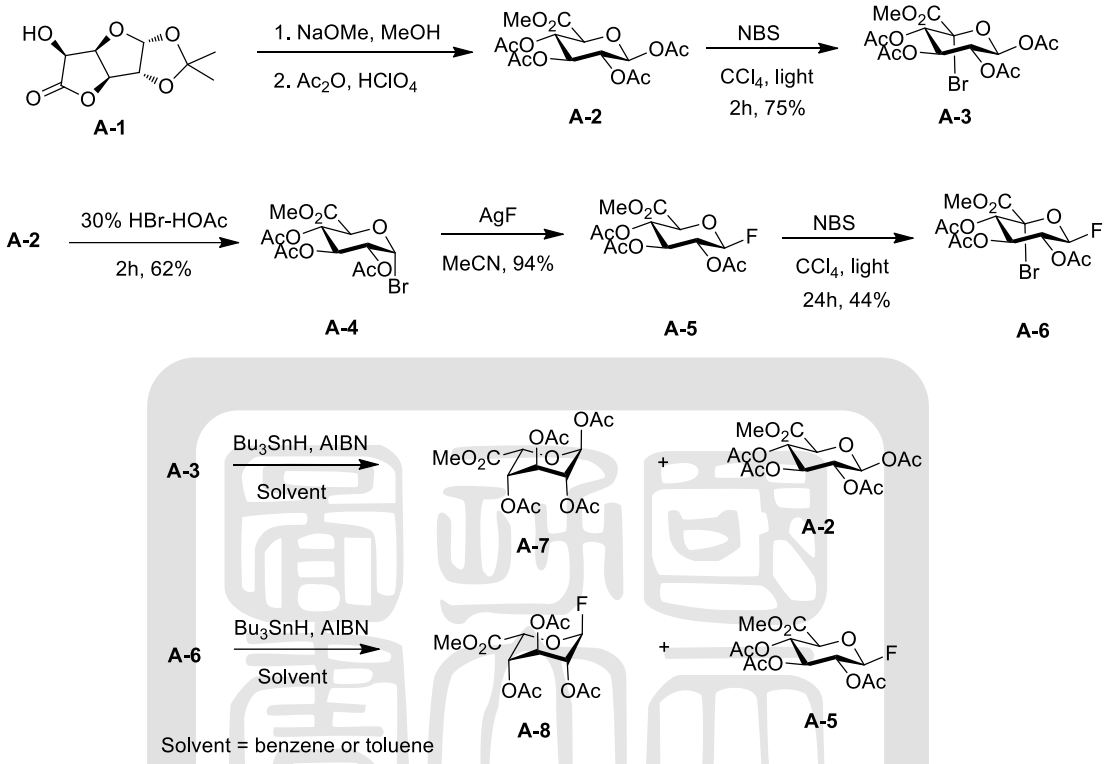

Scheme B. The strategy of synthesis $^{1}C_{4}$ conformer iduronic acid derivatives

In our case, the reductions of C-5 brominated **S-2** to get right conformer **S-3** is only 30%, there is less 60% transfer back to the initial material **S-1**. To overcome this conversion of right conformation, the methods of synthesis $^{1}C_{4}$ conformer iduronic acid derivatives were discussed by the literature search (Scheme B). In 2016, Vito Ferro and coworkers reported that **A-3** was reduced with tributyltin hydride in toluene at reflux the **A-7** to **A-2** was 1 : 5 and the **A-7** isolated in only 14% and this results is similar to the benzene as solvent condition (1 : 1.8). On the other hand, the same reaction has been reported by Wong and co-workers, the ratio of **A-7** to **A-2** was 2 : 1 in the benzene at reflux by the AIBN as the radical initiator. Recently, the synthetic route of substrate for MPS I showed the novel approach to get the high selectivity to obtained the $^{1}C_{4}$ conformer iduronic acid derivatives. Voznyi *et al.*

doi:10.6844/NCKU201900656

reported the reaction in toluene and get the product ratio of 2.6 : 1 in favor of **A-8** which was isolated in 67% yield. Actually, Gelb and coworkers obtained **A-8** exclusively in 64% yield when the reaction in benzene and the **A-5** didn't report any evidence of the formation and Vito Ferro and coworkers got the same result of obtained **A-8** in 65 %.

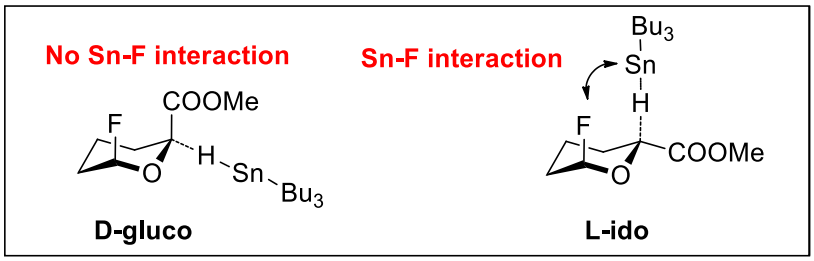

Figure C. The factors of Sn-F interaction affect the conformation

Based on the references, Vito Ferro and coworkers extended those work to evaluate the factor of Sn-F interaction affect the structures of $_{D}$-gluco and $_{L}$-ido. The results of calculation, the favored transition states is $_{L}$-ido because of the Sn interact with the fluoride and to lower the energy barrier (Figure C). This conclusion can correspond to the yield of products **A-7** (14%) and **A-8** (65%).

Motivation

Although the synthesis of iduronic acid derivatives are widely investigated, the structure of 2-O-sulfo-α-L-iduronic acid is less to report. It is challenging for us to develop the scaffold of IDS stabilizer. Whereas we inspired from the structure of arylsulfatase inhibitor, estrone sulfamate, is a steroid sulfatase inhibitor and the function group of sulfamate will interact with the FGly and FGH residue (Figure D). Due to the mechanism of sulfatase is reversible cycling pathway, the sulfamate will bond covalently in the active site block the cycling system and irreversible linkage on the enzyme to inactivation. However, the irreversible reaction was not suitable to the enzyme stabilizer and what we identify is the function of sulfamate can be a binder to the arylsulfatase.

doi:10.6844/NCKU201900656

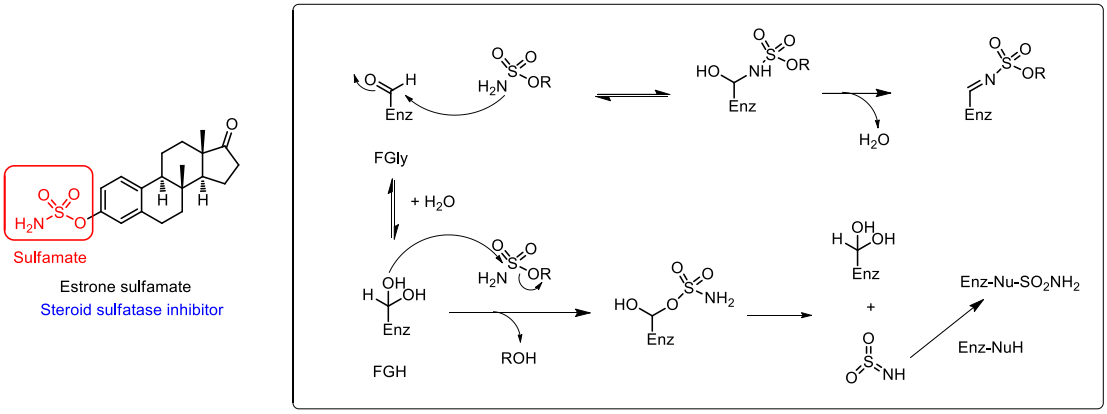

Figure D. Proposed mechanisms of sulfatase inhibitors

Herein, we hope to keep the function group of sulfate to binding with the active site and modify the C-1 moiety to increase the ability of IDS interaction. Based on the molecular modification of iduronic acid, the synthesis routes will be a reference to develop a new scheme of the enzyme stabilizers for IDS. Generally, we propose to the substrate mimic structure and design a non-cleavable moiety for the sulfate or surrogates on the iduronic acid. Besides, diversity-oriented synthesis approach will be applied to increase the structural diversity.

Design

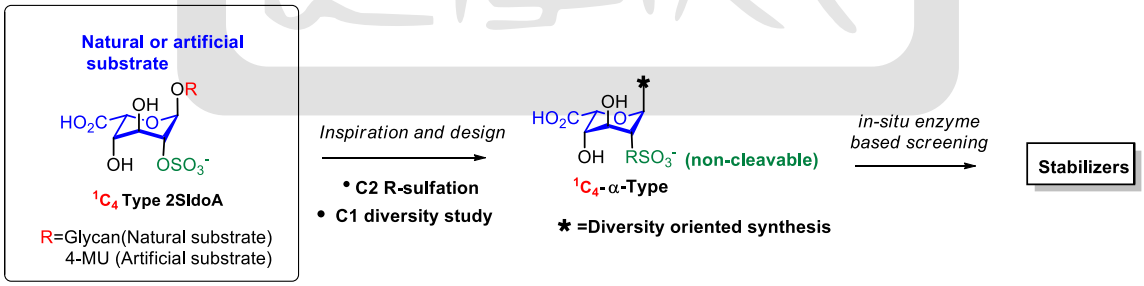

Scheme C. General strategy of synthesis of non-cleavable moiety scaffold

Based on the information of enzyme and preliminary data, we use the substrate mimic with non-cleavable moiety for the sulfate or surrogates in iduronic acid. We choose the $^1C_4$ conformer, which has more population of the natural or artificial substrate as the scaffold

doi:10.6844/NCKU201900656

(Scheme C). Additionally, the develop of C-1 diversity will interact with the amino acid nearby active site possibly. Both of the C-2 non-cleavable and C-1 diversity which could be a potential binder. Follow the principle of the best binder may be a best stabilizer or chaperone, this strategy will apply to discover powerful molecule as the stabilizer for enzyme drug.

Chemistry

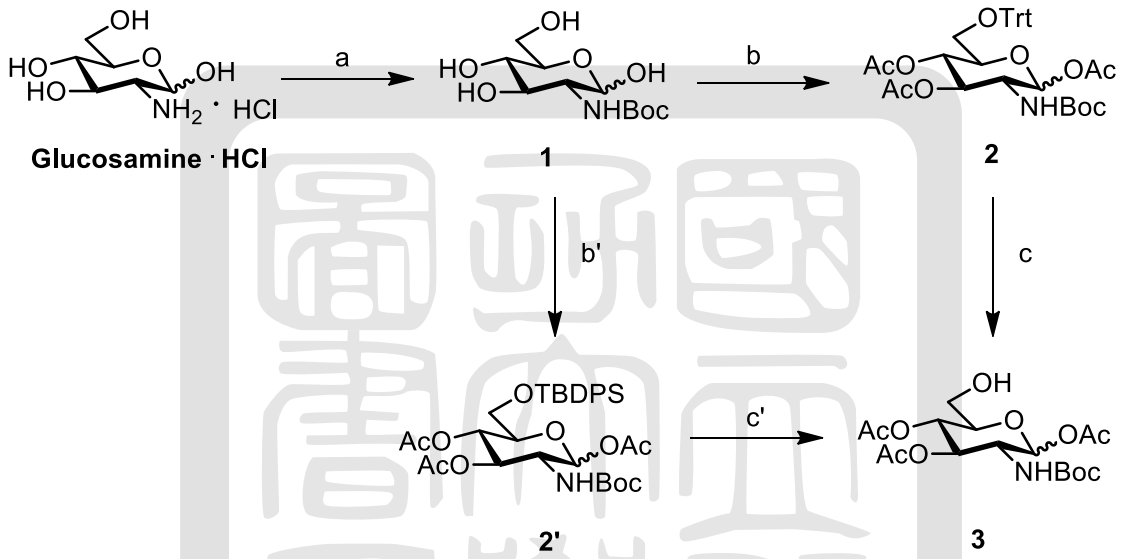

Scheme D. Reagents and conditions: (a) Boc_2O, Et_3N, 1,4-dioxane/H_2O, rt, 5h, 77%; (b)(1) TrtCl, pyridine, 80°C, 5h; (2) Ac_2O, pyridine, 0°C, o.n., 70% over two steps; (c) HCOOH, Et_2O, 0°C, 7h, 63%; (b')(1) TBDPSCl, pyridine, 60°C, o.n.; (2) Ac_2O, pyridine, 0°C, o.n., 80% over two steps (c') TBAF, THF, rt., o.n.; 82%

We assume the N-sulfate on C-2 will play a role to interact with the active site which will non-cleavable in the IDS. The starting the C-2 non-cleavable sulfate iduronic acid was prepared from glucosamine. As shown in Scheme D, the group of amine is protected by tert-butyl carbamate using the triethylamine in the couple solvents condition. When the reaction completed, the compound **1** as the white solid separated in the coupling solvents and then filtered and washed with EtOAc to obtained. Next, the hydroxyl group will be protected by acetyl group, but the primary alcohol on the C-6 need to oxidation to get the carboxyl group.

doi:10.6844/NCKU201900656

In the first, the hydroxyl group of C-6 selective protected by the trityl group and the other secondary alcohols can be acetylated to get the compound **2**. Before the oxidation on the primary alcohol, the formic acid can selective deprotection of trityl group to obtain the compound **3** and the N-Boc wouldn't deprotect in this acidic condition. However, the workup of **3** needed to using sodium bicarbonate ($NaHCO_3$) to quench the excess of formic acid slowly to the neutral condition. Because of the neutralization is time-consuming, so the silane group will be used to selective protection of primary alcohol and got the better yield.

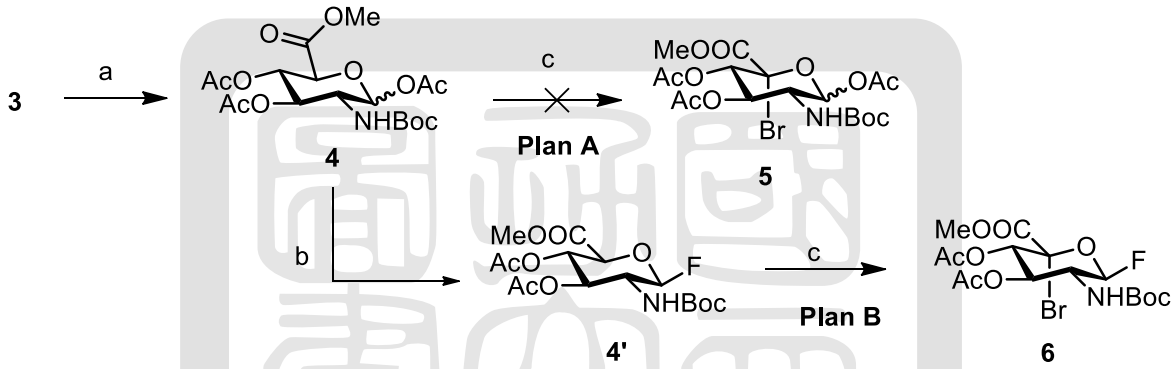

Scheme E. Reagents and conditions: (a)(1) TEMPO, BAIB, DCM/H_2O, rt. o.n.; (2) MeI, K_2CO_3, DMF, rt, 2h, 68% over two steps;(b) Bu_3SnOMe, DCM, reflux, 8h; (2) DAST, DCM, - 30ºC, 2h, 39% over two steps; (c) NBS, CCl_4, reflex, *hv*, 6h; 52%.

As shown in Scheme E, compound **4** was used the general condition of TEMPO oxidation and the carboxyl group will protect by the methyl ester bond. Next, bromination of **4** at the C-5 position under photo-induced radical conditions using N-bromosuccinimide gave **5**. Unfortunately, the result of plan A got a messy product detected by TLC. Therefore, we change the route to plan B which could get the pure product by purification. The compound **4** would selective hydrolysis by the tributyltin methoxide to obtain the compound of the hydroxyl group on the C-1. The purposed mechanism is the tin atom will coordinate to the oxygen atom on the sugar and lead the bond of C-O weakly to cleavage. The methoxide group in the Bu_3SnOMe will attack the acetyl group on the C-1 and move out the acetyl

doi:10.6844/NCKU201900656

group. Then work up the reaction, the product of selective hydrolysis on the C-1 is obtained (Figure E).

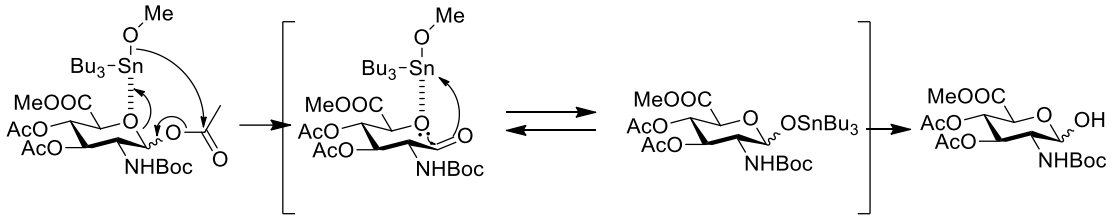

Figure E. Purposed mechanism of selective hydrolysis the acetyl group on the C-1

At this stage, the fluorine atom on the C-1 will be established by DAST reaction. Moreover, the electronegativity of fluoride ion is large and stable relatively, it is not easy to form a fluoro-carbon bonding because the fluoride ion has the ability of the base to affect the near hydrogen atom leading to elimination. At this moment using the electrophilic fluorinating reagent, Diethylaminotrifluoro Sulfur (DAST), which can activate the hydroxyl group at the C-1 position, and then immediately attacked by the S_N2 from the fluoride ion generated in the reaction. This reaction was carried out to obtain compound **4'**. Compared with other fluorinating reagents (such as AgF, KF), it can effectively shorten the reaction time and reduces side reactions. However, the products of α and β anomers are formed (α : β = 1 : 5) , and it is difficult to purification because the polarity is very close shown on the TLC (Figure F). Interestingly, we observe the crystal is formed in the tube which is the mixture of α and β compounds purified by the column chromatography. Next, we checked the crystal by the TLC is the product compound **4'** of β-form and test the solubility of dichloromethane、ether、ethyl acetate and hexanes. The compound **4'** is dissolving in the dichloromethane and ethyl acetate, hard to dissolve in the ether and insoluble to the hexane. Furthermore, it will use the method of recrystallization to purify compound **4'** because of the solubility for the biphasic recrystallization.

doi:10.6844/NCKU201900656

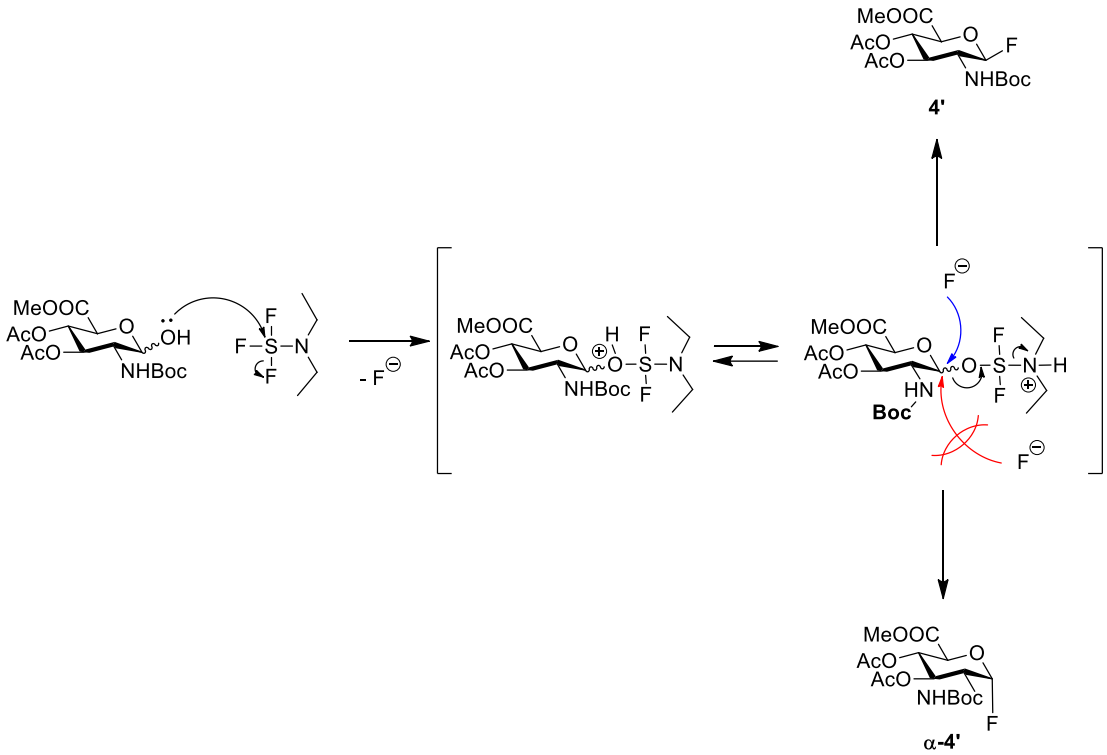

Figure F. Purposed mechanism of DAST reaction

To convert the stereochemistry of the C-5 position to got the $^{1}C_{4}$ conformer, the bromination of **4'** at the C-5 position under photo-induced radical conditions using N-bromosuccinimide gave **6**. In this reaction, the bromine only added in the axial position because the mechanism shown the methyl ester group can stabilize the free radicals generated at the C-5 position after photo-induced. On the other hand, the lone pair of electrons provided by the oxygen atoms on the ring is resulting anomeric effect would also cause the free radical orbital of the C-5 position to get the more stable axial position. Generally, the bromine radical generated by NBS will combine to the C-5 free radical to produce a single product **6** of the bromine atom in the axial position (Figure G). The compound **6** checked by the 1H NMR spectrum and occurred the peak of H-5' is disappeared (Figure H).

doi:10.6844/NCKU201900656

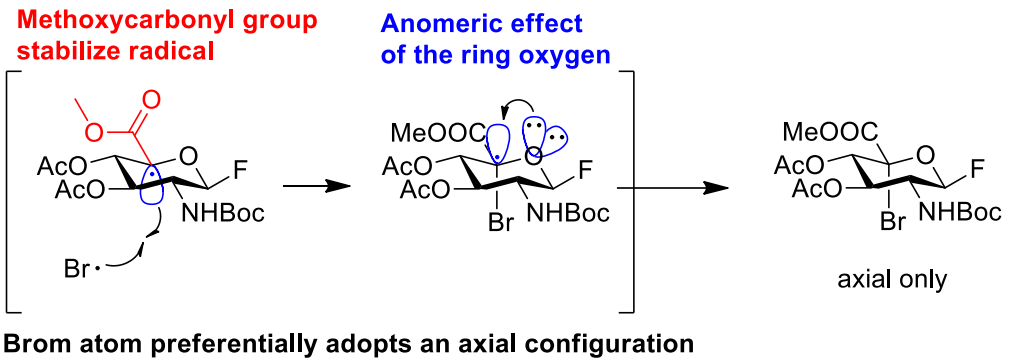

Figure G. Purposed mechanism of axial attack bromination

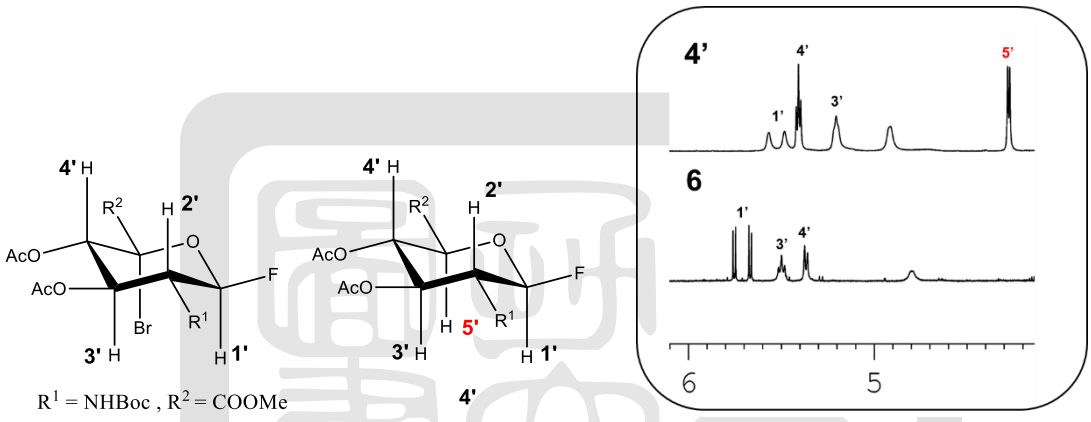

R^1 = NHBoc , R^2 = COOMe

Figure H. ^{1}H NMR of **4'** and **6**

Due to the low yield of compound **6** (2-39%), the mechanism would be discussed, and the condition of bromination will be improved (Table A). Actually, compound **4'** couldn't dissolve in the CCl_4 completely leading to the starting material would decompose at the photo-induced radical conditions. Even though the progress of bulbs lighting, the reaction would be heated and the CCl_4 refluxing in the bottle. When the reaction completely, there are some brown solid like the burnt things on the wall of the bottle. Notably, the benzene is usually used in the radical reaction, and the dissolution capacity is higher than CCl_4 can be observed in this case. However, the yield of compound **6** (18%) didn't improve, so that wasn't the solvent effect in this reaction (Entry 2). On the other hand, the model test is the compound **A-5** convert to **A-6**, the yield of compound **A-6** were acceptable 44-77% from references and the highest 80% in-house. As the results, the factor which caused the lower

doi:10.6844/NCKU201900656

yield is the C-2 substituent. Encouraged by literature, the N-Boc protecting group cannot tolerate the high temperature (150 ºC) and acidic condition (pH 3-4). The first test was cool down the reaction temperature by the blowing cooler air which cold by the ice water and close to the reaction bottle. The yield of compound **6** was 52% the same as before, and the temperature was be measured not higher than 80 ºC in the progress of reaction (Entry 3).

Table A. The condition of the C-5 bromination

Entry	Reaction condition	Time (h)	Yield (%)
1	NBS, CCl_4, *hυ*, reflux	6	2-39
2	NBS, benzene, *hυ*, reflux	6	18
3	NBS, CCl_4, *hυ*, cool down	6	52

Next, we tested other condition of bromination, which used the initiator and heated. There are two common initiators will be tested, AIBN and Bz_2O_2 at 80 ºC. Although the reaction was completed of AIBN as the initiator, the TLC pattern is messy and hard to purification. The condition of Bz_2O_2 added wasn't finish, and the TLC pattern was also messy (Table B).

Table B. The condition of initiator mediated bromination

Entry	Reaction condition	Temp (℃)	Time (h)	Yield (%)
1	NBS, CCl_4, AIBN, reflux	80	6	messy
2	NBS, CCl_4, Bz_2O_2, reflux	80	6	messy

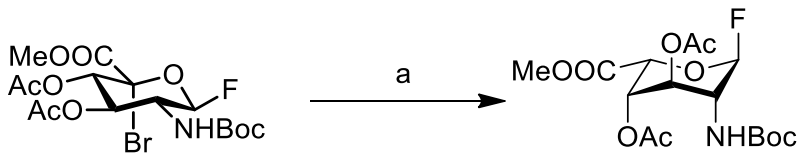

6 **7**

Scheme F. Reagents and conditions: (a) Bu_3SnH, AIBN, THF reflux; 46%

doi:10.6844/NCKU201900656

As described before, the 5-brominated compound **6** present in the tributyltin hydride, the free radical is carried out on the C-5 position. There is an opportunity to form a $^{4}C_{1}$ conformer (**4'**) and $^{1}C_{4}$ conformer (**7**). However, the fluoride on the C1 position is been reported the affinity between the fluoride atom and tributyltin (Scheme F). In this case, the product ratio of 4' to 7 is 1 : 2.5 checked by ^{1}H NMR and the yield of **7** is 46% by column chromatography. As the results of reaction, the conformation can be determined by the coupling constant is affected by the configuration of hydrogen are axial-equatorial or equatorial-equatorial. Based on NMR analysis and literature reports, compound **7** was confirmed to be a $^{1}C_{4}$ conformer because of the smaller coupling constants of $J^{4,5}$ = 1.6 Hz observed (Figure J).

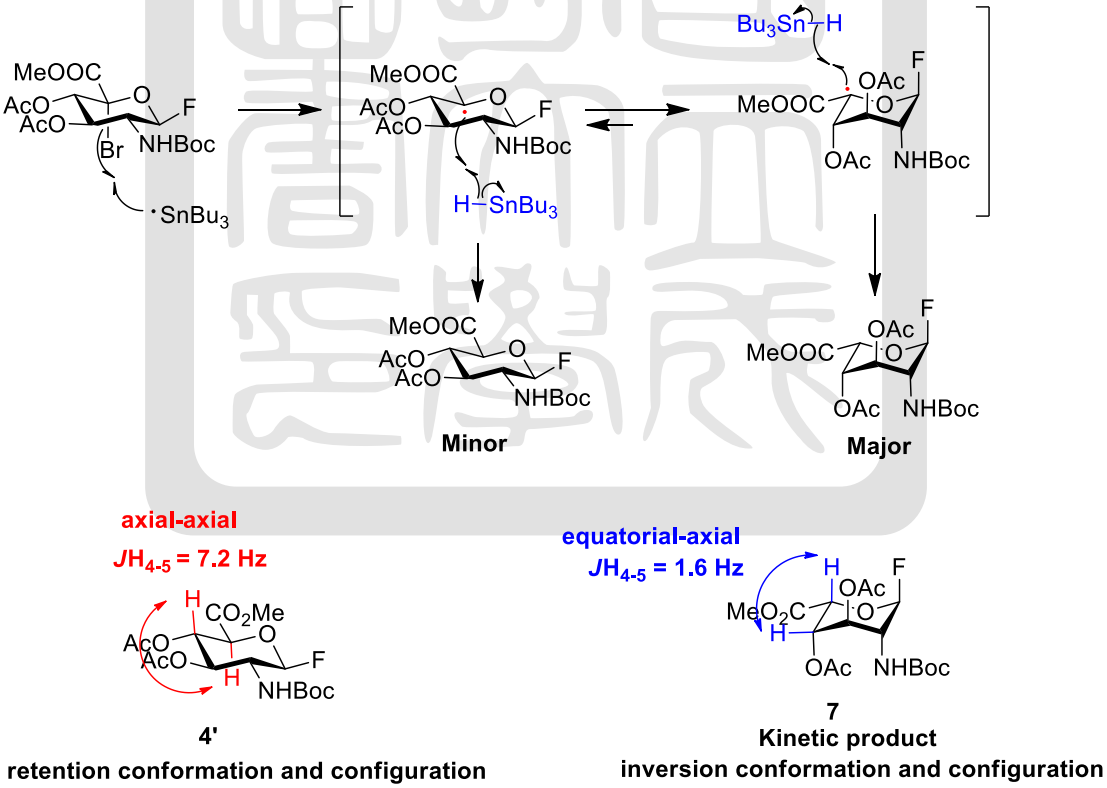

Figure J. Tributyltin hydride mediated the $^{1}C_{4}$ and $^{4}C_{1}$ conformers

doi:10.6844/NCKU201900656

Overall scheme

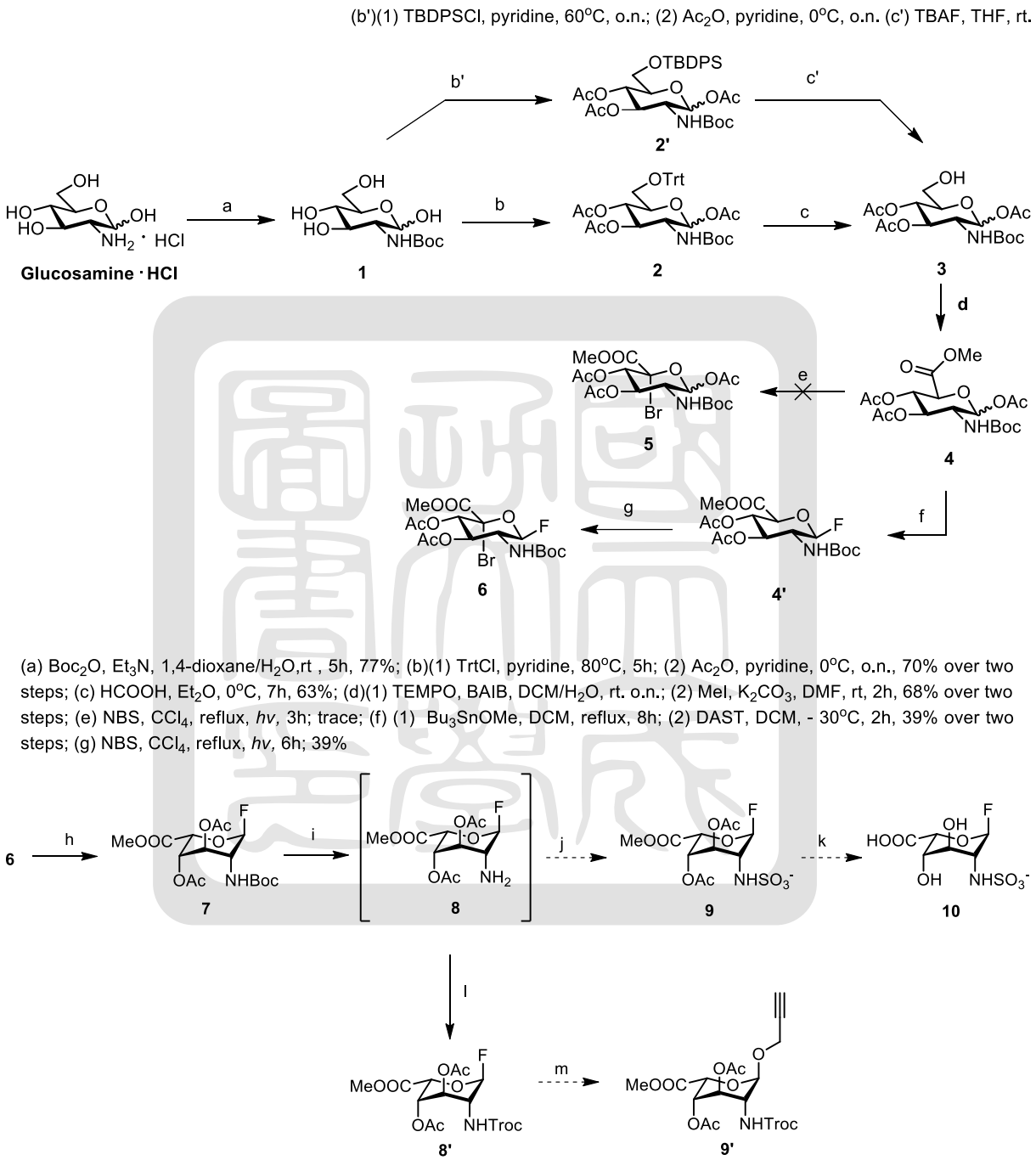

doi:10.6844/NCKU201900656